PNNL-10980
UC-512
Project Technical Information

The Incorporation of P, S, Cr, F, Cl, I, Mn, Ti, U, and Bi into Simulated Nuclear Waste Glasses: Literature Study

M. H. Langowski

February 1996

Prepared for
the U.S. Department of Energy
under Contract DE-AC06-76RLO 1830

Pacific Northwest National Laboratory
Richland, Washington 99352

Battelle

PNNL-10980
UC-512
Project Technical Information

The Incorporation of P, S, Cr, F, Cl, I, Mn, Ti, U, and Bi into Simulated Nuclear Waste Glasses: Literature Study

M. H. Langowski

February 1996

Prepared for
the U.S. Department of Energy
under Contract DE-AC06-76RLO 1830

Pacific Northwest National Laboratory
Richland, Washington 99352

DISCLAIMER

PACIFIC NORTHWEST NATIONAL LABORATORY
operated by
BATTELLE
for the
UNITED STATES DEPARTMENT OF ENERGY
under Contract DE-AC06-76RLO 1830

Printed in the United States of America

Available to DOE and DOE contractors from the Office of Scientific and Technical Information, P.O. Box 62, Oak Ridge, TN 37831; prices available from (615) 576-8401.

Available to the public from the National Technical Information Service, U.S. Department of Commerce, 5285 Port Royal Rd., Springfield, VA 22161


The document was printed on recycled paper.

SUMMARY

The incorporation of minor components (P, S, Cr, F, Cl, I), manganese, titanium, uranium and bismuth into glass is a function of composition and temperature. Redox state and basicity of the glass can also be important. Uranium, Mn, S, and Cr typically form more than one oxidation state in glass and properties of glass can be sensitive to oxidation state. Sulfate solubility, Cr(VI)/Cr(III) ratio, and Mn(III)/Mn(II) ratio in glass were reported to increase with basicity. Sulfur, F, Cl, and I volatilize significantly from glasses at high temperatures. Phosphate also was reported to volatilize but a factor of ten (or more) less than the halogens and sulfur. The solubility of U was found to be a function of oxidation state. U(VI) was reported to have a higher solubility in silicate glasses than U(IV). Mn and Cr were found in spinels and waste loading may be limited by spinel formation in glass. Chromium may also form chromate that may segregate from melts to form a water soluble layer. Sulfate segregation was also reported when the solubility of S was exceeded in oxidized glass,. The formation of gall at 1150°C was observed to remove phosphate, chromate, molybdate, boron, alkali and alkaline earths, rare earths and cesium from the melt. Titanium solubility is strongly affected by the presence of Al_2O_3. Fluorine, Bi and Ti were all reported to decrease viscosity in glass. Cl and iodine were found to have much lower solubility in silicate glasses than the other minor components (typically < 1 wt%). Enhanced corrosion of refractories was reported possible from Bi_2O_3 glasses. Metal piping was reported to be corroded by volatile Cl and S.

Setting limits for the additions of any of the potential waste loading inhibiting compounds for all waste glasses may not be practical due to the complexity of glass chemistry and the number of processing variables. The amount of each component that a waste glass can tolerate is dependent on many factors including minor component interactions, base glass composition, and processing conditions. More study is needed in each of these areas before solubility limits for particular composition can be predicted. The understanding of how each component is affected by these factors and the incorporation of this information into a model is the practical approach to glass formulation, melter selection, and pretreatment/blending strategy.

An evaluation of wastes from A, B, C, B, T, SX, AX, TY, BY, S, TX, and BX tank farms, Neutralized Current Acid Waste (NCAW), Double Shell Slurry Feed (DSSF), and remaining Double Shell Tank (DST) waste was conducted to estimate which waste glasses would be limited in waste loading by the minor components, Mn, Ti, U, and Bi. The maximum waste loading was estimated based on limited scoping studies and many unverified assumptions and extrapolations of property models. Predictions must be used with caution. Of the tank wastes assessed TF-B and TF-T predicted waste loading to be limited by P_2O_5. TF-SX was predicted to be limited by Cr_2O_3. Not enough information about U solubility or its interaction with Zr, Ce, F, and P was available to predict if any of the wastes would be limited by U. TF-C, TF-A, and TF-AX contained high amounts of MnO_2, but it is not known if waste loading would be limited by Mn. In TF-C, ZrO2 was predicted to limit waste loading before MnO_2. In TF-A and TF-AX, spinel was predicted to limit waste loading. The interaction between Fe, Mn and Cr to form spinel must be further studied to determine Mn's role in spinel to potentially limit waste loading. None of the evaluated wastes contained high enough TiO_2 concentrations to potentially limit waste loading. However, should pretreatment involve the addition of silico-titanates the interaction of TiO_2 with Al_2O_3 may potentially limit waste loading. TiO_2 may also increase crystallinity by acting as a nucleating agent.

None of the wastes contained high (> 1 wt%) amounts of Cl, I or S. However, the accumulation of salt layers in the batch blanket (cold cap) and cold cap chemistry both of which could affect melter operation have not been well studied. Molten salt segregation and enhanced volatility may

occur during processing of the assessed wastes.

Fluorine was present in amounts of < 1.56 wt% in the assessed wastes. Based on literature reports this amount should not limit waste loading. However, testing should be performed for verification and to assess interactive effects between F and other glass components. There is a possibility that CaF_2 could crystallize during the vitrification in TF-C. It is not known what effects this might produce on processing. Volatility of F may occur in the melter and cause problems for the offgas system.

Two wastes, TF-B and TF-T, contained significant amounts of Bi_2O_3. Though not expected to limit waste loading in these wastes (based on limited studies), the effect of the addition of Bi_2O_3 on viscosity needs to be determined so that modifications to glass formulation can be made to accurately predict melting temperature. TF-B and TF-T wastes were predicted to have waste loading limited by P_2O_5.

Acknowledgements

The author wishes to acknowledge and thank John Coblentz, Dong-Sang Kim, Mike Kupfer, Mike Elliot, Joe Perez, Rick Merrill, Kathy Whittington, Phyllis Shafer, Nick Hudson, Henry Schreiber, Sabrina Fu, Hong Li, John Vienna, Pavel Hrma, and the Hanford Technical Library staff.

List of Acronyms

CC	Complexant Concentrate
CST	Crystalline Silico-Titanates
CVS	Composition Variation Study
DST	Double Shell Tank
DSSF	Double Shell Slurry Feed
GED	Glass Envelope Definition
HLW	High Level Waste
HTM	High Temperature Melter
ICP-ES	Inductively Coupled Plasma Emission Spectroscopy
LFCM	Liquid-Fed Ceramic Melter
LLW	Low Level Waste
MCC-1	Materials Characterization Center-1
NCAW	Neutralized Current Acid Waste
PCT	Product Consistency Test
PFP	Plutonium Finishing Plant
PNL	Pacific Northwest Laboratory
PSCM	Pilot Scale Ceramic Melter
PVTD	PNL Vitrification Technology Development
SEM	Scanning Electron Microscopy
SRL	Savannah River Laboratory
SST	Single Shell Tank
TCLP	Toxicity Characteristic Leachate Procedure
TF	Tank Farm
TRAC	Tracks Radioactive Components
WV	West Valley
XRD	X-ray Diffraction

CONTENTS

SUMMARY iii

Acknowledgements v

List of Acronyms vi

List of Tables viii

List of Figures x

1.0 INTRODUCTION 1

2.0 CONCLUSIONS 2

3.0 WASTE COMPOSITIONS 4

4.0 CRITICAL COMPONENTS 4
- 4.1 Phosphorus 5
- 4.2 Chromate and Chromium Oxide 9
- 4.3 Sulfate 13
- 4.4 Manganese 17
- 4.5 Titanium Dioxide 18
- 4.6 Bismuth 20
- 4.7 Uranium 21
- 4.8 Chlorine and Iodine 23
- 4.9 Fluorine 27

5.0 ASSESSMENT OF WASTE LOADING LIMITATIONS FROM MINOR COMPONENTS FOR SELECTED WASTES 29

6.0 OTHER NEEDED STUDIES 31

7.0 REFERENCES 32

APPENDIX 57

List of Tables

Table 2.0.1. Preliminary Assessment of Minor Component Solubility Effects 38

Table 4.1.1. West Valley Glass Compositions WV-182 and WV-183 which formed Calcium Rare Earth Phases During Processing in PNL Melters 38

Table 4.1.2. HTM and CVS3 Selected Glass Compositions 39

Table 4.1.3. Phosphate Scoping Study Glasses 40

Table 4.1.4. Crystalline Phases Present Hanford Glasses: Scoping Studies and CVS3. 40

Table 4.1.5. West Valley Composition which Crystallized Li_3PO_4 and $Ca_3(PO_4)_2$ after heat treatment at 700°C for 100h 40

Table 4.2.1. Cr_2O_3 Scoping Study NCAW Glass Composition (Bates, 1987) 42

Table 4.2.2. High Cr_2O_3 High Level Waste Glass Composition 42

Table 4.2.3. Nuclear Research Institute High Cr Glasses 43

Table 4.2.4. High Cr_2O_3 Low Level Waste Glass Composition 44

Table 4.2.5. CVS2-68 and CVS2-69 Glass Compositions 44

Table 4.2.6. NCAW 87, CC, and PFP Others 45

Table 4.5.1. High Enriched Waste Concentrate (HEWC) Glass Composition That Crystallized Rutile in the Pamela Melter . . 46

Table 4.5.2. SRL-21 and SRL-131 base glass compositions (Schreiber, 1982) used to investigate the interaction of TiO_2 and U_3O_8 . . 46

Table 4.6.1. Bismuth Phosphate Simulant Waste Compositions (Kupfer, 1978 and Kupfer and Palmer, 1980) 47

Table 4.7.1. Summary of Uranium Interactions with Redox Sensitive Components 48

Table 4.7.2. Sodium Aluminophosphate Compositions (Schreiber, 1982) . . 48

Table 4.7.3. Simplified Formulation of PW-4b Calcine Composition 49

Table 4.8.1. Average Chlorine Decontamination Factors from PNL melter runs 49

Table 4.9.1 Compositions Used in F Scoping Studies (Bates, 1987c) 50

Table 5.0.1. Preliminary Waste Loading Assessment 51

List of Figures

Figure 4.2.1. Chromium equilibrium as a function of basicity number, B, at 1400°C (Kramer) 52

Figure 4.3.1. Sulfur Solubility and redox state distribution as a function of oxygen fugacity at various temperatures in SRL-131 melts 53

Figure 4.3.2. Relation of the imposed oxygen fugacity (-log fO2) to the analyzed redox ratio (log[reduced ion]/[oxidized ion]) of multivalent elements doped into SRL-131 melt at 1150°C (Schreiber et al., 1984b) 54

Figure 4.3.3. Temperature dependence of the sulfur diffusion coefficient (oxidized and reduced) as compared to the oxygen and water vapor diffusion coefficients for SRL-131 melts (Schreiber et al., 1988) 55

Figure 4.4.1. Manganese equilibrium as a function of the basicity number, B, at 900°C (Kramer) 55

Figure 4.7.1. The Proposed Structure Model of U(VI) in an Alkali Silicate Glass. Layers of uranyl are dispersed between layers of silica. Bottom: Detailed view of the uranyl sheet. (Veal et. al /Knapp et al.) 56

1.0 INTRODUCTION

Waste currently stored on the Hanford Reservation in underground tanks will be separated into High Level Waste (HLW) and Low Level Waste (LLW). The HLW melter will convert high-level and transuranic wastes to a vitrified form for disposal in a geological repository. The LLW melter will vitrify the low-level waste which is mainly a sodium solution. Characterization of the tank wastes is still in progress, and the pretreatment processes are still under development. Apart from tank-to-tank variations, the feed delivered to the HLW melter will be subject to process control variability which consists of blending and pretreating the waste. The challenge is then to develop glass formulation models which can produce durable and processable glass compositions for all potential vitrification feed compositions and processing conditions.

The work under HLW glass formulation is to study and model glass and melt properties as functions of glass composition and temperature. The properties of interest include glass melt viscosity, electrical conductivity, liquidus temperature, crystallization, immiscibility, and glass durability. It is these properties that determine the glass processability and acceptability of the waste glass. Apart from composition, some properties, such as viscosity and crystallization, are affected by temperature. The processing temperature may vary from 1050°C to 1550°C dependent upon the melter type. The glass will also experience a temperature profile upon cooling.

The purpose of this letter report is to assess the expected vitrification feed compositions for critical components with the greatest potential impact on waste loading for double shell tank (DST) and single shell tank (SST) wastes. The basis for critical component selection is identified along with the planned approach for evaluation. The proposed experimental work is a crucial part of model development and verification.

This work is conducted in accordance with the Pacific Northwest Laboratory (PNL) Vitrification Technology Development (PVTD) Project Work Plan (PWP) and completes milestone PVTD-C95-02.01P. The information obtained during this work will be used in support of glass formulation for the High Temperature Melter (HTM).

2.0 CONCLUSIONS

It may not be practical to determine limits for specific components (P, S, Cr, F, I,Cl, Mn, Ti, U, and Bi) due to the complexity of glass chemistry. Factors such as composition, temperature, heating rate, redox, or basicity may affect component solubility. Scoping tests and property composition models are necessary to predict approximate component solubility. Development of these models are crucial to increasing waste loading of glasses. The following conclusions describe which glass and melt properties are most likely to be affected by the presence of a specific component and factors which affect component solubility:

- TiO_2 may affect viscosity, liquidus temperature, crystallinity and durability. Based on the literature data the presence of Al_2O_3 strongly decreases the solubility of titania. Titania additions generally reduce the viscosity of HLW borosilicate glasses.

- The solubility of P_2O_5 in borosilicate glass is decreased by the presence of Li_2O, CaO, Nd_2O_3, La_2O_3, other rare earths, and SO_3. Durability is affected by the presence of Li_3PO_4. The formation of phosphate layer containing rare earth phosphate and/or calcium phosphate crystals formed during pilot scale testing. Melting rate was decreased by the phosphate layer. Scoping tests showed that molten sulfate segregation can remove phosphate from the glass resulting in the formation of a scum layer. The interaction of phosphate and sulfate is thus crucial to study.

- Waste form durability is decreased by the formation of water soluble chromates. Chromate (Cr(VI)) formation is a function of glass composition, redox, basicity, and temperature. Chromate formation increases with basicity and heat treatment in the temperature range of 800°C to 1000°C. Chromium is also present as Cr(III) in silicate glasses. Cr(III) is favored at temperatures > 1000°C and has a low solubility in glass. Crystals such as spinel or eskolaite (Cr_2O_3) may form when the solubility of Cr(III) is exceeded in glass. These crystals may agglomerate and settle causing problems in the melter.

- Bi_2O_3 may reduce viscosity and increase electrical conductivity. The latter through the possible formation of metallic films via the reduction of Bi(III) to Bi(0). Bi_2O_3 may improve durability slightly. Refractory corrosion may be increased in the presence of bismuth oxide. The possibility of the reduction of bismuth oxide to bismuth metal or the formation of insoluble bismuth sulfide precipitated should be investigated.

- U(IV) is less soluble than U(VI) and U(V). UO_2 precipitates if the solubility limit is exceeded for U(IV). The oxidation state of uranium is affected by the presence of other redox pairs, temperature, oxygen fugacity, basicity, and glass composition. The formation of U fluorite solid solutions has been observed from the heat treatment of oxide powders containing Ce-Nd-Fe-Mo-Zr-Cs-Ni-U-Sr-B-O. The possibility of U fluorite crystallization from glass should be investigated. Also the interaction of U and minor components such as F, SO_3, P_2O_5 should be studied as very little information is available on possible interactions.

- F decreases viscosity and volatilizes significantly. The solubility of F in glass is generally higher than solubility of other halogens. Interactions between F and other major and minor components (U, B, Cl, S, Ti, etc.) should be investigated.

- Iodine and Cl are volatilized in significant amounts. Cl has been reported to increase the

volatilization of F, Cs and Cr. The interaction of Sr and Cl should also be investigated as to assess volatility increases. Iodine has not been studied extensively and may cause foaming. If iodine is to be present in significant amounts in waste basic scoping studies are necessary.

- Sulfate is volatilized in significant amounts. The retention of SO_3 is affected by temperature, glass composition, and redox. Molten salt separation of sulfate can occur which can trap radionuclides, such as cesium, and increase their volatility. Sulfate may also pull phosphate, molybdates, chlorides, and chromates into the gall. The sulfate layer is generally water soluble. Formation of stable sulfate foams can reduce melting rate. Segregated sulfate can increase refractory corrosion and melting rate. Under reducing conditions metal sulfides can precipitate which can increase the risk of shorting out electrodes from joule-heated melters.

- Manganese solubility is expected to be limited by its interaction with Cr, Fe, and Ni to from spinel. Clinopyroxene can also contain Mn, but clinopyroxene is not expected to limit waste loading. Basic studies are necessary to determine the solubility of Mn as a function of these components, redox, basicity, and glass composition. Stable foams have been reported from the reduction of Mn(III) to Mn(II) and studies should determine the conditions under which the foam occurs.

- The increased processing temperature ranges will likely significantly influence the volatility rates of halides, Tc, Cs, Na, B, and other semivolatiles. Studies are needed to determine the volatility rates as a function of time, temperature and glass composition. Additives which may suppress volatility should be investigated to develop mitigation strategies. Components which may enhance volatility should be identified as pretreatment strategies may enable a reduction of these component to feeds containing quantities of volatile components.

Table 2.0.1 contains the preliminary assessment of minor component effects. Solubility numbers are highly dependent on glass composition and processing conditions and should be used with extreme caution. High numbers often represent special conditions such as high temperature, premelting of glass components, and tailoring of glass compositions to maximize the amount of a particular component. These ranges are intended to give some idea about the possible amounts which can be incorporated in silicate glasses. The ranges should not be interpreted and are not intended to mean amounts which can be incorporated into any glass. Scoping studies are necessary to provide more precise information about solubility limits in a particular glass.

3.0 WASTE COMPOSITIONS

Hanford waste compositions are determined using core sampling data and mass balance models (e.g., Tracks Radioactive Components (TRAC)) derived from records of chemical constituents which were released into the tanks. In addition, pretreatment methods (e.g., sludge washing) are incorporated into calculations to determine vitrification feed compositions. It should be noted that characterization of the waste is difficult due to the challenges associated with remote sampling of radioactive material, inhomogeneity of the waste within the tanks, and analytical challenges associated with determining the composition of the waste which contains a large potion of the elements in the periodic table as well as a variety of organic compounds. A variety of compositions have been generated and reported (Brevick (1994a and 1994b), Geeting et al., Miller et al., Lowe et al., May et al., and Weiss) as more information from core sampling and pretreatment processes have become available.

There are 28 double-shell tanks (DST) and 149 single-shell tanks (SST) containing an estimated 61 to 65 million gallons of waste. The waste consists of a liquid portion (supernate) and a solid portion (sludge or salt cake). The compositions in this report are in wt % or mass fraction and do not include compounds which would escape (decompose/volatilize) during vitrification such as oxides of carbon and nitrogen. The compounds are listed as oxides except for halogens. The waste compositions may change in the future and were based on the best available information.

4.0 CRITICAL COMPONENTS

Waste pretreatment, blending, and resulting compositions are subject to variabilities as several scenarios for waste retrieval and pretreatment are used (e.g., sludge washing) and as further waste characterization is performed. Melt processing temperature may also vary from 1050°C to 1550°C. Understanding the effects of the minor components (P_2O_5, SO_3, Cr_2O_3, F, I, and Cl) in the waste on glass properties, through appropriate experimental, model development, model verification and work are crucial to designing glasses for various waste compositions, pretreatment processes, and melter types. In addition, the effects of manganese, uranium, and bismuth (potential major components of waste) on glass properties need to be assessed. Wastes may contain as much as 23.7 wt% U_3O_8 which corresponds to $\approx$ 17.3 wt% in glass (predicted 73 wt% waste loading (WL) with TF-TX waste composition). Up to 8 wt% Bi_2O_3 may need to be incorporated in glass using high Bi_2O_3 wastes (estimated Bi_2O_3 amounts from TRAC data, Geeting and Kurath).

Uranium, Mn, I, Bi, P,S, F, Cr and Cl, were not included in the current Composition Variation Study (CVS) models because NCAW, the primary waste which has been used to study and develop the CVS, did not contain sufficient amounts of these components to impact the glass properties. As other wastes are likely to contain more of these components, it will be necessary to study their effect on glass and processing properties.

A liquidus temperature model which studies the effects of H_2O, Ni, Mn, Bi, P_2O_5, SO_3, F, and Cr_2O_3 in glass is currently being developed by the Centre for Research in Chemical Thermodynamics. This model will predict the equilibrium solubility limits of these components. Experimental work is necessary to validate the phase equilibria model.

Current CVS solubility limits and liquid-liquid separation limits for the minor components (P_2O_5,

SO_3, F, and Cr_2O_3) are based on extrapolation of Defense Waste Processing Facility (DWPF) data[1] and limited studies by Bates[2]. The constraints are $Cr_2O_3 \leq 0.5$ wt %, $SO_3 \leq 0.5$ wt %, F ≤ 1.7 wt % and $P_2O_5 \leq 1$ wt % in glass. The constraints were used to select the composition region for study (Hrma, 1992b) but were not used in the modeling of glass properties such as durability, viscosity and electrical conductivity. The constraints are potentially limiting to increased waste loading of glasses and may not be generally applied over the whole CVS composition region. The incorporation of any one component is dependent on factors such as temperature and overall glass composition. The constraints were developed from several small studies based on the HW-39 glass composition, one at a time experimental methods, or DWPF glass compositions as stated above. Thus, the constraints may be too small or too large for some compositions, and further study is required to determine limits and conditions under which the limits apply. The constraints were not meant and should not be taken to mean that a poor glass or a unprocessable glass would result if the constraints were exceeded in any glass.

The following sections describe in more detail the effects and characteristics of each minor component and the major components Bi and U on glass properties.

4.1 Phosphorus

Silica glass consists of SiO_4^{4-} tetrahedra in a three dimensional network. The Si-O internuclear distance is 1.62×10^{-10}m (Volf) and the Si-O-Si bond angles vary form 120° to 180°C (mean 145°) (Kingery et al.). Each Si^{4+} cation forms a single bond with each oxygen. Pure silica glass melts in the temperature range of > 1700°C. The percent ionic character if the Si-O bond is ≈ 45%.[3]

P_2O_5 forms PO_4 tetrahedra but in contrast, the P^{5+} cation forms three single bonds and one double bond with the four oxygen anions. The double bond is non-bridging such that pure phosphate glass already has 25% non-bridging oxygens compared to pure silica glass having nearly all

---

[1]Bates, S.O. 1987b. *Baseline Milestone HWVP-87-V110202B - Update of Glass Composition Boundaries of the Hanford Waste Vitrification Plant Project Reference Glass, HW-39.* HWVP-87-V110202B PRMC - 21000039. Pacific Northwest Laboratory, Richland, Washington.

[2]Bates, S.O., D.S. Goldman, and W.C. Richey. 1985. *A Letter Report Summarizing the Sulfate/Redox Relationship to Glass Melting Chemistry and Behavior.* Milestone 020207A. Pacific Northwest Laboratory, Richland, Washington.

Bates, S.O. and W.M. Bowen. 1987a. *Interim Milestone HWVP-86-V1122C - Report on Composition Variation Testing Conducted for the Hanford Waste Vitrification.* HWVP-86-V1122C. Pacific Northwest Laboratory, Richland, Washington.

Bates, S.O. 1987b. *Baseline Milestone HWVP-87-V110202B - Update of Glass Composition Boundaries of the Hanford Waste Vitrification Plant Project Reference Glass, HW-39.* HWVP-87-V110202B PRMC - 21000039. Pacific Northwest Laboratory, Richland, Washington.

[3]LaCourse, W.C., Course Notes, "Introduction to Glass Science", New York State University, Alfred, NY.

bridging oxygens. The P-O bond has an internuclear distance of 1.4 x10^{-10}m while the P=O bond is 1.62x10^{-10}m. The P-O-P bond angle is approximately 140°. P_2O_5 volatilizes at ≈359°C and thus has a strong tendency towards sublimation (Volf; Vogel, 1985). The percent ionic character of the P-O bond is ≈30%.[4] The remaining percentage is covalent. A pure P_2O_5 glass is very hygroscopic where as silica glass is not.

As a result of the strong P-O bond and the differing symmetry of the PO_4 tetrahedra, the solubility of P_2O_5 in silicate melts[5] at lower temperatures is low. On cooling, phase separation or crystallinity results in opacity. The structural differences between phosphate and silicate glasses, thus, result in limited solubility. There is a tendency to form SiP_2O_7 in the SiO_2-P_2O_5 system and to form BPO_4 in the B_2O_3-P_2O_5 system (Vogel, 1985).

Vogel (1985) reports that the high cation field strength of P^{5+} enables it to dominate the unmixing process in mixed systems such as Na_2O-B_2O_3-SiO_2-P_2O_5. It can gather alkali from the already unmixed borosilicate phase into an additional droplet phase rich in P_2O_5. CaO will also enter the P_2O_5 droplet phase and is the basis for the group of glasses called the phosphate opals. Phosphate added to a borosilicate glass by itself phase separates but does not provide deep enough opacity to meet commercial industry standards. The opacity arises from refraction and light scattering between the phases (Flannery et.al.). The phase separation may be liquid-liquid or liquid-crystal. Most commercially available (in U.S.) opal glasses are fluoride opal glasses based on the 3-10 volume percent crystallinity of CaF_2 or NaF. (See section on Fluorine for more details on fluoride opal glassed)

The addition of CaO to the following base glass: 70.7% SiO_2, 17% B_2O_3, 2.5%Al_2O_3, 6.5% Na_2O, 0.3% As_2O_3, 0.1wt% Sb_2O_3 increased the phase separated droplet size when P_2O_5 was held constant at 2.5% (Vogel, 1971). CaO was found to concentrate in the droplets and then cause the secondary precipitation of apatite. A secondary SiO_2 rich phase was also observed to form within the P_2O_5 droplets upon cooling with the addition of 3 wt% CaO. Opacity of the glass was still good (uniform)with a 3wt% CaO addition and the precipitation of apatite. Further increase of CaO leads to crystallization and growth which destroys the droplet phase and formed striae in the glass which renders the glass useless for commercial applications. The opacity of the glass was destroyed by this process. Changes in other properties such as thermal expansion and durability were not evaluated. Vogel also reported that the critical amount of CaO content which would destroy the homogeneous opacity of the glass would likely be different for each base glass composition. The addition of F or OH must be present to form hydroxyapatite.

The solubility of P_2O_5 is not as limited in an aluminosilicate melt as is reported for silicate melts. The situation is quite different. Alumina can go into 4 fold coordination using the net charge from the double bonded oxygen. The AlO_4 tetrahedra have a net negative charge while the PO_4 tetrahedra have a net positive charge. The two structures can form Al-O-P bonds which are similar to Si-O-Si bonds. If the molar ratio of P/Al is near or < 1, it is possible to incorporate much larger concentrations of P_2O_5 into silicate glasses. The exact concentrations are dependent on the base

---

[4]Ibid.

[5]A silicate melt is defined here as a melt containing silica or silica with any combination of alkali or alkaline earths. Alumina is specifically not included.

glass composition. A metal sealing glass with composition of SiO_2 50wt%, Al_2O_3 20wt%, CaO 16wt%, BaO 5wt% and P_2O_5 8 wt% was cited by Volf. However, the presence of alkali in an aluminosilicate glass can compete for the AlO_4 tetrahedra net negative charge, reducing the amount of P_2O_5 which can be incorporated into the glass and causing phase separation. Phase separation may also result in agglomeration of droplets or crystallization. Settling of crystals or a decrease durability may result. If the agglomerated droplets are less dense than the melt they will float to the top reducing melter throughput and producing an inhomogeneous glass.

Silicate glasses prepared with phosphate can exhibit molten separation and form a scum on top of the melt. WV-182 and WV-183 compositions (West Valley) were tested in the Pilot Scale Ceramic Melter Run 19 (PSCM-19) and in the Experimental Ceramic Melter (ECM). The formation of a calcium-rare earth phosphate refractory scum was observed in both tests (Perez, 1985 and Bunnell). Fe-Cr oxide phases were also observed to be part of the scum. Angular rare earth phosphate crystals were seen in a segregated layer produced during the processing of the WV-183 glass. The compositions are shown in Table 4.1.1. Laboratory crucible experiments using WV-182 were only able to produce the scum layer by using simulants and multiple additions to a hot crucible. Oxide and carbonate batches were not observed to form molten salt segregated layers. Another composition, WV-199n (composition not given in Bunnell) which were observed to segregate in the ECM melter but never formed a scum layer even after multiple additions with simulant in crucible tests. The mechanism and/or reason for the separation was not understood or always reproducible on a laboratory scale.

Recent scoping studies in HLW performed by PNL indicate that the separation was caused by the accumulation of sulfate (gall). In crucible studies using oxides and carbonates the WV-182 composition showed phosphate rich segregation after a gall formed at $\geq$ 1.5 wt% additions of sulfate. The gall observed in crucibles contained sodium, phosphorus, calcium, lanthanum, potassium, and sulfur. Spinel was also seen to accumulate in the surface layer. Increased amounts of Al_2O_3 visually increased the amount of scum on the surface of the glass. Based on this evidence, it is thought that during melter processing sulfate accumulates causing the segregation of P_2O_5, CaO, Li_2O, rare earths into a layer in the cold cap. The sulfate can then volatilize and leave behind crystalline calcium rare earth phosphates or other phosphates depending on the glass composition. The occurrence of crystallization is dependent on temperature and concentration of phosphate and other constituents. Segregation also appears to be increased by two other factors which are multiple additions of batch feed to crucibles and larger batch sizes. Multiple additions of feed produce a cold cap for a short time which is more similar to the conditions of the melter than a single batch. This appears to enhance the opportunity for segregation to occur. In small batch sizes there may not be enough of a particular component such as sulfate or phosphate to produce a visible segregation/accumulation on the surface of the melt or at the melt/cold cap interface. A larger batch size may segregate while a smaller batch size does not, even though the composition is the same. A more detailed study of these conditions is necessary to fully understand phosphate segregation.

Melter throughput is reduced by refractory scum formation because of mass and heat transfer difficulties. The layer can act as an insulator making temperature control of the batch difficult. The layer can also slow the diffusion of gases (increasing batch melting time) and reduce the volatilization of components such as cesium (radionuclide which could later possibly be leached out from the separated layer). In the case of a phosphate layer elements can preferentially separate and be removed from the bulk of the melt (e.g. CaO or Nd_2O_3). This can result in decreased durability of the product glass especially if the separation occurs upon cooling in the canister, increased viscosity of the layer or the melt, or may change the conductivity of the layer or the melt.

In scoping studies performed for the High Temperature Melter (HTM), neodymium phosphate crystallized from quenched glasses. In CVS3 studies, a sodium rare earth phosphate crystallized from quenched glasses. The rare earths present in the CVS3 glasses were Nd_2O_3, CeO_2, and La_2O_3. Compositions are shown in Table 4.1.2.

In addition to CaO and rare earth phosphate phase, alkali metal binary phosphate phases which are water soluble can form. In scoping studies performed at PNL, Li_3PO_4 was found to crystallize (by X-ray Diffraction (XRD)) in compositions where Li_2O exceeded 3.0 wt% in glass. Compositions are shown in Table 4.1.3 for these Plutonium Finishing Plant (PFP) Hanford glasses. Durability measurements showed that Li_3PO_4 is very soluble and can be washed out in the prewashes for PCT. Washes should be collected and analyzed so that the PCT data can be corrected or washes should be performed with a nonaqueous solvent. The PFP glasses were still much more durable than the environmental assessment (EA) glass (Jantzen, 1993) even though Li_3PO_4 crystallized from both quenched and CCC glasses (7-day normalized releases < 2.2 g/m^2). Crystallization data from these glasses are summarized in Table 4.1.4. No lithium phosphate crystals were observed optically from quenched glasses. However, after Canister Centerline Cooling (CCC) crystals were observed in an optical thin section of PFP 3.3 with similar morphology as seen by Buechele (1990, 1991). Further analysis is necessary to confirm that these are Li_3PO_4 crystals as $AlPO_4$ also crystallized from the CCC glasses. Other alkali phosphates observed during PNL studies include Na_3PO_4 and $Na_2Ca_4(PO_4)_2SiO_4$ phases which were detected by XRD in LLW glass studies.

A study by Jantzen (1986) on SRL 165 Stage 1 borosilicate glasses detected Li_3PO_4 crystallization when $\geq$ 4wt% P_2O_5 were added to the glasses. Durability measurements made from SRL lithium-borosilicate glasses with addition of P_2O_5 did not show decreased durability. The buffering capacity of the leachate containing phosphate was thought to effect the durability test. The crystalline phase reported by Jantzen (1986) was Li_3PO_4 which has been found to be soluble in water by Buechele (1990) when he tested West Valley waste borosilicate glasses. Buechele et al. recommended omitting the prewashes from the PCT test. It is possible that the Li_3PO_4 was washed out in the preliminary washing steps of the PCT test thereby affecting the PCT results of the Jantzen (1986) study. The West Valley composition which crystallized lithium phosphate is shown in Table 4.1.5. Buechele did not perform XRD on the glasses but evaluated crystallinity optically from thin sections. No Li_3PO_4 was seen visually in quenched glasses which is consistent with scoping study data from PNL. Lithium phosphate appeared after heat treatment of the glasses for either 3 or 100 hours at 700°C. The SRL composition was not reported.

Solubility limits are expected to be sensitive to the glass composition. Glasses containing up to 4.26 wt % P_2O_5, and 0.25wt% CaO, have been successfully processed in PNL melters (PSCM-9). Merrill and Janke (1993) incorporated $\approx$ 9.4 wt% of P_2O_5 into a high alumina ($\approx$20 wt%) borosilicate (30wt% SiO_2, 5wt% B_2O_3) glass with high alkaline earth (10.2 wt% MgO, 4.7 wt% CaO)and low alkali content without salt separation and with good durability (Toxicity Characteristic Leachate Procedure (TCLP) and Product Consistency Test (PCT)).

Needed Studies

The literature data shows composition to be an important variable in the incorporation of phosphate into a waste glass. The crystallization of several phosphate phases has been observed and evidence indicates that cold cap behavior is very important. The presence of Li_2O, CaO, Nd_2O_3, La_2O_3

(and other rare earths) and SO_3 can strongly decrease the solubility of P_2O_5 in borosilicate glasses. Lithium release was found to be increased by the presence of Li_3PO_4. However, more study is need to determine how other phosphate phases affect durability.

Crucible scoping tests showed that molten sulfate segregation can remove phosphate from the glass resulting in the formation of a scum layer. The interaction of phosphate and sulfate is thus crucial to study and appears to be most important in the cold cap. The investigation of cold cap chemistry and behavior (including temperature effects) is necessary to determine and predict phosphate behavior in the melter. Multiple additions of feed and different batch sizes should be evaluated to determine the effects on the phosphate segregation.

Only limited information for a particular composition will be obtained from single component studies. Statistically designed test matrices would help to determine the effect of overall glass composition on the incorporation of phosphate. It is also evident from scoping tests and literature data that setting limits on the incorporation of phosphate for all waste glasses is unwise due to the many variables which influence solubility. Modeling of data will be complicated but necessary to predict the behavior of phosphate.

4.2 Chromate and Chromium Oxide

Glasses prepared with high concentrations of Cr_2O_3 have limited solubility in the borosilicate matrix. If the redox equilibrium of Cr(VI)/Cr(III) in the glass melt reaches the value of 0.01, the alkaline chromates (Cr(VI)) are separated from the melt. The alkaline chromates concentrate as a yellow surface layer where they are relatively soluble in water leading to poor durability characteristics (Sussmilch, 1993). If the solubility of Cr(III) is exceeded, discrete particles of Cr_2O_3 form in the bulk of the melt. Macroscopic platelets with a metallic gloss precipitate may eventually form (equivalent to aventurine glass). Cr(II) can also be present in glass but usually only at high temperatures and under reducing conditions. Spinel formation has also been reported in high chrome glasses. Bates[6] performed a scoping study for Cr (0-2 wt % Cr_2O_3 in glass) for a NCAW waste composition and a 25 wt% waste loading. The waste loading was kept constant at 25 wt% while the amount of Cr_2O_3 was increased. The base composition is shown in Table 4.2.1. This study did not take into account the effects of other components on Cr incorporation into the glass except for Fe. Bates[7] observed an increase in viscosity (≈39°C increase in temperature for a viscosity of 10 Pa.s and a 2 wt% increase in Cr_2O_3) and crystallinity (1-5 wt %) with an increase in Cr concentration but did not see a significant effect on electrical conductivity or glass durability (MCC-1). Cr_2O_3 solubility was < 0.5 wt% Cr_2O_3 in HW39. Spinel ($FeCr_2O_4$) was the only phase observed above 1 wt% Cr_2O_3. Below 1wt% $(Fe, Cr)_2O_3$ and spinel were both observed.

Temperature and time have a significant effect on the Cr(VI)/Cr(III) ratio in the batch. Higher

---

[6]Bates, S.O. and W.M. Bowen. 1987a. *Interim Milestone HWVP-86-V1122C - Report on Composition Variation Testing Conducted for the Hanford Waste Vitrification.* HWVP-86-V1122C. Pacific Northwest Laboratory, Richland, Washington.

[7]ibid.

temperatures favor Cr(III) (Volf) causing Cr(VI) to reduce and liberate oxygen.

$1/2Cr_2O_3 + 3/4O_2 <=> CrO_3$

From the thermodynamic equation:

$\ln K = -\Delta H/RT + I$
where: K=redox equilibrium constant
ΔH=enthalpy
T= absolute temperature
I=constant

It can be seen that as the temperature increases the redox equilibrium constant, K, decreases and the lower oxidation state is favored (Paul).

Longer heat treatment times at medium temperatures ≈ 800°C favor the oxidation of Cr(III) to Cr(VI). However, the ratio of Cr(VI)/Cr(III) is also a function of the activities of all the redox ions in the glass, the activity of oxygen and oxygen ion, the reaction constant (K) and the composition of the glass. The melter feed is likely to experience a wide range of temperatures and residence times from the time it enters the cold cap and exits the melter. If enough chromate forms in the cold cap, it may float on the surface of the melt and cause inhomogeneity in the glass and poor durability. A scoping study performed by PNL showed chromate formation after batch material was heated at 800°C for 24 h for a Hanford waste glass initially containing 6.2wt% Cr_2O_3. This particular glass was made without the visible formation of the orange red chromate phase when melted at 1450°C and quenched. However, when batch material was subjected to the isothermal hold at the lower temperature of 800°C, an orange red phase developed which was readily soluble in water. ICP analysis confirmed the presence of Cr. The composition is shown in Table 4.2.2. Durability releases from the quenched glass was much less than the EA glass. The quenched glass contained a significant amount crystalline Cr_2O_3. The presence of Cr_2O_3 doesn't appear to significantly decrease durability. This is consistent with Bates' work.[8]

The presence of sulfate may also affect the amount of chromate in the glass as it can draw chromate into the molten sulfate layer. In scoping tests performed by PNL, sulfate gall layers were observed to draw Cr and Mo from the glass during melting at 1150°C. When the gall was rinsed with water Cr and Mo were in soluble forms most likely as chromate and molybdate. More testing is necessary to investigate the interactive affects between sulfate and higher concentrations of Cr_2O_3 (> 1 wt%). It is possible that the gall could keep Cr (VI) from reducing at temperatures >1000°C. Thus, Cr would be fixed in its more soluble form. The interaction of sulfate and Cr in the cold cap is thus important to study.

The basicity of the melt is important to the incorporation of Cr. The more acid the glass the more likely the Cr(III) will be present in the glass. Cr(VI) is favored in basic melts (Nath et al.). The following set of equations show this relationship:

---

[8]Bates, S.O. and W.M. Bowen. 1987a. *Interim Milestone HWVP-86-V1122C - Report on Composition Variation Testing Conducted for the Hanford Waste Vitrification.* HWVP-86-V1122C. Pacific Northwest Laboratory, Richland, Washington.

$$1/2Cr_2O_3 + 3/4O_2 \iff CrO_3$$
$$2SiO_{4/2} + R_2O \iff 2SiO_{3/2}O + 2R^+$$
$$2[SiO_{3/2}O]^- + CrO_3 \iff [CrO_4]^{2-} + SiO_{4/2}$$

$$1/2Cr_2O_3 + 3/4O_2 + R_2O \iff [CrO_4]^{2-} + 2R^+$$

where: R = Li, Na, or K... etc.

Cr(VI) is not present as an ion ionically bonded to other oxygen ligands in the glass but as $[CrO_4]^{2-}$ group (Paul, 1982). This was verified by spectroscopic investigations. The addition of TiO_2 and B_2O_3 have been reported to help in the incorporation of Cr into glass (B_2O_3 by Volf, TiO_2 by Sussmilch, and both by Kramer) Both of these components significantly increase the acidity of the glass melt. A study by Paul and Douglas looked at the Cr(III)/Cr(VI) ratio as a function of alkali oxide. Cr(VI) was produced in higher concentrations in K than Na and Li binary silicate glass matrix. In terms of relative basicity, K>Na>Li. Volf states that in the presence of M_2O oxides (where M= Li, Na, or K... etc.) chromate formation occurs above 200°C and reaches a maximum in the temperature range of 800-1000°C.

Kramer looked at the formation of chromate as a function of basicity number (b). The basicity number is calculated by the following formula:

$$b = 119 - \sum_{i=1}^{n} x_i B_i$$

where: b = basicity number

x_i = mol fraction of component i

n = number of cation components in glass

B_i = cation – oxygen bond strength of component i (Sun, 1947)

Kramer found that as the basicity number of the glass increased, Cr(VI)/Cr(III) ratio increased (see Figure 4.2.1). The data shown in Figure 4.2.1 is from a study by Nath et al. Kramer has replotted the data as a function of basicity number. The regression equation was found to be:

$$\log[Cr(VI)/Cr(III)] = -10.51 + 6.66\log b$$

A possible redox equation, reported by Kramer, is:

$$(CrO_8)^{10-} \iff Cr^{3+} + 13/2O^{2-} + 3/4O_2$$

Glasses with 4 wt% soluble Cr_2O_3 have been prepared by the Nuclear Research Institute in the Czech Republic as a fluorescence spectroscopy standard for the Federal Republic of Germany. The compositions of Cr and Cr-4 glasses are shown in Table 4.2.3. Both of these glasses were melted at temperatures > 1500°C. The glasses are high alkali and high temperature in order to dissolve more Cr(III) into the glasses. No durability measurements were made. The 4 wt%

Cr_2O_3 is a high amount of Cr to dissolve in glass based on studies by Bates[9], Hrma et al. (1994a), and Bickford(1986). This amount may not be repeatable with other compositions and appears to be highly dependent on the glass composition and temperature.

Settling of spinel containing Cr in joule-heated melters has been observed by Perez et al. (1986). PNL scoping tests, using the PFP composition shown in Table 4.1.3, have also observed the settling in crucibles of Cr_2O_3 and spinel. However, in LLW glass containing 2 wt% of Cr_2O_3, no settling was observed. The glass did not contain spinel, only Cr_2O_3. The composition is shown in Table 4.2.4. The LLW glass contains very little Fe and thus spinel is not likely to form. This suggests that settling and agglomeration may be more of a problem when spinel or a combination of spinel and Cr_2O_3 are present. The study of settling and agglomeration however, involves many variables and more study is necessary before any firm conclusions can be made.

Volf reports that $CrCl_3$ volatilizes readily and that the addition of Cl should be avoided to glasses containing Cr. The interactive effects of Cr and Cl should be investigated based on this report.

Hrma et al. (1994a) observed Cr to crystallize in spinel and eskolaite (Cr_2O_3) in the 123 glasses studied. Two high Cr glasses were produced for the CVS2 study (Hrma et al., 1994a). CVS2-68 contained 3 wt% Cr_2O_3 and Complexant Concentrate (CC) others (May et al.). CVS2-69 contained 2.4wt% Cr_2O_3 and PFP others (May et al.). Table 4.2.5 shows the major components of glass composition. CVS2-68 and CVS2-69 glasses were compared to CVS2-73 and CVS2-74 glasses, respectively. CVS2-73 and CVS2-74 contained the identical nine major CVS components (SiO_2, B_2O_3, Na_2O, Li_2O, CaO, MgO, Fe_2O_3, Al_2O3, and ZrO_2) but contained Neutralized Current Acid Waste (NCAW)-87 others (Hrma et al., 1994a). The others for CVS2-68, 69, 73 and 74 are shown in Table 4.2.6. The glasses with NCAW-87 others contained 0.09 wt% Cr_2O_3 and 0.21wt% Cr_2O_3 and were respectively compared to CVS2-68 and CVS2-69. The liquidus temperature (Cr_2O_3 crystals) for CVS2-68 and CVS2-69 increased to >1114°C from 816°C and 1066°C respectively. The viscosity also increased from 8 to 12 Pa·s at 1150°C. Durability was not affected. The change in others involved other components besides Cr_2O_3 so that the changes in viscosity may not be attributed entirely to Cr_2O_3.

Schreiber (1983) investigated the interaction of Cr with U in glass. He found that Cr(VI) oxidized U(V) to U(VI). The reaction was reported to go to completion. In addition the presence of Fe(III) protects U(V) from reduction to U(IV) by Cr(II). Schreiber (1981) also reported that Cr and Ti interact in glass. Cr(II) was reported to reduce Ti(IV) to Ti(III). The data was determined in limited studies with ≈ 1 wt% of each redox sensitive component. Results may be different based on glass composition and amount of redox component.

Needed Studies

The literature data shows composition, redox, and temperature to be an important variables in the incorporation of chromium into a waste glass. Investigation in these areas are necessary to predict solubility, oxidation state, and the effects on glass properties. More study is necessary in the area of settling and agglomeration of Cr(III) phases in order to determine if a particular melter type can tolerate a specific amount of spinel and Cr_2O_3.

---

[9]Bates, S.O. and W.M. Bowen. 1987a. *Interim Milestone HWVP-86-V1122C - Report on Composition Variation Testing Conducted for the Hanford Waste Vitrification.* HWVP-86-V1122C. Pacific Northwest Laboratory, Richland, Washington.

Crucible scoping tests showed that molten sulfate segregation can remove chromate from the glass. The interaction of chromate and sulfate is thus crucial to study. The investigation of cold cap chemistry and behavior (including temperature effects) is necessary to determine and predict Cr_2O_3 behavior in the melter. The interaction of Cr and Cl should also be investigated as Cl is reported to increase the volatility of Cr.

Only limited information for a particular composition will be obtained from single component studies. Statistically designed test matrices would help to determine the effect of overall glass composition on the incorporation of chromate/Cr_2O_3.

4.3 Sulfate

Sulfate in glass is used as a refining and homogenizing agent in commercial glass production. It also helps in the dissolution of silica sand (increases melting rate) and by stirring the glass through bubble evolution. (Kim et al., 1992). The refining effect is based on thermal decomposition and starts near 1200°C and is most efficient at 1450°C (Volf). The following equation is applicable to the thermal decomposition:

$$2Na_2SO_4 \Rightarrow 2Na_2O + 2SO_2 + O_2$$

Alkali metal sulfate solubility in glass is poor and usually does not exceed 1wt% (Volf). Molten salt separation occurs, when the glass becomes oversaturated, which can remove alkali from the melt. This may affect the viscosity of the bulk melt but even more importantly sulfate salts are volatile and water soluble. Schreiber et al. incorporated up to 6.5 wt% SO_3 in a West Valley borosilicate glass when excess sulfate was added and an immiscible sulfate layer was present.

In addition, sulfate foam can form at $T > 1400°C$ which reduces melter throughput by forming an insulating layer (Kim et al., 1991). This layer makes temperature control difficult and can trap gases or volatile species such as Cs. Foaming in soda-lime-silica glasses due to sulfate decomposition has been studied by Kim et. al (1991 and 1992) and and Hrma et al. (1994). Sulfate solubility is sensitive to the glass composition, basicity of the melt, oxidation/reduction state of the glass melt, temperature, and melt heating rate. The following reactions (Goldman) describe the incorporation of sulfur under oxidizing conditions as in the flint glasses:

$$SO_2(g) + 1/2O_2(g) = SO_3(g)$$
$$SO_2(g) + 1/2O_2(g) + O^{2-}(melt) = SO_4^{2-}(melt)$$
$$SO_3(g) + O^{2-}(melt) = SO_4^{2-}(melt)$$

From the equations, sulfate solubility increases with the oxygen anion activity in the melt. Thus, sulfate solubility increases with basicity of the melt. The alkali oxides increase basicity so that the solubility of sulphate increases with increasing alkali. In addition, sulphate solubility decreases with increased reducing conditions (decreasing partial pressure of O_2 (pO_2)). Log-log plots of %S (or percent SO_3) in the melt as a function of partial pressure of SO_3 (pSO_3) or $pSO_2pO_2^{1/2}$ should be linear with a slope of one at constant temperature. Plots as a function of pO_2 should also be linear with a slope of 1/2.

Under very oxidizing conditions Schreiber et al. (1987) report that sulfate may dissolve as the pyrosulfate ion by the reaction:

$2SO_2(g) + O_2(g) + O^{2-}(melt) = S_2O_7^{2-}(melt)$

Log-log plots of %S (or percent SO_3) in the melt as a function of $pSO_2p^{1/2}O_2$ should be linear with a slope of two.

Under reducing conditions as in amber glasses the following reactions apply (Goldman):

$1/2S_2(g) + O_2(g) = SO_2(g)$
$1/2S_2(g) + O^{2-}(melt) = 1/2O_2(g) + S^{2-}(melt)$
$SO_2(g) + O^{2-}(melt) = 3/2O_2(g) + S^{2-}(melt)$

The equations show that sulphide solubility increases with increasing reducing conditions. Log-log plots of %S (or percent SO_3) in the melt as a function of $pS_2^{1/2}pO_2^{-1/2}$ (or $pSO_2pO_2^{-3/2}$) should be linear with a slope of one. Plotted as a function of pO_2 the slope should be -3/2.

Schreiber et al. (1987) experimentally demonstrate that the solubility of sulphur (as sulphate or sulfide) forms a V-shaped curve with the pO_2 (see Figure 4.3.1). The study was done using SRL-131 glass. The glass composition is shown in Table 4.5.2. The %S as a function of pO_2 curve goes through a minimum before increasing to the maximum of sulphate or sulphide. The minimum results from the formation of SO_2 and/or SO_3 which are intermediate steps to the formation of sulphate from sulfide. The gaseous SO_2 and SO_3 have limited solubility in glass resulting in a minimum %S in the glass. As the melt temperature increases sulphate solubility decreases and sulphide solubility increases. The region of minimum solubility shifts in the oxidizing direction as temperature increases. This means that less sulphate is soluble as the temperature increases. Sulphate and sulphide are expected to co-exist only over a very narrow range of oxygen fugacities. At 1150°C, the range was found to be 10^{-9} bar to 10^{-11} bar in SRL-131 melts. The only redox state of sulfur incorporated into the SRL-131 melt was S^{6+} (SO_4^{2-}) and S^{2-} (Schreiber et al., 1990). Intermediate redox states such as elemental sulphur, and sulfite ion were not stable in the melt. Polysulfide ions (e.g., S_x^{2-} and S_y^{2-}) were observed when oxidized melts were placed in reducing atmospheres but after time these ions would form sulfide ions (Schreiber et al., 1988).

Reducing sulfate to sulfide to increase sulfur solubility may not be a good idea for joule-heated melters due to the dangers of forming transition metal sulfides such as NiS which are virtually insoluble in glass once formed. These sulfides could settle and agglomerate to form a conductive sludge on the bottom of the melter. This may short the melter electrodes. In Figure 4.3.2, the redox ratio for various components studied in SRL-131 frit at 1150°C as a function of oxygen fugacity is shown. From the position of the S^{2-}/SO_4^{2-} line it can be seen that as conditions are made more reducing, metal sulfides will precipitate from the melt before the metallic phases. Schreiber et al. (1987) recommended a lower limit of 10^{-9}bar for oxygen fugacity. At more reducing conditions the precipitation of metal sulfides was predicted to become a significant problem.

The formation of a sulphate bloom (gall) or segregated layer (often white in color) occurs if the melt is oversaturated with sulfate according to the following equation (Volf):

$2Na_2O$ (from glass) $+2SO_2 + O_2 = 2Na_2SO_4$

In scoping tests performed by PNL, the formation of gall at 1150°C was observed to remove phosphate, chromate, molybdate, boron, alkali and alkaline earths, rare earths, and cesium from

the melt.[10] Li_3PO_4 was observed to crystallize in the gall layer and was confirmed by XRD. Other phosphate phases containing calcium and lanthanum were detected by SEM or energy-dispersive x-ray spectrometry (EDS) analyses (see phosphate section for more detail on the interaction of phosphate and sulfate). Twenty borosilicate glass compositions were studied to examine several parameters believed to influence sulfate solubility. The parameters studied included waste loading, glass basicity, alumina content, and phosphate content. The mass transfer of cesium oxide in one glass was also studied. The five waste loading glasses had increasing sulfate contents from 0.7 to 1.9 wt% SO_3 in glass. The maximum sulfate solubility in these borosilicate-based waste glasses was 1.15 wt.%. However, this limit was dependent on the melt time, surface area to volume ratio, and whether the crucible was covered or open. Gall was first observed on the surface of the third glass in the series with a batched sulfate content of 1.3 wt.%. Glass basicity was estimated using glass compositions (in mole %) and the relative basicity numbering system that uses bond strengths determined by Sun. Basicity numbers for the five waste glasses ranged from 30.08 to 45.14 and had sulfate solubilities range from 0.6 wt.% to 1.3 wt.%, respectively. The solubility of sulfate was found to increase with glass basicity. The effect of alumina on sulfate solubility was studied by changing the glass composition of alumina. The Al_2O_3 content varied from 0.0 wt.% to 15.0 wt.% and had respective sulfate solubilities range from 1.1 wt.% to 0.9 wt.%. The solubility of sulfate was thus observed to decrease slightly with increasing Al_2O_3. The effect of phosphate on sulfate solubility was studied by varying the phosphate in four waste glasses. The phosphate content varied from 0.5 wt.% to 8.0 wt.% and had a corresponding sulfate solubility range from 1.0 wt.% to 1.4 wt.%, respectively. The amount of P_2O_5 which remained in the glass as the phosphate content increased from 0.5 wt.% to 8.0 wt.% was 0.08 wt.% to 6.0 wt.% P_2O_5, respectively. The phosphate was either drawn into the gall or volatilized. Li_3PO_4 crystals were found in the gall. The two highest phosphate compositions exhibited Li_3PO_4 scum formation (3.5 wt% and 8 wt%). The scum was not readily water soluble like the gall. The layer had to be physically scraped from the surface of the glass whereas the gall is easily separates by gently tapping the crucible or by washing with water. Cesium was found to segregate into the gall and to volatilize.[11] This is consistent with what is reported by Stefanovskii and Lifanov. Specifically, sodium sulfate and chloride can segregate and form a molten salt layer which can trap cesium and strontium radionuclides. The decomposition of the molten salts leads to enhanced volatility of the radionuclides.

Sulfate segregation was observed to be a function of temperature in further PNL scoping tests. Gall formation did not occur in several high temperature HLW and LLW glasses which were melted at 1350°C. It is believed that the high temperature promoted sulfate volatilization rather than gall formation. In the LLW glasses segregation was observed at temperatures <1350°C. Further testing of the HLW glasses is in progress to determine if separation occurs at lower temperatures.

Schreiber et al. (1987) observed the formation of a sulfate-rich crystalline layer on the melt at temperatures of 1050°C and lower at oxygen fugacities of 10^{-4} bar. At 1150°C, however the crystalline layer did not form. Sulfur super saturation in oxidized melts was also reported to be possible with subsequent bubble formation (if a surfactant is present, also with foaming) by either increasing melt temperature or by decreasing the oxygen fugacity (redox state) of the melt.

---

[10]Studies by G. Sullivan, H. Li, and MH Langowski.

[11]Sullivan, G. 1994. *High Level Waste Sulfate Study* (student report)

In the sulfate study performed by Bates[12] sulfate solubility was investigated as a function of iron redox. The Fe^{2+}/Fe^{3+} ratio was varied from 0 to 2.5 for 0.5 wt % and 1.0 wt % sulfate in the glass for a NCAW waste composition at 25% waste loading. Sulfate solubility decreased with iron redox ratios > 0.3. Solubility decreased from both 1 wt % and 0.5 wt % SO_3 glass compositions to 0.15 wt % SO_3 in glass. The effects of other components on sulfate incorporation in the glass were not evaluated.

Schreiber et al. (1988) investigated the diffusion properties of sulfur in SRL-131 glass. The diffusion coefficient of the sulfur gases as a function of temperature was expressed as:

$$\log D = -3.08 - (3300/T)$$

where T is in (°K). The diffusion coefficients were found to be the same for both sulfate in oxidized melts and sulfide in reduced melts. This indicated that the rate limited step must be similar for both situations and is likely the diffusion of $SO_2(g)$. In Figure 4.3.3, the temperature dependence of the sulfur diffusion coefficient is compare to the oxygen and water vapor diffusion coefficients. The activation energy for O_2 diffusion was about five times higher than both water, sulphide and sulphate. The latter three had approximately the same activation energy. The temperature dependence was found to fit a Arrhenius type relationship of $D=D_oe^{-E/RT}$, where D=diffusion coefficient, Do = constant, E =activation energy, R=gas constant, and T=temperature (°K). From the figure it can be seen that O_2 and gaseous sulfur diffusion at about the same rate at 1150°C but that at 1050°C gaseous sulfur diffused much faster. Water diffusion is about an order of magnitude faster than gaseous sulfur.

Schreiber et al. (1990) also investigated the interaction of iron and nickel on sulfur redox. Iron did not affect sulfur redox or solubility and sulfur did not affect iron redox under most conditions. In a narrow range of oxygen fugacities of 10^{-9}bar to 10^{-11}bar at 1150°C, high iron concentrations (10wt%) were seen to enhance sulfide solubility. At 10^{-10} bar and 1 wt% total iron sulfur solubility was ≈ 0.06wt% this increased to ≈ 0.6wt% when the total iron was increased to 10wt%. Nickel did not affect sulfur redox or solubility and sulfur did not affect nickel redox.

Needed Studies

Sulfate studies are crucial to understanding the formation of phosphate rare earth refractory scum layers in the melter/cold cap as well as the segregation of radionuclide components such as Cs. The precise conditions under which segregation is promoted or mitigated have not been well studied. Investigations which determine the segregation of sulfate as a function of temperature, time, and composition (emphasis on interaction with other minor components and components found in segregate layers) are necessary. Multiple additions of feed and different batch sizes should be evaluated to determine the effects on the sulfate segregation. The study of the cold cap processes is necessary to fully understand the segregation mechanisms and to develop mitigation strategies. After laboratory scale studies are completed, small scale melter tests would provide further understanding of segregation.

The solubility of sulfate and sulfide as a function of composition, redox, and temperature should

---

[12]Bates, S.O., D.S. Goldman, and W.C. Richey. 1985. *A Letter Report Summarizing the Sulfate/Redox Relationship to Glass Melting Chemistry and Behavior.* Milestone 020207A. Pacific Northwest Laboratory, Richland, Washington.

also be studied. Some melter types may be operated under more reducing conditions and at higher temperatures which should reduce sulfate solubility. Sulfate foam formation becomes favorable at higher temperatures. Conditions under which stable foams form should be assessed as well as possible mitigation strategies. Interactions between sulfate and other components has not been well studied. The possibility that sulfate volatility and/or solubility may be enhanced or reduced through the addition of additives should be investigated so that appropriate modification of glass composition can be determined.

4.4 Manganese

A possible sludge pretreatment process involves the use of $KMnO_4$. This would result in increased levels of MnO in the waste glass. Mn is already present in the waste in significant quantities. NCAW is approximately 2.14 wt% MnO_2. TRAC data also indicates that Mn is present in the Hanford waste in as high as 11.5wt% MnO_2.

Manganese is present in glass as Mn(II) and/or Mn(III). Mn(III) is unstable at high temperatures and is reduced to Mn(II). At 1150°C in a borosilicate melt, Schreiber (1984b) reports about 10% of Mn is present as Mn(III) and 90% as Mn(II). This is similar to redox ratio reported by Lucktong and Hrma for a $3Na_2O7B_2O_3$ melt. Mn(IV) is very unstable and starts to liberate oxygen at 530°C (Volf). Mn(II) glasses are colorless, but oxidize during cooling to faint yellow or brown. Mn(II) has been reported to fluoresce both green and red depending on the glass composition (Kreidl (1945), Linwood et al.). An intense violet color or pink is produced by Mn(III). Though glass compositions in this document, report Mn as MnO_2 it is highly unlikely that there is any Mn(IV) in the glass (This was a convention adopted from SRL). Conventional (in commercial glasses) usage reports Mn and MnO. MnO and Mn_2O_3 are the forms most likely to be in glass. Mn is used as a colorant in commercial brown bottle glasses with Fe or Cr. A typical combination is 4.5 wt% MnO and 1.5 wt% Fe_2O_3.

Solubility of Mn in simple silicate glasses is not reported to be a problem (Nelson et al.). Volf mentions a glass with 20wt% MnO. However, in waste glasses which contain Fe_2O_3 and Cr_2O_3 the formation of spinels containing Mn has been observed (Hrma, et al.(1994a), Bickford et.al.(1986), Turcotte et al., and Buechele et. al (1990)). In CVS2 (Hrma et. al, 1994a), three glasses were prepared with higher Mn. CVS2-55, 56 and 66 contained 2.8, 4.64, and 1.45 wt% MnO_2, respectively. No crystals were detected by XRD in Canister Centerline Cooled (CCC) samples of CVS2-55 and CVS2-56. Spinel was detected in CVS2-66. Optically, CVS2-55 contained corundum crystals which contained Fe and Cr. CVS2-56 did not show any crystals optically except spinel near the crucible walls. CVS2-66 showed spinel dispersed through the sample. In addition SEM/EDS showed Fe,Cr, Ni, and Mn to be in the spinel crystals of CVS2-66. This data shows that Mn may enter spinel or may not. Clinopyroxene ($CaMgSi_2O_6$) can also contain Mn, but clinopyroxene is not expected to limit waste loading. The liquidus temperature is usually < 1000°C as observed in 123 CVS glasses (Hrma et al., 1994a).

Foaming of borosilicate glasses has been reported by Lucktong et al. The reduction of Mn(III) to Mn(II) occurs as the glass is heated causing the liberation O_2. This generation of oxygen can result in foaming.

Schreiber (1983) reports that Mn(III) interacts with U(V) oxidizing it to U(VI). Mn(III) also interacts with Fe(II) oxidizing it to Fe(III). Mn(III) was found to oxidize Fe(II) before oxidizing U(V) (Schreiber, 1984a). The data was determined in limited studies with ≈ 1 wt% of each redox sensitive component. Results may be different based on glass composition and amount of redox

component.

Kramer plotted Mn(III)/Mn(II) as a function of basicity number at 900°C for alkali borate glasses. The plot is shown in Figure 4.4.1. The Mn(III)/Mn(II) ratio was observed to increase with basicity. The regression equation was found to be:

$\log[Mn(III)/Mn(II)] = -5.04 + 2.94 \log b$

A possible redox reaction was given as $(MnO_4)^{5-} <=> Mn^{2+} + 7/2O^{2-} + 1/4O_2$. The data was replotted by Kramer from a study by Paul and Lahiri.

Needed Studies

Mn(III) was observed to increased with basicity in alkali borate glasses. The effect of basicity on Mn redox in borosilicate glasses should be assessed to determine if Mn(III) is present in sufficient amounts to create a stable foam at high temperatures. High MnO compositions should be investigated further for possible foaming problems. The affect of other redox sensitive components (Fe, Cr, etc.) on MnO should also be studied to determine if foaming is generated. The interaction of MnO and spinel (Fe, Cr, and Ni spinels) should be further investigated in order to determine whether MnO can influence the liquidus temperature or the amount of spinel in the glass. The effect should be assessed for its impact on waste loading and solubility.

4.5 Titanium Dioxide

Titanium has recently become of interest due to the possible use of crystalline silico-titanates (CST) as the ion exchange material for cesium removal.[13] This would likely increase the amount of TiO_2 in HLW Hanford glasses through the addition of the CST recycle. Currently there is no constraint for titania as the waste itself has not been reported to contain significant amounts of TiO_2 (May and Watrous, 1992 and Boomer, 1993). DWPF currently has a waste solubility limit of <1wt % TiO_2 in glass (Bickford, 1990).

Ti can be present in glass in oxidation states of 2,3,4. Ti(IV) is preferred while 3 and 2 form under reducing conditions. Ti(III) also forms at temperatures above 1000°C. Schreiber (1982) investigated the redox pair Ti(III)/Ti(IV) in SRL 21 and SRL 131 borosilicate glasses at 1150°C. About 5% of the total titanium concentration is Ti(III) at $\approx 10^{-14.5}$bar O_2 partial pressure. Ti(II) occurs only rarely in glass. Ti(IV) can be in coordination numbers of 4, 6, and 8. Studies (Volf) have shown that 4 and 6 can exist simultaneously in glass. The presence of fluorine promotes a coordination of 6 and the formation of $[TiF_6]^{2-}$. Higher amounts of F are reported to be retained in the glass when TiO_2 is present. However, considerable volatility of titanium can also occur in the form of TiF_4 when F is present in the glass (Volf). TiO_2 does not volatilize up to 1640°C if F is not present. Titanium oxygen compounds in glass are $[TiO_3]^{2-}$ and $[TiO_4]^{4-}$(Volf).

Ti is classified as an intermediate glass former. It is readily meltable and improves the acid resistance of glass. TiO_2 combines with P_2O_5 to form very stable glasses. Titania forms a series of very low thermal expansion glasses with SiO_2 from 5 to 11 wt% of TiO_2. The solubility of

---

[13]Goheen, R.S. and D.E. Kurath. 1994. *Conceptual Study of In-Tank Cesium Removal using an Inorganic Ion Exchange Material*, TWRSPP-94-015. Pacific Northwest Laboratory, Richland, Washington.

titanium dioxide is sensitive to the glass composition. The solubility of TiO_2 increases in silica glasses as the amount of alkali and alkaline earth metals are increased. K_2O is particularly effective at increasing the solubility of TiO_2. Up to 20 wt% of TiO_2 can be added to a soda-titania-silica glass. Rutile, anatase or titanium silicates crystallize in the glass if solubility limits are exceeded. Zinc, Mg, Al, and B decrease the solubility of Ti in silicate glasses. Microcrystallinity forms as these components increase (Volf).

In Na_2O-TiO_2-B_2O_3-SiO_2 up to 45mole % of TiO_2 can be incorporated if 30mole% Na_2O is present. Replacement of SiO_2 with TiO_2 in the sodium borosilicate system results in improved chemical durability (Volf).

TiO_2 is used as a nucleating agent in lithium and magnesium aluminosilicate systems for the production of glass ceramics. TiO_2 is effective due to its poor solubility in alumina rich glasses. About 3-4 wt% TiO_2 is used to nucleate glass ceramics in the Li_2O-Al_2O_3-SiO_2 system and 8-10 wt% in the MgO-Al_2O_3-SiO_2. Rutile crystallized in the Pamela melter outlet channel when glasses with 1.55 wt% TiO_2 and 20.68 wt% Al_2O_3 were melted. The bottom drain plugged several times and rutile crystals formed in the glass which had remained in the outlet channel for an amount of time (Ewest and Wiese). The glass composition is shown in Table 4.5.1. This glass was designed to be processed with a viscosity of 12 Pa·s at 1150°C which is higher than the 4 to 6 Pa·s range recommended by SRL and PNL. The glass was redesigned to have a viscosity of 6 Pa·s and TiO_2 was removed from the composition.

In SRL glasses, when the solubility limit for TiO_2 in lithium aluminoborosilicate waste glasses was exceeded, $LiAlSiO_4$ crystallized. Since TiO_2 is used as a nucleating agent in lithium aluminosilicate systems this is consistent. Ferrite solubility also decreased with increase in TiO_2 (Plodinec 1979 and 1980). Only a slight decrease in viscosity was observed by Plodinec (1979) in the 1150°C range from 0 to 11wt% TiO_2.

Thus, in waste glasses which contain significant amounts of alumina, the titania solubility is expected to be extremely limited. Scoping studies are necessary to provide data for property composition model development and to determine precise limits for glass compositions. Based on the literature data, titania is much more soluble is systems without the presence of alumina. However, other components may also affect the solubility of titania. In particular, boron interaction with titania should be investigated. B_2O_3 is reported to facilitate nucleation in titanium containing glasses (Volf).

Extensive liquid-phase separation is reported by Galakhov (1987 and 1988) in the Li_2O-Al_2O-TiO_2-SiO_2 system in the temperature range of 700-800°C. The addition of 2-3 mole percent titania to Li_2O-Al_2O-SiO_2 system resulted in phase separation. Phase separation can affect crystallinity and durability of the waste glass and should be investigated when looking at increased amounts of titania.

Schreiber (1982b) investigated the effects of titanium on uranium incorporation into glass structure. He found that Ti(III) reduces U(V) to U(IV). The reduction of U(V) to U(IV) was observed to go to completion. Ti(III) and U(V) were not found to coexist. Titanium was found to increase the solubility of uranium in SRL-21 and SRL-131. Compositions for SRL-21 and SRL 131 are shown in Table 4.5.2. Without titanium and under reducing conditions (-log (fugacity O_2) ≈ 12.5 about 9wt% of UO_2 was soluble in both glasses. The amount increased to 11wt% for SRL-21 and to 13wt% UO_2 in SRL-131. U(IV) solubility thus, increased with the addition of

titanium. Under oxidizing conditions (-log $fO_2 \approx 0.7$) the solubility was 40wt%. This was attributed to the fact that U(VI) and U(V) are the species present in the melt and their solubility being higher since it is usually UO_2 (U(IV)) which precipitates out from the glass.

Volf cautions about the behavior of titania during melting. Due to its density of 4.26 it may separate during melting and settle to the bottom of the furnace. However, the meltability of glasses also improves because titania forms a eutectic with SiO_2 and Na_2CO_3. In addition, the deformability of Ti(IV) is high and also contributes to the meltability. Viscosity is decreased in the high temperature range when TiO_2 is substituted for silica. However in the working range the glass is shortened.

Needed Studies

The solubility of titania has been reported to be a strong function of glass composition. Investigation of Hanford HLW waste compositions to determine the solubility of titania should be performed. The effect of Al, B, F, and the alkali on Ti solubility should be studied. Mg and Zn should be studied if glass compositions are predicted to contain significant amounts of either component. The relationship between titania and glass properties should also evaluated with particular emphasis on viscosity.

4.6 Bismuth

Currently there is no CVS constraint for Bi. Bi is reported to be a major component in wastes generated from the $BiPO_4$ process. Specifically the TRAC data indicates that B, BX, BY, T, TX and TY SST tank farms contain significant amounts of bismuth. In addition, some C tanks and U-110 tank also contain significant amounts of bismuth (Boomer, 1993). The CVS study has been expanded to include bismuth for this reason. Bismuth solubility in borosilicate glasses may have some limit based on its effect on properties, but this limit may be eclipsed by the constraint for phosphate (or another component) present in the waste glass.

Bi_2O_3 is a conditional glass former like Al_2O_3. It forms a bulk glass only in a binary or in multi-component mixtures with other oxides. However, Bi has properties in glass most similar to Pb due to their similar electronic configurations and almost identical weights (Volf). The most stable oxidation state of bismuth in glass is Bi(III). Bi(V) is unstable and Volf reports that only Bi(III) is encounter in glass. Heynes and Rawson reported the maximum content of bismuth which forms a glass with silica to be 84 wt%. Speranskaya et al. (1968) report a lower amount of 65 wt% Bi_2O_3 maximum (35wt% SiO_2) forms under conventional glass-forming conditions. The high refractive index of high bismuth glasses has made them useful in reflecting highway paints (Kreidl, 1983).

Kupfer (1978b) vitrified 1st and 2nd cycle $BiPO_4$ simulant wastes. The simulant compositions are shown in Table 4.6.1. The glasses contained up to $\approx$ 13.0 wt% Bi_2O_3 (40% waste loading). Glasses were clear dark green-brown and durable when tested by the Soxhlet leach method.

Kupfer and Palmer (1980) prepared glasses using simulated 3rd cycle bismuth phosphate process waste simulant. Simulant containing up to 37.6 wt% Bi_2O_3 (11.3 wt% Bi_2O_3 in glass, 30% waste loading) were vitrified. The simulant composition is shown in Table 4.6.1. The glasses were transparent when quenched, but bismuth glasses devitrified when cooled slowly at a rate of 15°C/min, from 1100 to 400°C. No bismuth crystalline phases formed. The devitrification was

likely caused by the high amounts of P_2O_5, La_2O_3, Cr_2O_3 and MnO present in the glass and not by bismuth. The primary crystallization phase was tridymite. Smaller amounts of Cr_2O_3, spinel, and $LaPO_4$ were also identified in the slowly cooled sample.

Bismuth glasses are reported to strongly attack refractory materials and melt at relatively low temperatures (Volf). In a study by Palmer tin oxide, molybdenum, and inconel 690 electrodes were corroded more by $BiPO_4$ glasses than other glasses which did not contain bismuth.

The addition of Bi_2O_3 is predicted to decrease the viscosity of glass similarly to PbO, but may improve the durability. During the preparation of high bismuth CVS3 glasses the addition of bismuth was observed to decrease the melting temperature. In addition, under reducing conditions bismuth glasses tend to form a metallic mirror on the surface of the glass (Volf).

Needed Studies

It is important to study the effects of bismuth in borosilicate glasses because significant impacts on corrosion of refractories, electrical conductivity, and viscosity are reported in the literature. The processing of waste glass, the development of models based on composition, and waste loading may be affected. The relationship between bismuth, glass composition, and glass properties has not been well studied for waste glasses and should be investigated. Interactive effects may exist and assessment of glasses for crystallinity and segregation involving bismuth should be performed. The effects of bismuth on the corrosion of refractories and electrodes should be investigated to determine if the amounts in Hanford waste glasses will produce an adverse impact.

4.7 Uranium

Uranium is not present in glass as U_3O_8. U_3O_8 is a binary oxide expressed as $UO_2 \cdot 2UO_3$ (Volf). However, the convention uses U_3O_8 when reporting U concentrations in glass. Uranium is usually present in glass in the tetravalent or hexavalent state but can form oxidation states of 3, 4, 5, 6 in glass. Schreiber et al. (1982a) has studied the redox properties of uranium (typical quantities of < 1 wt% in glass) in SRL frits. Schreiber (1983) found U(IV), U(V), and U(VI) to be the most important in molten glass. U(VI) was observed to be quite soluble (≈ 40 wt% UO_3) in the glasses tested, but U(IV) had a limited solubility (≈ 9wt% UO_2). U(IV) precipitated readily as UO_2 (Schreiber, 1983). Redox state thus strongly affected the solubility of U in borosilicate glass. Uranium interaction with redox sensitive components is shown in Table 4.7.1. A summary of interactions with Ti, Cr, and Mn are discussed in the respective sections of this report. Ce was found to oxidize U(V) to U(VI) but this reaction was only partially complete. The presence of Fe(III)-Fe(II) redox couple acts as a redox buffer towards uranium system minimizing the effects to U(V) (Schreiber et.al., 1985). The solubility of U is thus a function of redox state, concentration of selected other redox sensitive components, temperature, and oxygen partial pressure. Veal also reports that U solubility may be a function of alkali content as well.

Conflicting reports of the effect of uranium on glass durability are present in the literature. Volf reports that uranium dioxide dissolves to form uranyl salts (UO_2^{2+}), when present in acidic glasses, and that uranium salts do not improve the chemical durability of glass. Feng, however, found a slight improvement in the durability of glasses with the addition of small amounts of UO_2 (≈0.56wt%) and ThO_2 (≈3.58wt%) in the study of West Valley nuclear waste glasses. Schreiber et al. (1985) studied the MCC-1 durability from SRL-131 glass (see Table 4.5.2) containing 5 to 6 wt% U_3O_8. No difference in leachability of uranium was observed based on uranium redox state (≈18 g/m^2 normalized uranium release). U(IV), U(V) and U(VI) were all observed to leach at the

same rate and amount. The species found in the solution was U(VI) suggesting that U(IV) and U(V) were rapidly oxidized at the glass leachate interface. A yellow surface film enriched in uranium formed on leached glasses. As uranium concentrates at the surface, the crystalline phase of schoepite ($UO_3.2H2O$ or $UO_2(OH)_2.H_2O$) formed. The layer was not protective and was observed to be brittle and to spall off easily. The amount of uranium in the leachate was observed to be a function of how rapidly schoepite formed and the mineral's equilibrium with the solution. Both are functions of time and temperature. Schreiber et al. (1985) also reported that the solubility of uranium in solution would be expected to change under different Eh and pH conditions. U(IV) would be favored under reducing and lower pH conditions. U(IV) is more insoluble than U(VI) and therefore the solubility of uranium in the leachate would be expected to decrease. This is consistent with the Eh-pH diagram (Pourbaix) for uranium which shows a larger insolubility region for UO_2 or U(IV) than for U(VI).

Interactive effects may exist between U_3O_8 and P_2O_5. However, Schreiber (1982c) investigated the solubility and redox chemistry of U_3O_8 in two sodium aluminophosphate glasses. Compositions are shown in Table 4.7.2. He found similar behavior exhibited in these glasses as in borosilicate glasses. U(IV) was less soluble that U(VI) and precipitated as UO_2 when the solubility limit was exceeded. The redox conditions influenced the solubility significantly. At low oxygen fugacities ($\log fO_2 = -6$), UO_2 precipitated in the melt at equilibrium temperatures of 1250°C, 1350°C, and 1450°C. Up to 15 wt% U_3O_8 was tested and found to be soluble as U(VI) and U(V) in the aluminophosphate glass in air ($\log fO_2 = -0.7$). Higher amounts than 15wt% U3O8 were not tested. No segregated phosphate phases were reported, however, the glass did not contain CaO, Li_2O, or the rare earths. It should be noted that $Ca_3(PO_4)_2$ which has been reported to crystallize from sodium borosilicate glasses (Vogel, 1971), containing small amounts of Al_2O_3, does not necessarily crystallize from higher amounts of Al_2O_3 glasses (Merril and Janke). Therefore, the formation of a uranium phosphate may still be possible in a borosilicate glass. Farges et al. reported that U(IV) is accommodated in apatite ($Ca_5(OH, F)(PO_4)_3$), zircon, thorite, titanite, and uranium oxide natural minerals. The potential for U and P containing crystals should be explored based on this evidence.

Volf reports that U reacts with fluorine to form gaseous UF_6 (at room temperature) so that the presence of F and U in glass is undesirable. Farges et al. were unable to detect any U-F or U-Cl complexes by EXAFs in the silicate glasses they tested. However, the amounts of $UO_2 < 1$ wt% and F, Cl < 2.5 wt%. Larger amounts are contained in some Hanford wastes and may produce different results (see TF-C and TF-DST wastes in Table 5.0.1). The interaction of U and halogens should be studied to ascertain whether complexes form in the glass which may promote volatility such as UF_6.

McCarthy and Davidson investigated the crystalline phases which crystallized from PW-4b material shown in Table 4.7.3. Simplified subsystems containing 2 to 10 of the components of PW-4b were used to systematically study the formation of phases. The ratios of components were kept the same subsystems as in PW-4b. Uranium was found to form fluorite (structurally similar with CeO_2) solid solutions in powders heat treated in the 750°C to 1350°C temperature range. The fluorite solid solutions formed in the Ce-Nd-U, Ce-Nd- Fe-Mo- Zr- U, Ce-Nd-Fe-Mo-Zr- Ni-Sr-U, and Ce-Nd-Fe-Mo-Zr- Ni-Sr-U-Cs subsystems. The formation of perovskite solid solutions was also thought to contain U because $SrUO_3$ (perovskite) is know to exist.

In a review by Veal et al. on actinides in silicate glasses, the solubility and possible structure of U is discussed. The solubility of U(IV) is reported to be < 10wt% in borosilicate glasses and to be relatively independent of alkali concentration. U(VI) is reported to have a much higher solubility

of 20 mole% in sodium trisilicate glass and 25 mole% in sodium disilicate glass. The amount of alkali appears to increase the solubility of U(VI). U(IV) can be in either 6-fold or 8-fold coordination (Veal et al.). U(V) is in octahedral coordination with tetrahedral compression (Schreiber, 1985). U(VI) prefers 6-fold coordination (Veal et. al and Schreiber, 1985). The lower solubility of U(IV) is attributed to the fact that it does not readily substitute for Si(IV) due to the large ionic size mismatch[14] and because Si(IV) is in 4-fold coordination. U(VI) in contrast was theorized to have a higher solubility because it could form a layered structure as shown in Figure 4.7.1. Layers of uranyl are dispersed between layers of SiO_4 tetrahedra and are weakly bonded by alkali. Extended X-ray Absorption Fine Structure (EXAFS) studies of U(VI) showed a high concentration of U neighbors surround each U in the glass suggesting a strong tendency for U(VI) to form clusters. Similar studies of U(IV) did not show the same tendency to cluster.

In uranium single component study by Bates, MCC-1 data showed an increase in normalized release of U from 2.4 g/m^2 to 5.1 g/m^2 as U_3O_8 increased from 0.15 to 8 wt%.[15] Releases for Si, B, Li, and Na were below the EA glass values by more than 50% and did not vary more than 2 g/m^2 over the range tested. The NCAW simulant waste loading in the test glasses was 25 wt%. No evidence of uranium phase separation was observed over the uranium concentration range tested. In addition, the amount of Fe in the chromite spinel phase [Fe (Fe, Cr)$_2O_4$] was observed to decrease with an increase in U_3O_8. Above 2 wt% U_3O_8 in glass, the chrome crystallite phase was thought to be Cr_2O_3. No change in the properties of viscosity or electrical conductivity were observed over 0 to 8 wt% additions of U_3O_8 in glass. The effects of matrix components were not studied.

Needed Studies

The interaction of U with Ce, Nd (and other rare earths), Fe, Mo, Zr, Ni, Sr, U, Cs should be studied to determine the possibility of the formation of $U_{fluorite}$ and $U_{perovskite}$ solid solutions in glass which may limit waste loading. Recently, estimated compositions include wastes with as high as 23.7wt% U_3O_8 (See assessment section). Compositions with > 8 wt% U_3O_8 should be studied to ascertain the effects of U on glass properties in high concentrations. Glass composition effects on U solubility should be evaluated (e.g., alkali, F, etc.). In addition, the substitution of Nd for U should be evaluated to determine if Nd effects glass properties in the same manner as U.

The effect of redox on U solubility should be expanded for in Hanford high level compositions which may have higher amounts (>1 wt%)and combinations of Mn, Cr, Ce, Ti, and other redox sensitive components than reported in the literature. The effect of higher temperature should also be determined as this would favor increased amounts of U(IV).

4.8 Chlorine and Iodine

Chlorine and iodine have a limited solubility in borosilicate glasses. In a commercial glass, such as Pyrex, Cl usually does not exceed 0.1 wt% . For a soda-lime-silica glass of composition, 75 wt%

---

[14]Si(IV) ionic radius 0.41Å, U(IV) ionic radius 0.89Å to 1.00Å (depends on coordination)

[15]Bates, S.O. and W.M. Bowen. 1987a. *Interim Milestone HWVP-86-V1122C - Report on Composition Variation Testing Conducted for the Hanford Waste Vitrification.* HWVP-86-V1122C. Pacific Northwest Laboratory, Richland, Washington.

SiO_2, 9.2 wt% CaO, and 15.8 wt% Na_2O at 1400°C approximately 1.4 wt% Cl was soluble (Volf). Unlike F, which significantly substitutes for O in a SiO_4^{4-} tetrahedra, Cl and I do so only in a very limited quantity. Volf attributes this to the similarity in effective radius between F^-, OH^- and O^{2-}. It is likely then the volatility of F < Cl < I if ionic radius is the only factor considered. The data from PSCM-23 supports that volatility of F < Cl (DF's=> 6.6 Cl, 9.2 F). However, data on I volatility was not available as I was not present in the melter feed.

Chlorine volatilizes in significant quantities and can also increase the volatility of other components such as F (Volf) and Cs (Spalding). Chlorine has been reported to form a molten salt layer with sulfate over silicate melts. Cesium and strontium radionuclides have been reported to concentrate in this layer. The phase decomposition of the sulfate/chloride layer leads to the volatilization of Cs and Sr (Stefanovskii and Lifanov). Thus, Cl can enhance the volatility of radionuclides. Chlorine in the offgas stream also increases the corrosion of piping and other metal parts. Severe corrosion of offgas metal parts occurred during LFCM2 from Cl and S containing compounds (Goles and Sevigny). Furthermore, the potential for a steam explosion from the presence of molten salts in liquid-fed melters has been reported by Goles and Sevigny. It was not always clear from the literature what species of Cl or I volatilized. In many cases no attempt was made to determine the species. In the case of Cl, Na or Cs were often present in corrosion products or collected particles along with Cl. Cl can volatilize as NaCl, CsCl, Cl_2, HCl. Iodine was reported to volatilize as gaseous I_2 (Spalding, Button et al., Volf, Scott et al.).

NaCl is added to commercial glass batches because it decreases the melt surface tension and increases melting rate through better wettability of batch particles. The amount is usually < 2wt%. NaCl combines with Na_2CO_3 to give a eutectic at of 838°C, 213°C below the melting temperature of soda. The eutectic fluid reacts faster with SiO_2 resulting in intensified melting. NaCl and KCl have been used as refining agents in commercial glass melting. The refining effect occurs intensely between 1100 to 1200°C and liberates gaseous HCl by the following reaction:

$$2NaCl + H2O + SiO_2 \Rightarrow Na_2SiO_3 + 2HCl \quad \text{(Volf)}$$

Above 804°C the volatilization of NaCl occurs with an intensification at ≈ 1300°C (Volf). However, as shown by Spalding (1994), significant amounts of Cl can volatilize in the 800 to 1000°C temperature range. In commercial melting NaCl has also been used to adjust the thickness of the cold cap. By increasing NaCl the thickness was reduced and by decreasing it was increased.

It has been suggested that photochromic glasses might provide important clues as to increasing the amount of chlorine or iodine in glass. Increasing the solubility of Cl in glass may help reduce Cl volatility by reducing the thermodynamic driving force of Cl diffusion to the melt service. Since Cl volatilization occurs (largely from the cold cap) during melting and is a function of the melt and vapor properties, it is unlikely that the crystallization of silver halides as in commercial photochromic glasses (which occurs later during cooling the glass) will reduce Cl volatility during melting. Araujo et. al states that silver halide precipitation from many glasses is not possible and that it is largely a function of having high solubility in the glass at high temperature, but low solubility of silver halides at low temperature. It would probably be necessary to have small evenly dispersed halide crystallites present in the melter at melting temperature to reduce volatility. Typically photochromic glasses use a mixture of halides to produce small silver halide crystallites which are precipitated from a homogeneous glassy matrix (Paul). The amount of Cl is approximately < 2 wt% the average being less than 1wt%. The average crystallite size is about 100 Å. Ag is usually less than 0.7wt%. Activated by u.v. radiation, silver separates from the halogen induces a darkening color change. After the source of light is removed, silver recombines with the

halogens and the glass is again transparent. Br, F, and I can be used as well Cl to form the metal halide compound. Polyvalent oxides of As, Sb, Sn, Pb, Cu, and Cd can increase the sensitivity and photochromic absorbance. The total halogens does not usually exceed 5 wt%. Thus, the amount of Cl in photochromic glasses is not much more than what is typically present as an impurity in commercial glasses (i.e. <1 wt%).

A potential problem also exists with the use of Ag. Silver ion readily reduces to silver metal leading to increased risk for the settling of Ag metal into a conductive sludge on the bottom of the melter. Schreiber et al. (1984b) reports that at 1150°C for a borosilicate glass SRL-131 (@ partial pressure of air), about 80 wt% of the Ag is present as metal and 20 wt% as Ag(+1 oxidation state). The factors which should be considered are electrical conductivity increase from the addition of Ag, the amount of AgI or Ag metal crystallinity that could be tolerated by the melter (i.e., primarily the amount of settling in melter which would not inhibit processing), durability, viscosity increases from the precipitation of crystallites, liquidus temperature, volatility, and environmental concerns. Scoping studies would be necessary to determine the feasibility of using photochromic composition to incorporate Cl.

Chlorine has also been used to cause opalization when added in amounts of > 2 wt% KCl. Chlorine can react with Ca and P to produce apatite. There are two types of opal glasses. These are spontaneous and heat treated. Most commercial opal glasses are heat treated to grow the crystallites which cause opalescence. Spontaneous opals form crystals upon cooling. Chlorine volatilization occurs during melting and is a function of the melt and vapor properties. It is unlikely that opacifying the glass will reduce Cl volatility (largely from the cold cap) during melting since opalization of the commercial glasses occurs later during cooling or reheating. It would probably be necessary to have small evenly dispersed apatite crystallites present in the melter at melting temperature to reduce volatility. However, scoping studies need to be performed to determine the feasibility of using apatite to trap chlorine. The factors which should be considered are the amount of apatite crystallinity that could be tolerated by the melter (i.e., primarily the amount of settling in melter which would not inhibit processing if apatite were crystallized in the melter), thermal expansion mismatches which might cause cracking during cooling, durability, viscosity increases from the precipitation of crystallites, liquidus temperature, volatility, and environmental concerns. Furthermore, the addition of Ca and P to produce apatite may cause the formation of a Ca rare earth phosphate scum layer which was reported during the PSCM-19 melter run (Perez et al., 1985).

Some evidence exists that B may help to increase the solubility of Cl. Button et al. observed that Cl could substitute for O in lithium borate glasses. Up to 14 wt% Cl was soluble in lithium borate glasses (12.7 mol% $(LiCl)_2$-23.4 mol% Li_2O-63.6 mol% B_2O_3) melted at 940°C. Cl due to its valency of -1 is non-bridging when it binds to B. The O/B ratio was observed to decrease as Cl was added to the glass. However, the reduction in Cl vaporization losses is attributed by Button to be due to lower melting temperatures and shorter soak times in the lithium borate system when compared to silicate glasses. Araujo et al. theorized that nickel chloride complexes could form in potassium aluminoborosilicate glasses based on color changes observed when Ni was present in the glass. It is possible that Ni might therefore affect Cl solubility. However, the glasses investigated had a starting amount of 1 wt% Cl and the amount of NiO was 0.25 wt% so the affect may be for small concentrations. It was not clear from the paper if the presence of NiO actually increased Cl solubility only that color changes were observed which were attributed to chloride complexes of Ni.

Chlorine DF's from PNL joule-heated melters (runs PSCM-1 thru 8 and LFCM 4, 6, 7) ranged from 1.5 to 6.6 and are listed in Table 4.8.1. The DF's show that Cl is very volatile and losses

from the melter were high. About 83 wt% of submicron particulate compositions from PSCM-4 consisted of NaCl. Offgas line deposits formed during melter idling periods contained 20-90 wt% NaCl and as high 30 wt% S. The melter runs were performed under a variety of conditions (e.g., feed rate, plenum temperature, offgas flowrate, pH, etc.) with feeds of different composition. This may account for the variability of the DF's. Offgas deposits containing alkali borates, chlorides, fluorides, chromates and sulfates have also been reported by Jantzen (1991) during the operation of the Scale Glass Melter (SGM). Jantzen (1992) also investigated the presence of compounds in a DWPF canister filled during Campaign 10 of the SGM. Sodium and potassium chlorides, sulfates and borates were found on the interior canister walls, neck and shoulder above the melt line Thus, these compounds appear to be volatilizing during the pouring of the glass from the melter as well as during vitrification.

Iodine DF's have not been measured in most PNL melter runs because the melter feeds did not contain I or was at such a low concentration that I was not detected in the offgas (NCAW waste target was 4.5×10^{-6} wt% I- or 1.25×10^{-6} wt% I- in glass). Perez and Nakaoka reported an iodine DF of 1.3 for vitrification in PSCM (run number not specified). LFCM-8 had a iodine DF of ≈ 1.[16] The as batched concentration of iodine was 0.01wt% in glass, but based on the reported DF very little iodine ended up in the glass. Goles and Nakaoka recommend for a HWVP design specification for I a DF of 1. Scott et al. report that nearly all volatile iodine out-gasses in reprocessing steps that occur prior to calcination or vitrification and this may be why there is not an abundance of literature on the volatility of iodine from glass. Iodine is released primarily as I_2 gas. However, Scott et al. state that Hg has been observed to volatilize as Hg_2X_2 compounds, where X is a halogen. Scott also present a discussion of I- recovery methods (using scrubbers) from the offgas based on the reviews of Holladay (1979) and Burger et al. (1983). Knox and Farnsworth studied the volatility of I-131 from spray calcined feed. About 31 wt% of I-131 volatilized at 800°C.

Needed Studies

Solubility limits for Cl and I are dependent upon several factors including glass composition and temperature. Scoping studies would need to be performed to obtain more precise information about Cl and I solubility in glass.

The interactive effects between Cl and S, F, Cr, P, Sr, and Cs should be studied to determine effects on glass properties, segregation, and volatility. Studies should also evaluate if other components are affected by the presence of Cl. Investigations should consider additives which may reduce Cl volatility or increase Cl solubility. The effect of temperature on Cl solubility, segregation, and volatility should also be evaluated. If the formation of a crystalline compound is investigated as a possible method for increasing Cl solubility, settling and agglomeration of crystals should be evaluated in crucibles and small scale melters. Effects on electrical conductivity should also be evaluated. Multiple additions of feed and different batch sizes should be evaluated to determine the effects on the chloride segregation. The study of the cold cap processes is necessary to fully understand the segregation mechanisms and to develop mitigation strategies. After laboratory scale studies are completed, small scale melter tests would provide further understanding of segregation.

---

[16]Perez, J.M., L.D. Whitney, W.C. Buchmiller, J.T. Daume, and G.A. Wyatt. 1994. HWVP Pilot-Scale Vitrification System Campaign - LFCM-8 Summary Report, PHTD-K963, Rev. 0. Pacific Northwest Laboratory, Richland, Washington.

Iodine studies should determine if there are any additives which might increase I solubility in glass and reduce its volatility. The effect of temperature on I solubility and volatility should also be evaluated. If the formation of a crystalline compound is investigated as a possible method for increasing I solubility, settling and agglomeration of crystals should be evaluated in crucibles and small scale melters. Effects on electrical conductivity should also be evaluated.

4.9 Fluorine

Fluorine has an effective radius which is close to oxygen and the hydroxyl group, OH^-. It can partially substitute for either of these in glass. The monovalent, F^-, cannot, however, form bridging bonds between silica tetrahedra and therefore decreases melt surface tension and viscosity in the glass. The behavior of fluorine in glass is substantially different than other halogens (e.g. Cl and I) because the ionic radii of other halogens are larger and therefore do not readily substitute for O. The behavior of other halogens (i.e., other than F) in glass should not be inferred from the behavior of F.

F is used as a refining agent in commercial glass melting and usually added with sulfate. F decreases the melt surface tension and increase melting through better wettability of batch particles. Fluorine increases the diffusion of bubbles by decreasing melt viscosity and surface tension. A typical refining mixture is 0.7-0.8 wt% CaF_2 by wt of glass, 0.3-0.5 wt% NaCl by wt of batch., 0.5 wt% Na_2SO_4 by wt of glass. Experimental evidence by Volf shows that CaF_2 forms NaF in the melt. NaF combines with Na_2CO_3 to give a eutectic mixture with a melting point of 700°C. The fluid eutectic reacts faster with SiO_2 intensifying melting.

Fluorine has a limited solubility in glass. Fluorine is soluble in silicate glasses at high temperatures, but separates in the form of droplets or crystals at lower temperatures. If the solubility limit for fluorine is exceeded in a soda-lime-silicate glass, opacity of the glass results from the formation of compounds of NaF or CaF_2. A group of silicate based glasses called opal glasses is based on this phenomena. Opal glasses based on F generally contain 3-5% fluorine and are based on the soda-lime-silica system (Flannery et al.). In silicate glasses containing phosphate and calcium, fluorine can cause the precipitation of apatite. Most clear commercial glasses have at most 0.6% fluorine.

The addition of elements which can increase coordination number (y), such as Al (y=4 or 6) Ti (y=4, 6, or 8) and B(y=3 or 4), can increase the solubility of F in glass. This is due to the fact that screening around the cation is satisfied by the remaining O^{2-} anions after some have been replaced by F^-. In aluminate glasses up to 7 wt% of the oxygen has been replaced by fluorine. Parker et al. (1984) reported up to 7.1 wt% retained in glass (base composition of 67 wt% SiO_2, 17 wt% Na_2O, 12 wt% CaO and 4 wt% Al_2O_3) but with considerable volatilization losses (i.e., 31wt% of F volatilized). Volf also reported that F can form $[FeF_6]^{2-}$ complexes with Fe in glass.

Wang et al. reported up to 11.7 wt% of F was retained in a glass of 9.37 mole% Al, 7.18 mole% B, 16 mole% Ca, 4.39 mole% Fe, 14.61 mole% Mg, 12.72 mole% Na, 35.65 mole% Si. The 11.7 wt% F represented ≈ 57 wt% retention of the original amount of F (20.5wt% F was originally present in the batch). In addition, Wang et al. employed special melting techniques[17] to

---

[17] SiO_2, $CaCO_3$, Fe_2O_3, CaF_2, H_2BO_3, and Na_2CO_3 were premelted at 1300°C for 1 h. The glass was crushed and MgF_2 and AlF_3 added. The mixture was then melted at 1100°C for 1 h followed by 1200°C for 2.5 h.

reduce volatilization. The glass devitrified after 2 hours at 1000°C to produce 14 vol% crystallinity. Phases present included calcium magnesium aluminum fluorosilicate, pargasite ($(Ca, Na)_{23}(Mg,Fe^{2+}, Fe^{3+}, Al)_5(Al,Si)_8O_{22}F_2$), and fluorite ($CaF_2$). A radioactive glass of similar composition was also melted by Wang et al. This glass, F4-20, contained 13.8wt% F (analyzed). It also devitrified after 2 hours at 1000°C to produce ≈12 vol% crystallinity. The phases present in the radioactive glass included fluorite and fluorophlogopite ($K_2(Mg,Fe^{2+})_6[Si_6Al_2O_{20}]F_4$).

Fluorine volatilizes from silicate melts in the form of fluorides (e.g.SiF_4, AlF_3, ZnF_2, NaF, Na_3AlF_6, TiF_4, F_2 or BF_3). Volatilization is generally greater in borosilicate glasses when compared to soda-lime silica glasses because of the formation of BF_3 which is gaseous at ambient temperature (b.p. -101°C) (Volf). In contrast, NaF melts at 988°C and CaF_2 melts at 1378°C and are therefore more stable fluorides. Chlorine may enhance the volatilization of F by increasing the separation of F from the melt (Volf).

Parker et al. reported 27 to 38 wt% volatilization loss from various soda-lime-aluminosilicate glasses. Retention of fluorine was seen to increase from 62% to 73% when Ca^{2+} was replaced by other divalent cations in the following order $Mg^{2+} < Ca^{2+} < Zn^{2+} < Sr^{2+} < Ba^{2+}$. F was lost primarily as SiF_4 and NaF. However, F may also volatilize as AlF_3, ZnF_2, Na_3AlF_6, and HF. Alumina was also observed to improve retention of fluorine slightly. Reported retention increased from 64% to 70% as SiO_2 was replaced by alumina from 0 to 8 wt%. As stated earlier, 7.1 wt% F was retained in soda-lime-aluminosilicate glass but 31% of the F was volatilized.

Fluorine reacts with sulphate in commercial glasses resulting in accelerated melting. This occurs according to Mahring's reaction (Volf):

$$Na_2SO_4 + CaF_2 = Na_2O + CaO + (SO_2 + F_2)$$

As stated earlier, the addition of F reduces the viscosity of silicate melts. In a scoping study Bates[18] prepared 5 glasses in the range of 0.3 to 5 wt% F. The compositions of these glasses are shown in Table 4.9.1. The temperature at which the viscosity is a 100P (T100P°C) was found to decrease by 21 °C when 2.7 wt% F was added to HW39 glass. Electrical conductivity was unchanged. No significant changes were observed for MCC-1 results. PCT was not performed. Between 5 and 10 wt% CaF_2 crystallized from quenched glass containing 4.8wt% F. Glasses containing < 4.8 wt% F were found to be amorphous by XRD.

Needed Studies

Investigations should consider additives which may affect F volatility and solubility (e.g. TiO_2, Al_2O_3, B_2O_3, Na_2O, CaO, Cl, S, U, etc.). The effect of temperature on F solubility and volatility should also be evaluated. The relationship between F and glass properties should be evaluated with particular emphasis on viscosity, durability, segregation, and volatility of glass components. If the formation of a crystalline compound is investigated as a possible method for increasing F solubility, settling and agglomeration of crystals should be evaluated in crucibles and small scale melters. Multiple additions of feed and different batch sizes should be evaluated to determine the effects on the fluoride segregation. The study of the cold cap processes is necessary to fully

[18]Bates, S.O. 1987c. *Interim Milestone HWVP-867-V110202C - Report on FY87 Glass Variability Testing Conducted for the Hanford Waste Vitrification.* Program. Pacific Northwest Laboratory, Richland, Washington.

understand the segregation mechanisms and to develop mitigation strategies. After laboratory scale studies are completed, small scale melter tests would provide further understanding of segregation.

5.0 ASSESSMENT OF WASTE LOADING LIMITATIONS FROM MINOR COMPONENTS FOR SELECTED WASTES

Table 5.0.1 shows a summary of preliminary waste loading assessment of estimated waste compositions of tank farms (TF) TF-B, TF-T, TF-SX, TF-C, TF-A, TF-AX, TF-TY, TF-BY, TY-S, TF-U, TF-TX, TF-BX. DSSF, TF-DST, Case C, and NCAW waste compositions are also shown. DSSF is a type of feed contained in several tanks called double shell slurry feed. TF-DST is the double shell tanks, not necessarily in one tank farm. Case C is the reference DST and SST Waste Blend[19]. Appendix A contains an explanation assumptions and the calculation sheets used to prepare Table 5.0.1. The maximum waste loading was estimated based on many unverified assumptions and extrapolations of property models and must be used with caution.[20] The property models are based on data largely determined from glasses prepared with simulated NCAW-87 which is similar to the NCAW-91 shown in Table 5.0.1. This waste did not contain high amounts of troublesome components (e.g. Cr, P, S, Cl, F, etc.). The property models for glass formulation/waste loading predictions are used by converting the glass composition into the ten components considered in CVS (SiO_2, B_2O_3, Na_2O, Li_2O, CaO, MgO, Fe_2O_3, Al_2O3, ZrO_2, and Others). The Others component is NCAW others. Troublesome components are not accounted for by the CVS property models at relative levels different than what is contained in the NCAW composition.

An evaluation of the wastes for TF-B, TF-T, TF-SX, TF-C, TF-DST, TF-A, TF-AX, TF-TY, TF-BY, TY-S, DSSF, TF-U, TF-TX, TF-BX, Case C, and NCAW was conducted to estimate which wastes glasses would be limited in waste loading by the minor components, Mn, Bi, Ti, and U. TF-B and TF-T were estimated to have waste loading limited by P_2O_5. An arbitrary limit of 3 wt% P_2O_5 was set for the waste loading assessment. This limit was based on limited scoping tests where HLW quenched glasses were prepared in small crucibles without phosphate crystallinity or segregation. The glasses contained 3 wt% P_2O_5, rare earths < 8wt %, Li_2O < 3wt%, SO_3 < 0.20wt% or CaO < 1.2wt%. However, as stated in the phosphate section of this report, less than 3 wt% P_2O_5 caused problems in PSCM-19. Conflicting with this limit is PSCM-9 where > 4 wt% P_2O_5 was processed in the melter without problems. If sulfate accumulation occurred during the processing of TF-B or TF-T, it is likely that the combination of CeO_2 and P_2O_5 in these wastes could result in the formation of a phosphate layer. If sulfate does not accumulate, the preliminary waste loading limits is a best estimate for processability given the current information available. More testing of these compositions are necessary to determine more precise estimates.

---

[19]Letter, R.W. Powell, WHC to J.M. Creer, PNL, "Double Shell Tank/Single-Shell Tank Waste Blend Composition for High-Level Waste Vitrification Process Testing" 9452712, dated May 19,1994.

[20]It is not the scope of section 5.0 to discuss the limits based on all components/properties other than the minor components, Bi, Mn, Ti, and U. The complete discussion of the preliminary waste loading assessment limitations is presented in Lambert, S.L. 1994.^@ *TWRS High-Level Waste Feed Processability Assessment Report*, WHC-SP-1143, Westinghouse Hanford Company, Richland, WA. See this document for more information.

The 3 wt% P_2O_5 limit may also be in some cases too limiting. Higher amounts of P_2O_5 (>3 wt%) have been made in the laboratory without phosphate scum layer formation though some quenched crystallinity was present in amounts up to 7 vol%. If this crystallinity could be tolerated in the melter and the durability of the glass was unaffected, this glass may be processable. Depending on the glass composition P_2O_5 has been incorporated in as high as 28 wt%. This particular glass was transparent and contained 22.1 wt% CaO, 22.2 wt% SiO_2 and 20.7 wt% Al_2O_3 and so was really a calcium aluminophosphosilicate glass rather than a borosilicate glass. Other properties were not tested. The important thing to stress is that it may be the cold cap chemistry (interaction with sulfate) which has limited the processing of P_2O_5 in borosilicate glasses in the past not the fact that P_2O_5 is insoluble in a particular composition. In order to confirm this, small scale melter studies of high phosphate compositions should be performed and the cold cap chemistry studied.

It should be noted that TF-B and TF-T also contain high amounts of Bi_2O_3. This compound may affect the waste loading limit. Though no Bi_2O_3 crystalline phases have been observed in very limited studies, the behavior of Bi_2O_3 is an unknown and a study is necessary to rule out an affect on waste loading. Bi_2O_3 has been reported to decrease viscosity and increase corrosion of refractories so that processing issues are significant and worth investigation.

TF-SX waste loading was estimated to be limited by Cr_2O_3. The preliminary waste loading limit was 13 wt%. This is very low and could be increased depending on how much undissolved Cr_2O_3 and spinel a particular melter could tolerate without processing problems. The shape and size of the crystals could also affect settling and agglomeration characteristics of the melt. The formation of chromate and the interaction between sulfate and chromate has not been well studied in waste glasses. This may affect the limit for Cr_2O_3.

Sulfate did not appear to be limiting in any of the wastes shown in Table 5.0.1. However, if sulfate were to accumulate in the melter cold cap it could potentially trap phosphate, chlorides, molybdates, and radionuclides in a gall. This would lead to increased volatility of cesium and chlorine. Also refractory rare-earth or calcium phosphates could retard melting rate. The sulfate layer is not durable and cesium would be leachable from it. It is not known what levels of sulfate in the melter feed could lead to accumulation. The accumulation of sulfate may not occur until a certain amount of feed has been processed or may not occur at all. More study is need in this area in order to better understand the cold cap chemistry and its relation to melting rate, volatility, and formation of refractory phosphates.

MnO_2 is high (> 2.14 wt%) in TF-C, TF-A, and TF-AX wastes. Because MnO has a tendency to enter spinel it may limit waste loading through the formation of spinel. The affect on liquidus temperature and its precise interaction with Fe, Cr, and Ni are unknown and may therefore limit waste loading. In TF-C, Fe, Ni, and Mn are all high. However, the amount of ZrO_2 is sufficiently higher and is predicted to limit waste loading rather than spinel.

U_3O_8 is high (>2 wt%) in TF-B, TF-SX, TF-C, TF-A, TF-AX, TF-TY, TF-BY, TY-S, TF-U, TF-TC, TF-BX, Case C and NCAW wastes. Not enough information is available to determine if U_3O_8 will affect waste loading. Though the solubility of UO_3 is reported to be ≈ 40wt% in a borosilicate glass tested by Schreiber, interaction effects may exist between U and other glass components. Fluorite solid solutions containing U have formed from mixed oxides during calcining (see uranium section). The mixed oxides contained Ce, Nd, Fe, Mo, Zr, Ni, U, Cs, Sr, and Ba. Potential interactions between U and these components as well as F and S should be investigated in order to obtain more information about waste loading limitations.

Fluorine was present in amounts < 1.56 wt% amounts in the assessed wastes. Based on literature reports this amount and less should not limit waste loading. There is a possibility that CaF_2 could crystallize during the vitrification in TF-C. It is not known what effects this might produce on processing. Volatility of F may occur in the melter and cause problems for the offgas system.

None of the evaluated wastes contained high TiO_2 concentrations which would potentially limit waste loading. However, should pretreatment involve the addition of silico-titanates the interaction of TiO_2 with Al_2O_3 may potentially limit waste loading. TiO_2 may also increase liquidus temperatures by acting as a nucleating agent.

None of the wastes contained high (> 1 wt%) amounts of Cl, I or S. However, the accumulation of salt layers in the cold cap and cold cap chemistry both of which could affect melter operation have not been well studied. Molten salt segregation and enhanced volatility may occur during processing of the assessed wastes.

6.0 OTHER NEEDED STUDIES

This report has focused primarily on issues of solubility. However, the increased processing temperature ranges will likely significantly influence volatility rates of halides, Tc, Cs, Na, B, and other semivolatiles. Studies are needed to determine the volatility rates as a function of time, temperature and glass composition. Additives which may suppress volatility should be investigated to develop mitigation strategies. Components which may enhance volatility should be identified as pretreatment strategies may enable a reduction of these component to feeds containing quantities of volatile components.

7.0 REFERENCES

Araujo, R.J. and D.W. Smith. 1980. "The effect of boron coordination on halogen solubility, nickel color, and photochromism in potassium aluminoborosilicate glasses," *Phys. and Chem. of Glasses*, 21(3):114-119.

Bickford, D.F. and C.M. Jantzen. 1986. "Devitrification of Defense Nuclear Waste Glasses: Role of Melt Insolubles," *J. Non- Crys. Solids*, 84:299-307.

Bickford, D.F., A. Applewhite-Ramsey, C.M. Jantzen, and K.G. Brown. 1990. "Control of Radioactive Waste Glass Melters: I, Preliminary General Limits at Savannah River," *J. Am. Ceram. Soc.*, 73(10):2896-902.

Boomer, K.D. 1993. *Tank Waste Technical Options Report* - Appendix D. WHC-EP-0616, Rev. 0. Westinghouse Hanford Company, Richland, Washington.

Brevick, C. H. 1994a. "Historical Tank Content Estimate for the Northeast Quadrant of the Hanford 200 East Area," WHC-SD-WM-ER-349, Rev. 0. ICF Kaiser Hanford Company, Richland, Washington.

Brevick, C. H. 1994b. "Historical Tank Content Estimate for the Southwest Quadrant of the Hanford 200 West Area," WHC-SD-WM-ER-352, Rev. 0. ICF Kaiser Hanford Company, Richland, Washington.

Buechele, A.C., X. Feng, H. Gu, and I.L. Pegg. 1990. "Alteration of Microstructure West Valley Glass by Heat Treatment," in *Materials Research Society Symposium Proceedings*, Ed. V.M. Oversby and P.W. Brown (MRS, Pittsburgh, PA), Vol 176, pp. 393-402.

Buechele, A.C., X. Feng, H. Gu, I.S. Muller, W. Wagner, and I.L. Pegg. 1991. "Effects of Composition Variations on Microstructure and Chemical Durability of West Valley Reference Glass," in *Materials Research Society Symposium Proceedings*, Ed. P.A. Abrajano and L.H. Johnson (MRS, Pittsburgh, PA), Vol 212, pp. 141-152.

Bunnell, L.R. 1988. *Laboratory Work in Support of West Valley Glass Development*, PNL-6539 UC-510. Pacific Northwest Laboratory, Richland, Washington.

Burger, L.L. and R.D. Steele. 1983. *The Status of Radioiodine Control for Nuclear Fuel Reprocessing Plants*, PNL-4689. Pacific Northwest Laboratory, Richland, Washington.

Button, D., R. Tandon, H. Tuller, and D. Uhlmann. 1980. J. Non-Cryst. Solids, 42(1/3):297.

Ewest, E. and H. Wiese. " High level Liquid Waste Vitrification with the Pamela Plant in Belgium." IAEA-CN-48/177, pp. 269-280.

Farges, F., C.W. Ponader, G. Calas, and G.E. Brown, Jr. 1992. "Structural environments of incompatible elements in silicate glass/melt systems: II. U^{IV}, U^{V}, and U^{VI}." *Geochim. Cosmochim. Acta* 56:4205-4220.

Feng, X. 1988. *Compositional effects on chemical durability and viscosity of nuclear waste glasses--systematic studies and structural thermodynamic models* , Order no. 8820009, UMI, Ann

Arbor, Michigan.

Flannery, J.E. and D.R.Wexell. 1986. "Opal Glasses" in *Advances in Ceramics, vol 18, Commercial Glasses.* Ed. D.C. Boyd, J.F. MacDowell. American Ceramic Society Press, Columbus, OH.

Galakhov, F. Ya and B.G. Varshal. 1987. "Liquid Phase Separation in the Li_2O-Al_2O_3-TiO_2-SiO_2 System." Translated from Fiz. Khim. Stekla, 13(4):481-488.

Galakhov, F. Ya and V.T. Vavilonova, V.I. Aver'yanov, and T.V. Slyshkina. 1988. "An Experimental Determination of the Region of Liquid-Liquid Phase Separation in the Li_2O-Al_2O_3-TiO_2-SiO_2 System." Translated from Fiz. Khim. Stekla, 14(1):38-46.

Geeting, J.G.H. and Kurath, D.E. 1993. *Preliminary Assessment of Blending Hanford Tank Wastes.* PNL-8589 UC-721. Pacific Northwest Laboratory, Richland, Washington.

Goldman, D.S. 1985. "Redox and Sulfur Solubility in Glass Melts."; pp. 74-91 in *Gas Bubbles in Glass.* Prepared by the Technical Committee 14 of the International Commission on Glass. Institute du Verre, Charleroi, Belgium.

Goles, R.W. and G.J. Sevigny. 1983. *Off-Gas Characteristics of Defense Waste Vitrification Using Liquid-Fed Joule Heated Ceramic Melters*, PNL-4819 UC-70, Pacific Northwest Laboratory, Richland, Washington.

Goles, R.W., and R.W. Nakaoka. 1990. *Hanford Waste Vitrification Program Pilot-Scale Ceramic Melter Test 23*, PNL-7142, UC-721, Pacific Northwest Laboratory, Richland, Washington.

Herborn, D.I. and Smith, D.A. 1992. *Hanford Waste Vitrification Plant Preliminary Safety Analysis Report.* WHC-SD-HWV-PSAR-001, Rev. 0. Westinghouse Hanford Company, Richland, Washington.

Heynes, M.S.R. and H. Rawson, 1957. "Bismith trioxide glasses." J. Soc. Glass Technol. Vol 41:347T-249T.

Holladay, D. W. 1979. *A Literature Survey: Method for the Removal of Iodine Species from Off-Gases and Liquid Waste Streams of Nuclear Power and Fuel Reprocessing Plants with Emphasis on Solid Sorbents*, ORNL/RM-6350, Oak Ridge National Laboratory, Oak Ridge, Tennessee.

Hrma, P. R. and G. F. Piepel. 1992b. *Property / Composition Relationships for Hanford Waste Vitrification Plant Glasses -- Preliminary Results Through CVS - II Phase 2.* Pacific Northwest Laboratory, Richland, Washington.

Hrma, P. R., G. F. Piepel, P. E. Redgate, and D. S. Kim. 1994a. *Property / Composition Relationships for Hanford Waste Vitrification Plant Glasses -- Results Through CVS-II Phase 4, PVTD-93-03.01C.* To be published. Pacific Northwest Laboratory, Richland, Washington.

Hrma, P. and D. Kim. 1994b. "Sulphate mass balance and foaming threshold in a soda-lime glass," *Glass Technology*, 35(3):128-134.

Jantzen, C. M. 1986. "Phosphate Additions to Borosilicate Waste Glass Cause Phase Separation," memorandum dated April 15. DPST-86-389. Westinghouse Savannah River Company, Aiken, South Carolina.

Jantzen, C.M. 1991. "Glass Melter Off-gas System Pluggages: Cause, Significance, and Remediation," Proceeding of the 5th International Symposium on Ceramics in Nuclear Waste Management, G.G. Wicks, D.F. Bickford, and R. Bunnell (Eds.) American Ceramic Society, Westerville, OH, pp. 621-630.

Jantzen, C.M. 1992. *Inorganic Analyses of Volatilized and Condensed Species within Prototypic Defense Waste Processing Facility (DWPF) Canistered Waste (U)*, WSRC-MS-92-260, Westinghouse Savannah River Company, Aiken, South Carolina.

Jantzen, C. M., N. E. Bibler, D. C. Beam., CL Crawford, and MA Pickett. 1993. *Development and Characterization of the Defense Waste Processing Facility (DWPF) Environmental Assessment (EA) Glass Standard Reference Material (U).* WSRC-MS-93-124, Westinghouse Savannah River Company, Aiken, South Carolina.

Kim, D.S. and P. Hrma. 1991. "Foaming in Glass Melts Produced by Sodium Sulfate Decomposition under Isothermal Conditions." *J. Am. Ceram. Soc.*, 74(3):551-55.

Kim, D.S. and P. Hrma. 1992. "Foaming in Glass Melts Produced by Sodium Sulfate Decomposition under Ramp Heating Conditions." *J. Am. Ceram. Soc.*, 75(11):2959-63.

Kingery, W.D., H.K. Bowen, and D.R. Uhlmann. 1976. *Introduction to Ceramics*, John Wiley and Sons, New York, NY.

Knox, C.A. and R.K. Farnsworth. 1981. *Behavior of radioactive iodine and technetium in the spray calcination of high-level waste*, PNL-3741. Pacific Northwest Laboratory, Richland, Washington.

Kreidl, N.J. 1945. "Recent Studies on the Fluorescence of Glass," J. Opt. Soc. Am. 35(4):249-257.

Kreidl, N.J. 1983. "Inorganic Glass-Forming Systems." in *Glass Science and Technology.* ed. D.R. Uhlmann and N. J. Kreidl. Academic Press, NY.

Kupfer, M.J. 1978. *Vitrification of Hanford Bismuth Phosphate and Uranium Recovery Process Sludges*, RHO-LD-60. Rockwell Hanford Operations, Richland, Washington.

Kupfer, M.J. and R.A. Palmer. 1980. *Physical and Chemical Characterization of Borosilicate Glasses Containing Hanford High-Level Wastes*, RHO-SA-189. Rockwell Hanford Operations, Richland, Washington.

Kramer, F.W. 1991. "Contribution to basicity of technical glass melts in relation to redox equilibria and gas solubilities." Glastech. Ber. 64(3):71-80.

Linwood, S.H. and W.A. Weyl. 1942. "The Fluorescence of Manganese in Glasses and Crystals," J. Opt. Soc. Am. 32(8):443-453.

Lowe, S.S., 1991. *Preliminary Material Balances for Pretreatment of NCAW, NCRW, PRP and*

CC Wastes. WHC-SD-WM-TI-492, Rev. 0. Westinghouse Hanford Company, Richland, Washington.

Lucktong, C. and P. Hrma. 1988. Oxygen Evolution During MnO-Mn3O4 Dissolution in a Borosilicate Melt," *J. Am. Ceram. Soc.*, 71(5):323-28.

May T.H. and Watrous, R.A. 1992. *Hanford Waste Vitrification Plant Feed Processability Assessment*, WHC-SP-0705. Westinghouse Hanford Company, Richland, Washington.

McCarthy, G.J. and M.T. Davidson. 1975. "Ceramic Nuclear Waste Forms: I, Crystal Chemistry and Phase Formation," Ceramic Bulletin 54(9):782-786.

Merrill, R.A. and D.S. Janke. 1993. "Results of Vitrifying Fernald OU-4 Wastes," PNL-SA-21856, Pacific Northwest Laboratory, Richland, Washington.

Miller, W.C., D.W. Hamilton, L.K. Holton, and J.W. Bailey. 1991. *Hanford Waste Vitrification Systems Risk Assessment - Final Report*, WHC-EP-0421. Westinghouse Hanford Company, Richland, Washington.

Nath, P. and R.W. Douglas. 1965. "Cr^{3+}-Cr^{6+} equilibrium in binary alkali silicate glasses." Phys. and Chem. of Glasses, 6(6):197-202.

Nelson and White. 1980. "Transition metal ions in silicate melts-I. Manganese in sodium silicate melts," *Geochim. Cosmochim. Acta* 44:887-893.

Palmer, R.A. 1980. *Interactions Between Candidate Melter Electrode Materials and Defense Waste Glass Melts*, RHO-SA-173. Rockwell Hanford Operations, Richland, Washington.

Paul, A. 1982. *Chemistry of Glasses*, Chapman and Hall, London.

Paul, A. and D. Lahiri. 1966. "Manganous-manganic equilibrium in alkali borate glasses." *J. Am. Ceram. Soc.*, 49(10):565-568.

Parker, J.M., J.A.M. Aldulaimy, and Q.A. Juma'a. 1984. "Volatilisation from fluoride opal melts," *Glass Technology* , 25(4):180-187.

Perez Jr., J.M., L.R. Ethridge, D.S. Goldman, R.W. Goles, P.A. Scott, B.M. Wise. 1985. *West Valley Pilot -Scale Melter Experiment PSCM-19/19E Run Summary*, 7H35-85-2. Pacific Northwest Laboratory, Richland, Washington.

Perez Jr., J.M.and R.W. Nakaoka. 1986. "Vitrification Testing of Simulated High-Level Radioactive Waste From Hanford," *Waste Management '86 (Ed. R.G. Post) Proceedings of the Symposium in Waste Management at Tucson, AZ, March 2-6, 1986*, 2:495-505.

Plodinec, M.J. 1979. "Development of Glass Compositions for Immobilization of Savannah River Plant Waste." *Scient. Basis Nuclear Waste Management.*, Ed. G.J. McCarthy, 1:31-35.

Plodinec, M.J. 1980. "Improved Glass Compositions for Immobilization of SRP Waste." *Scient. Basis Nuclear Waste Management.*, Ed. C.J.M. Northrup, Jr., 2:223-229.

Pourbaix, M. 1974. Atlas of Electrochemical Equilibria in Aqueous Solutions. National

Association of Corrosion Engineers, Houston, TX.

Schreiber, H.D. and G.B. Balazs. 1981. "Mutual Interactions of Ti, Cr, and Eu redox couples in silicate melts," *Phys. and Chem. of Glasses*, 22(4):99-103.

Schreiber, H.D. and G.B. Balazs. 1982a. "The chemistry of uranium in borosilicate glasses. Part 1. Simple base compositions relevant to the immobilisation of nuclear waste." *Phys. and Chem. of Glasses*, 23(5):139-146.

Schreiber, H.D., G.B. Balazs, P.L. Jamison, and A.P. Shaffer. 1982b. "The chemistry of uranium in borosilicate glasses. Part 2. Base compositions containing titanium relevant to the immobilisation of nuclear waste." *Phys. and Chem. of Glasses*, 23(5):147-153.

Schreiber, H.D., G.B. Balazs, and B.J. Williams. 1982c. "Chemistry of Uranium in Aluminophosphate Glasses." *J. Am. Ceram. Soc.*, 65(9):449-453.

Schreiber, H.D., L.M. Minnix, and B.E. Carpenter. 1983. "The chemistry of uranium in borosilicate glasses. Part 3. Mutual interactions of oxidising agents (Ce^{4+}, Cr^{6+}, Fe^{3+}, and Mn^{3+}) with uranium in a base composition relevant to the immobilisation of nuclear waste." *Phys. and Chem. of Glasses*, 24(6):155-165.

Schreiber, H.D., L.M. Minnix, G.B. Balazs, and B.E. Carpenter. 1984a. "The chemistry of uranium in borosilicate glasses. Part 4. The ferric-ferrous couple as a potential redox buffer for the uranium redox state distribution against oxidising agents in a borosilicate melt." *Phys. and Chem. of Glasses*, 25(1):1-10.

Schreiber, H.D., G.B. Balazs, B.E. Carpenter, J.E. Kirkley, L.M. Minnix,and P.L. Jamison. 1984b. "An Electromotive Force Series in a Borosilicate Glass Forming Melt," J. Am. Ceram. Soc., 67(6):C106-C108.

Schreiber, H.D., G.B. Balazs, and T.N. Solberg. 1985. "The chemistry of uranium in borosilicate glasses. Part 6. The leaching of uranium from glass." *Phys. and Chem. of Glasses*, 26(2):35-45.

Schreiber, H.D., S.J. Kozak, P.G. Leonard and K.K. McManus. 1987. "Sulfur chemistry in a borosilicate melt: Part 1. Redox equilibria and solubility," *Glastech. Ber.*, 60(12):389-398.

Schreiber, H.D., S.J. Kozak, P.G. Leonard, K.K. McManus, and C.W. Schreiber. 1988. "Sulfur chemistry in a borosilicate melt: Part 2. Kinetic properties," *Glastech. Ber.*, 61(1):5-11.

Schreiber, H.D., S.J. Kozak, C.W. Schreiber, D.G. Wetmore, and M.W. Riethmiller. 1990. "Sulfur chemistry in a borosilicate melt: Part 3. Iron-sulfur interactions and the amber chromophore," *Glastech. Ber.*, 63(3):49-60.

Scott, P.A., R.W. Goles, and R.D. Peters. 1985. *Technology of Off-Gas Treatment for Liquid-Fed Ceramic Melters,* PNL-5446 UC-70, Pacific Northwest Laboratory, Richland, Washington.

Spalding, B.P. 1994. "Volatilization of Cesium-137 from Soil with Chloride Amendments during Heating and Vitrification," *Environ. Sci. Technol.*, 28:1116-1123.

Stefanovskii, S. V. and F.A. Lifanov. 1989. "Glasses for immobilization of sulfate-containing

radioactive wastes," Translated from *Radiokhimiya*, 31(6):129-134.

Sun, K. H. 1947. "Fundamental Condition of Glass Formation," *J. Am. Ceramics Soc.*, 30(9):227-281.

Sussmilch, J., and A. Jouan. 1993. "The Vitrification of Accident Wastes from the Nuclear Power Plant A-1 in Slovakia." in *Proceedings of Environmental Remediation and Environmental Issues Vol 3*, R. Baschwitz et al. eds. American Society of Mechanical Eng.

Turcotte, R.P., J.W. Wald, and R.P. May. 1980. "Devitrification of Nuclear Waste Glasses" *Scient. Basis Nuclear Waste Management.*, Ed. C.J.M. Northrup, Jr., 2:223-229.

Veal, B.W., J.N. Mundy, and D.J. Lam. 1987. "Actinides in Silicate Glasses," in *Handbook on the Physics and Chemistry of the Actinides*, Ed. A.J. Freeman and G.H. Lander. Elsevier Scientific Publishers, New York.

Vogel, W. 1971. *Structure and Crystallization of Glasses.* Pergamon Press, Oxford, England.

Vogel, W. 1985. *Chemistry of Glass.* American Ceramic Society, Columbus, OH.

Volf, M. B. 1984. *Glass Science and Technology, 7: Chemical Approach to Glass.* Elsevier Scientific Publishers, New York.

Wang, E., H. Kuang, K.S. Matlack, A.C. Buechele, and S.Fu. 1994. "Effect of Fluoride on Crystallization in High Calcium and Magnesium Glasses." *Scient. Basis Nuclear Waste Management.*, Ed. A. Barkatt and R.A, Van Konynenburg, 333:473-479.

Weiss, R.I. 1986. *TY Tank Farm Waste Characterization Data.* RHO-WM-TI-1 P. Rockwell International, Richland, Washington.

Table 2.0.1. Preliminary Assessment of Minor Component Solubility Effects

Compo-nent	Approximate Solubility Range*	Comment
P_2O_5	<1 wt% (with presence of sulfate gall)	Highly dependent on glass composition. Could be much higher especially if Al_2O_3 present and Li_2O, CaO, S and rare earths absent. Solubility range based on limited screening studies. More study needed.
Cr_2O_3	< 4 wt% < 1 wt% (more typical in borosilicate waste glasses)	Cr_2O_3 crystallinity or the formation of spinel with other transition elements may limit. Dependent upon how much crystal settling and agglomeration can be tolerated in the melter (i.e. melter type). Redox/basicity/temperature important. Chromate formation in cold cap possible. More study needed.
Cr(VI)	< 2 wt%	Durability strongly decreased by presence of chromate. Volatility may be a problem. More study needed.
SO_3	< 1.5 wt %	Dependent on glass composition, redox, melt temperature. Volatility expected to be a problem. Foaming and gall formation possible. More study needed.
MnO	< 20 wt% could be much less if Fe, Ni, Cr present	Formation of spinel with other transition elements may limit. Dependent upon how much crystal settling and agglomeration can be tolerated in the melter (i.e. melter type). Foaming possible. Redox/basicity/temperature important. Dependent on glass composition. More study needed.
TiO_2	< 4 wt%	Dependent on glass composition. Could be significantly higher if Al_2O_3 is not present. More study needed.
Bi_2O_3	not expected to limit waste loading	Refractory corrosion or affect on viscosity may limit waste loading. Dependent on glass composition. More study needed.
UO_2	<10 wt%	Redox components can oxidize U(IV) so it does not limit solubility in glass. Dependent on glass composition. Interactions with other components may limit. More study needed.
U(V) and U(VI)	not expected to limit waste loading	Dependent on glass composition. More study needed.
Cl and I	Cl < 1.4 wt% I < 1 wt%	Dependent on glass composition and temperature. Volatility expected to be a high. More study needed.
F	0.5 wt% to 13.5 wt%	Dependent on glass composition and temperature. Volatility expected to be a high. Decreases viscosity and may cause phase separation. More study needed.

* The solubility ranges were determined based on limited data available in the literature and should be used with extreme caution.

Table 4.1.1. West Valley Glass Compositions WV-182 and WV-183 which formed Calcium Rare Earth Phases During Processing in PNL Melters

Component	WV-182 (wt%)	WV-183 (wt%)
SiO_2, wt%	44.7	44.6
B_2O_3	12.7	15.5
Na_2O	15.1	14.7
Li_2O	--	--
CaO	3.0	0.7
Cr_2O_3	0.68	0.7
Rare Earths	3.2	2.0
P_2O_5	2.6	2.6
Others	18.0	19.2

Table 4.1.2. HTM and CVS3 Selected Glass Compositions

Compo-nent	SW-1 HTM (wt%)	SW-2 HTM (wt%)	CVS3-37 (wt%)	CVS3-38 (wt%)	CVS3-39 (wt%)	CVS3-40 (wt%)
SiO_2, wt%	34.0	25.0	52.1	51.1	50.0	48.9
B_2O_3	0.	9.0	0.05	0.05	0.05	0.05
Na_2O	9.7	9.7	12.1	11.8	11.6	11.3
Li_2O	0	0	2.8	2.7	2.7	2.6
Nd_2O_3	4.5	4.5	5.9	5.8	5.6	5.5
La_2O_3	0.2	0.2	0.3	0.3	0.3	0.2
CeO_2	1.4	1.4	1.7	1.6	1.6	1.6
Al_2O_3	19.0	19.0	4.8	4.7	4.6	4.5
CaO	1.0	1.0	1.2	1.2	1.2	1.2
P_2O_5	16.3	16.3	3	5	7	9
Others	13.9	13.9	16.1	15.8	15.4	15.2

Table 4.1.3. Phosphate Scoping Study Glasses

Component	PFP 3.3 (wt%)	PFP 5.3-2 (wt%)	PFP 5.3-3 (wt%)	PFP 7.3 (wt%)
SiO_2	52.2	51.1	52.3	50.0
B_2O_3	13.6	13.3	13.7	13.1
Na_2O	4.2	4.1	4.2	4.0
Li_2O	7.2	7.0	7.2	6.9
Nd_2O_3	0.2	0.2	0.2	0.2
La_2O_3	0.05	0.05	0.06	0.05
CeO_2	0.1	0.1	0.1	0.1
Al_2O_3	8.7	8.5	8.7	8.3
CaO	0.9	0.8	0.9	0.8
P_2O_5	3.3	5.3	5.5	7.3
Cr_2O_3	2.4	2.4	0	2.3
Others	7.2	7.0	7.2	6.9

Table 4.1.4. Crystalline Phases Present Hanford Glasses: Scoping Studies and CVS3.

Glass Name	Phosphate Crystalline Phases Present in Quenched Glasses by XRD	Approximate Vol% (Semi-quantitative)
SW-1 (HTM)	$NdPO_4$	3 %
SW-2 (HTM)	$NdPO_4$	5 %
CVS3-37	none	none
CVS3-38	$Na_3(RE)(PO_4)_2$ RE=Nd, La, Ce	1 %
CVS3-39	$Na_3(RE)(PO_4)_2$ RE=Nd, La, Ce	3 %
CVS3-40	$Na_3(RE)(PO_4)_2$ RE=Nd, La, Ce	7 %
PFP 3.3	Li_3PO_4	2 %
PFP-5.3-2 (2.4 wt% Cr_2O_3)	Li_3PO_4	3 %
PFP 5.3-3 (No Cr)	Li_3PO_4	5 %
PFP 7.3	Li_3PO_4	4 %

Table 4.1.5. West Valley Composition which Crystallized Li_3PO_4 and $Ca_3(PO_4)_2$

after heat treatment at 700°C for 100h

Component	Reference 5 (wt%)
Al_2O_3	6.45
B_2O_3	12.89
CaO	0.68
CeO_2	0.16
Cr_2O_3	0.14
Fe_2O_3	12.02
K_2O	3.18
Li_2O	2.71
MnO_2	1.01
Na_2O	9.82
NiO	0.25
P_2O_5	2.37
SO_3	0.23
SiO_2	41.16
ThO_2	3.56
TiO_2	0.80
UO_2	0.59
ZrO_2	0.32
Others	1.66

Table 4.2.1. Cr_2O_3 Scoping Study NCAW Glass Composition (Bates, 1987)

Component	NCAW (wt%)
SiO_2	51.3
B_2O_3	9.6
Na_2O	10.4
Li_2O	3.8
CaO	2.9
MgO	0.8
Fe_2O_3	11.1
Al_2O_3	4.3
ZrO_2	0.6
Cr_2O_3	1.3
Others	3.9

Table 4.2.2. High Cr_2O_3 High Level Waste Glass Composition

Component	45% Waste Loading High Cr Glass (wt%)
SiO_2	40.24
B_2O_3	9.19
Na_2O	9.37
Li_2O	6.33
CaO	0.28
MgO	0.03
Fe_2O_3	2.10
Al_2O_3	24.32
ZrO_2	0.03
Cr_2O_3	6.22
Others	1.89

Table 4.2.3. Nuclear Research Institute High Cr Glasses

Component	Cr (wt%)	Cr-4 (wt%)
SiO_2	50.6	51
Al_2O_3	1.5	1.5
B_2O_3	6	8
Na_2O	15	18.02
K_2O	2.5	2.48
CaO	5	5
SrO	0.5	0.5
BaO	3	
MnO	5	5
ZnO	2	5
CuO	1	
NiO	0.5	
CoO	1	
Cr_2O_3	4	4
As_2O_3	0.8[a]	0.3[a]
Ta_2O_5	0.94	
UO_3	0.5	
F	0.8[a]	

[a]heavy volatilization

Table 4.2.4. High Cr_2O_3 Low Level Waste Glass Composition

Component	wt%
SiO_2	55.66
B_2O_3	4.9
Na_2O	19.61
CaO	3.92
Al_2O_3	11.76
Cr_2O_3	2.0
Others	2.14

Table 4.2.5. CVS2-68 and CVS2-69 Glass Compositions

Component	CVS2-68 (mass fraction)	CVS2-69 (mass fraction)
SiO_2	0.5040	0.5660
B_2O_3	0.1355	0.0781
Na_2O	0.0797	0.0664
Li_2O	0.0696	0.0713
CaO	0.0007	0.0079
MgO	0.0002	0.0032
Fe_2O_3	0.0046	0.0334
Al_2O_3	0.1640	0.0816
ZrO_2	0.0001	0.0005
Cr_2O_3	0.0297	0.0238
Others-Cr_2O_3	0.0119	0.0678

Table 4.2.6. NCAW 87, CC, and PFP Others

Component	CVS2-73 & CVS2-74 NCAW-87 Others (wt%)	CVS2-68 CC Others (wt%)	CVS2-69 PFP Others (wt%)
Cr_2O_3	2.24	71.3	25.93
F	5.37	13.6	1.2
P_2O_5	1.79	-	35.54
SO_3	4.93	0.2	7.51
PdO	0.90	-	1.5
Rh_2O_3	0.90	-	0.7
RuO_2	2.69	-	0.7
CdO	13.43	-	1.2
CuO	2.69	-	2.00
K_2O	-	3.9	-
MnO_2	2.69	6.4	16.32
MoO_3	5.37	1.7	-
Nd_2O_3	22.09	-	1.9
PbO	-	-	1.6
SeO_2	-	-	3.9
ZnO	-	2.9	-
NiO	10.30	-	-
La_2O_3	11.19	-	-
CeO_2	2.69	-	-
Cs_2O	2.69	-	-
BaO	1.79	-	-
Pr_6O_{11}	1.79	-	-
SrO	1.79	-	-
Rb_2O	0.90	-	-
Sm_2O_3	0.90	-	-
Y_2O_3	0.90	-	-
sum	100	100	100

Table 4.5.1. High Enriched Waste Concentrate (HEWC) Glass Composition That Crystallized Rutile in the Pamela Melter

Component	HEWC Glass Composition (wt%)
SiO_2	38.75
B_2O_3	21.7
Na_2O	8.64
Li_2O	3.10
TiO_2	1.55
CaO	3.88
Al_2O_3	20.68
SO_3	0.9
Others	0.8

Table 4.5.2. SRL-21 and SRL-131 base glass compositions (Schreiber, 1982) used to investigate the interaction of TiO_2 and U_3O_8

Oxide component	SRL-21* (base composition) (wt%)	SRL-131* (base composition) (wt%)
SiO_2	52.5	57.9
TiO_2	10.0	1.0
ZrO_2	-	0.5
B_2O_3	10.0	14.7
La_2O_3	-	0.5
CaO	5.0	-
MgO	-	2.0
Na_2O	18.5	17.7
Li_2O	4.0	5.7

*U varied from 1 to 45 wt% in base composition

Table 4.6.1. **Bismuth Phosphate Simulant Waste Compositions (Kupfer, 1978 and Kupfer and Palmer, 1980)**

Component	1st Cycle $BiPO_4$ Simulant (wt%)	2nd Cycle $BiPO_4$ Simulant (wt%)	3rd Cycle $BiPO_4$ Simulant (wt%)
Na_2O	8.7	15.3	8.0
Fe_2O_3	25.0	22.4	-
Cr_2O_3	3.4	2.2	10.3
ZrO_2	0.3	-	-
Bi_2O_5	34.7	35.6	-
Bi_2O_3	-	-	37.6
SiO_2	17.1	13.7	-
CeO_2	0.4	-	-
P_2O_5	9.9	10.2	10.8
SO_3	0.2	0.2	0.3
F-	0.2	0.3	1.0
La_2O_3	-	-	16.5
MnO_2	-	-	15.5

Table 4.7.1. Summary of Uranium Interactions with Redox Sensitive Components

Component	Redox Reaction with U	Completion
Ti	Ti(III) + U(V) => U(IV) + Ti(IV)	yes
Cr	Cr(VI) + 3U(V) => Cr(III) + 3U(VI)	yes
Ce	Ce(IV)+ U(V) => Ce(III) + U(VI)	Partial
Mn	Mn(III) + U(V)=>Mn(II) + U(VI)	yes
Fe	none	no

Table 4.7.2. Sodium Aluminophosphate Compositions (Schreiber, 1982)

Component	SPIKE (wt%)	ROVER (wt%)
Na_2O	22.3	21.2
P_2O_5	51.1	49.0
Al_2O_3	26.6	29.8

Table 4.7.3. Simplified Formulation of PW-4b Calcine Composition

Component	wt%
CeO_2	14.8
Nd_2O_3	22.6
Fe_2O_3	9.9
MoO_3	16.9
ZrO_2	13.4
Cs_2O	7.5
SrO	5.7
NiO	2.9
UO_2	6.3

Table 4.8.1. Average Chlorine Decontamination Factors from PNL melter runs

Run Name	Chlorine DF's
PSCM-1	3.1
PSCM-2	3
PSCM-3	4
PSCM-4	5
PSCM-5	1.5
PSCM-6	2.9
PSCM-7	6.4
PSCM-8	4.7
PSCM-19	--
PSCM-23	6.6
LFCM-4	2.2
LFCM--6	2.7
LFCM-7	--

Table 4.9.1 Compositions Used in F Scoping Studies (Bates, 1987c)

Component	HW39 (wt%)	HW39, 2% F (wt%)	HW39, 3% F (wt%)	HW39, 4% F (wt%)	HW39, 5% F (wt%)
Al2O3	4.55	4.22	4.03	3.85	3.67
Na2O	10.50	10.30	10.19	10.08	9.96
Fe2O3	11.77	10.90	10.43	9.96	9.48
SiO2	51.21	51.16	51.13	51.10	51.07
ZrO2	0.62	0.58	0.56	0.53	0.51
F	0.32	2.00	3.00	4.00	5.00
SO4	0.4	0.44	0.42	0.40	0.38
B2O3	9.56	9.56	9.56	9.56	9.56
Li2O	3.75	3.75	3.75	3.75	3.75
Others	7.32	7.09	6.93	6.77	6.62

Table 5.0.1. Preliminary Waste Loading Assessment

	P2O5		Cr2O3	Zr-phase		Spinel				Durability (Na)			Si (low)	Al			
Oxide	TF-B (Wt%)	TF-T (Wt%)	TF-SX (Wt%)	TF-C (Wt%)	TF-DST (Wt%)	TF-A (Wt%)	TF-AX (Wt%)	TF-TY (Wt%)	TF-BY (Wt%)	TF-S (Wt%)	DSSF (Wt%)	TF-U (Wt%)	TF-TX (Wt%)	TF-BX (Wt%)	Oxide	Case C (Wt%)	NCAW (Wt%)
SiO2	0.76	0.49	9.37	0.06	8.31	0.32	0.57	29.20	5.84	2.13	29.44	18.85	17.33	21.37	SiO2	10.00	4.03
B2O3					0.47		0.00				0.00				B2O3	0.08	0.01
Na2O	52.19	56.03	33.93	10.38	31.98	17.31	51.89	22.29	23.75	69.31	66.00	39.89	30.07	25.14	Na2O	25.30	21.42
Li2O					0.01		0.00								Li2O	0.00	0.00
CaO	0.03	0.00	1.24	9.39	0.79	0.03	2.79	0.00	5.66	0.00	0.62	0.00	0.01	0.12	CaO	2.06	0.79
MgO					0.27		0.00				0.00				MgO	0.08	0.20
Fe2O3	7.93	8.95	12.76	11.00	8.75	59.60	23.52	15.42	9.89	2.70	0.00	2.28	3.91	5.91	Fe2O3	11.00	28.21
Al2O3	1.20	0.66	22.74	7.55	2.65	1.48	1.46	10.06	12.33	13.20	2.00	16.73	15.83	22.98	Al2O3	13.00	9.04
ZrO2	0.22	0.42	0.01	25.85	35.20	0.04	0.05	2.52	0.22	2.93		0.30	0.40	0.33	ZrO2	7.08	15.11
"Others"	37.67	33.45	19.93	35.77	11.56	21.23	19.71	20.51	42.31	9.74	1.94	21.96	32.45	24.14	Others	31.41	21.19
Total	100.00	100.00	100.00	100.00	100.00	100.00	100.00	100.00	100.00	100.00	100.00	100.00	100.00	100.00	Total	100.00	100.00
Key "Others" Components																	
Bi2O3	6.43	8.83		0.05				0.33	0.03			0.04	0.05	0.04	Bi2O3	1.95	
CeO2	4.23	5.38	2.07	0.03	0.08	0.48	0.33	1.05	1.99	1.11		2.24	2.76	2.96	CeO2	2.73	0.60
Cr2O3	0.02	0.02	3.92	0.01	0.40	0.00	0.43	0.03	0.00	0.72	0.02	0.19	0.01	0.00	Cr2O3	0.45	0.26
F	0.72	0.50	0.04	1.56	1.43	0.00	0.01	0.04	0.52	0.12	0.07	0.07	0.12	0.17	F	0.56	0.10
La2O3	0.04	0.12			0.66										La2O3	0.43	0.65
MnO2	0.48	1.09	1.67	7.76	0.87	7.18	11.48	0.10	0.41	0.46	0.00	0.21	0.75	0.84	MnO2	1.82	2.14
NiO	0.23	0.03	0.30	5.69	0.47	0.22	0.66	0.00	11.64	0.17	0.00	0.01	0.25	1.25	NiO	2.27	2.30
P2O5	14.20	15.39	0.42	0.28	0.34	0.02	0.02	3.47	1.82	0.54	0.02	0.74	4.10	2.56	P2O5	4.71	0.87
SO3	0.18	0.03	0.22	0.16	0.43	0.41	0.02	0.59	0.23	0.28	0.07	0.06	0.51	0.54	SO3	0.34	0.65
SrO	0.00	0.00	0.01	0.00	0.02	0.02	0.00	0.00	3.45	0.00	0.00	0.00	0.00	0.05	SrO	0.41	0.12
U3O8	9.95	1.88	9.19	19.87	2.67	12.76	6.51	14.71	21.99	5.89	0.01	18.35	23.72	14.12	U3O8	14.30	4.74
Subtotal	36.47	33.27	17.84	35.40	7.37	21.09	19.45	20.32	42.08	9.29	0.19	21.90	32.27	22.53	Subtotal	29.97	12.43
Balance	1.20	0.18	2.09	0.37	4.19	0.14	0.26	0.19	0.23	0.44	1.75	0.06	0.18	1.62	Balance	1.44	8.76
Estimated Maximum Waste Loading* (wt%)																	
1050°C	21	19	13	31	24	13	28	58	46	35	38	55	61	54	1050°C	45	
1150°C	21	19	13	35	31	17	36	68	51	36	38	63	64	63	1150°C	50	33
High-T	21	19	13	44	38	25	46	84	64	39	41	65	73	70	High-T	62	50

*The maximum waste loading was estimated based on many unverified assumptions and extrapolation of the property models, and must be used with caution.

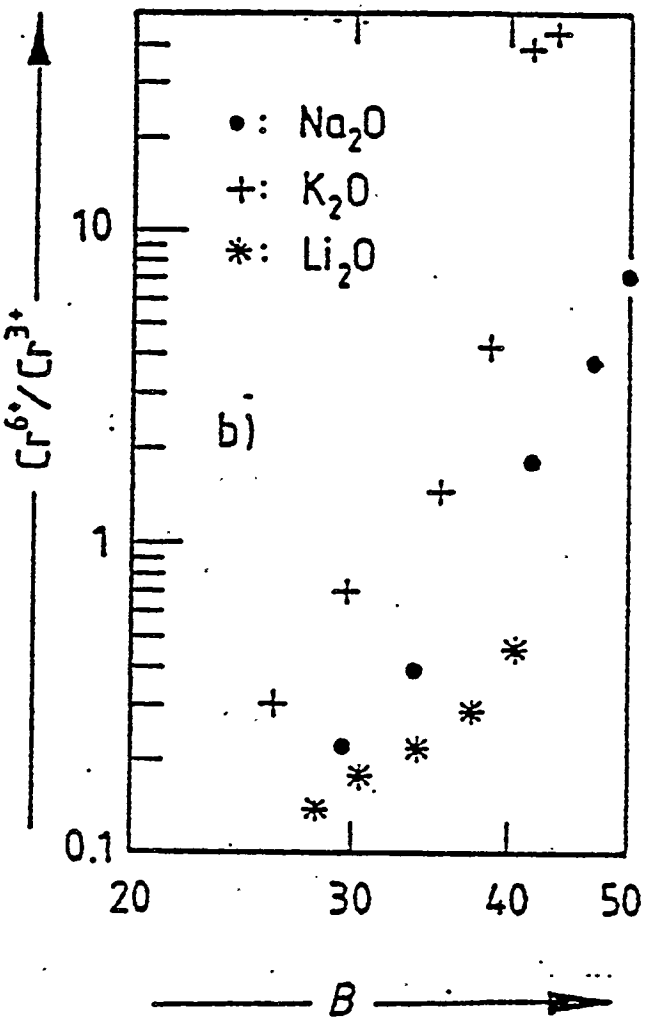

Figure 4.2.1. Chromium equilibrium as a function of basicity number, B, at 1400°C (Kramer)

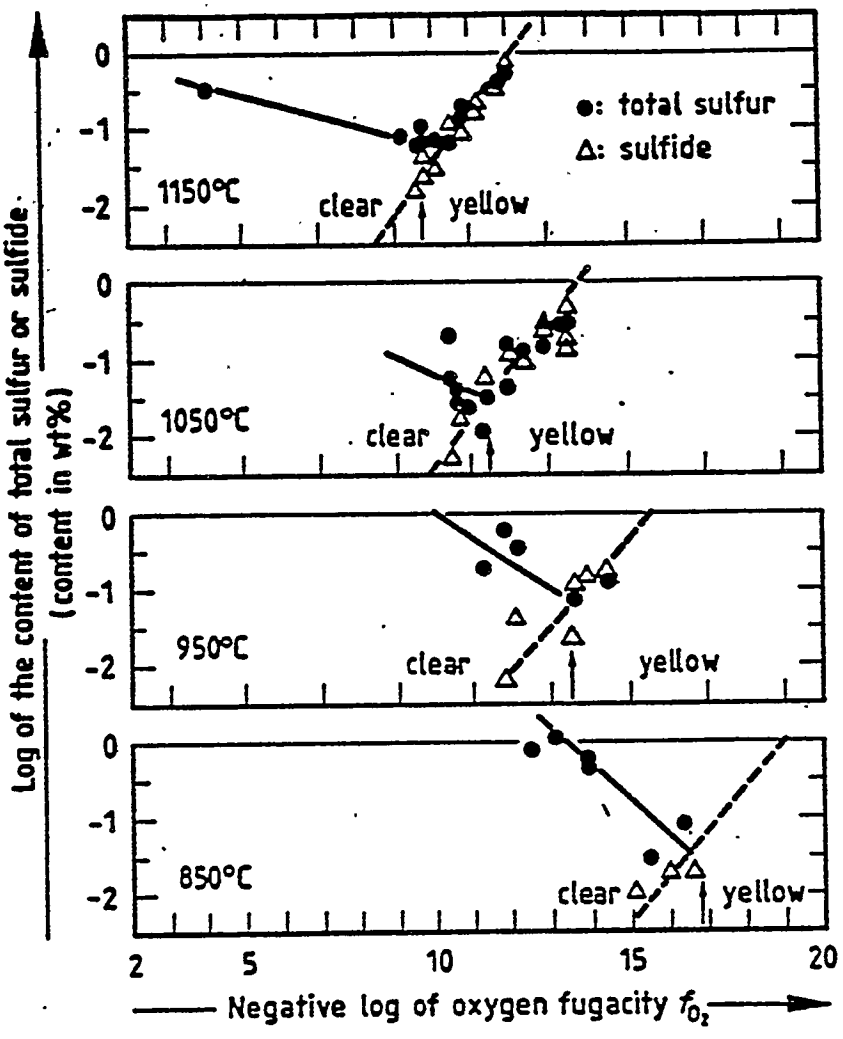

Figure 4.3.1. Sulfur Solubility and redox state distribution as a function of oxygen fugacity at various temperatures in SRL-131 melts. Sample atmosphere of $CO_2/CO/SO_2$ contained 15% SO_2. Solid lines represent the solubility of the sulfate ion as a function of the imposed oxygen fugacity, whereas the dashed line indicates the similar relation for the sulfide ion. The critical oxygen fugacity at which the color changes from clear to yellow is also indicated (Schreiber et al., 1987).

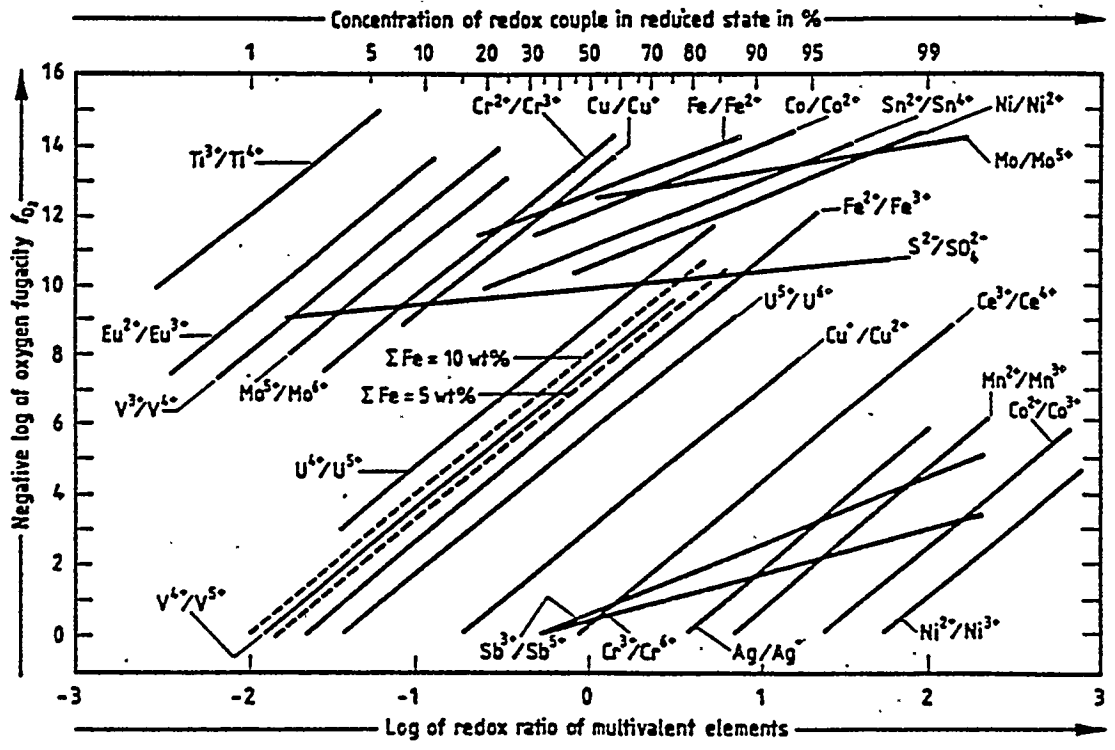

Figure 4.3.2. Relation of the imposed oxygen fugacity (-log fO2) to the analyzed redox ratio (log[reduced ion]/[oxidized ion]) of multivalent elements doped into SRL-131 melt at 1150°C (Schreiber et al., 1984c). Arabic numerals following the element symbols represent the redox couple for that relationship (1wt% redox element). Dashed lines represent the Fe^{3+}/Fe^{2+} redox couple in a glass containing 5 or 10 wt% total iron.

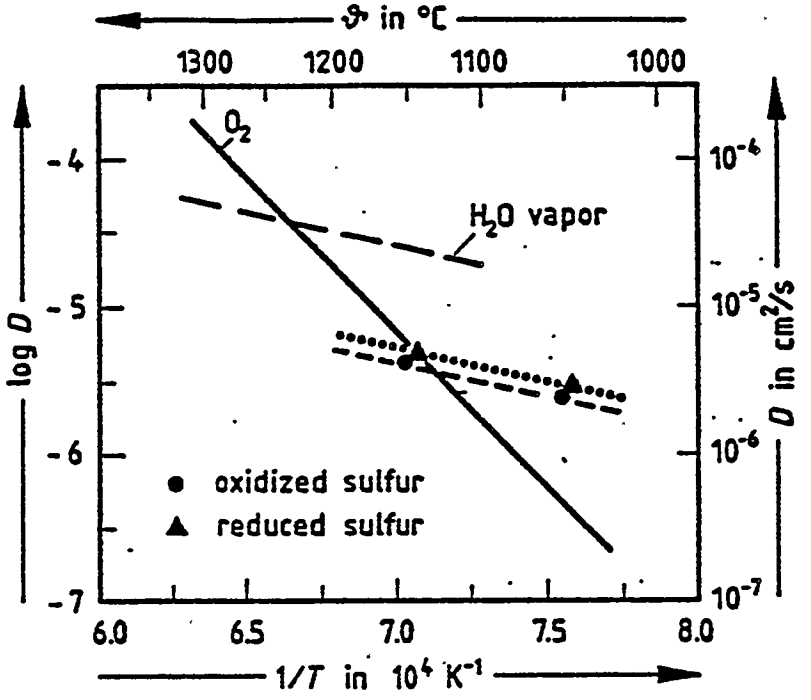

Figure 4.3.3. Temperature dependence of the sulfur diffusion coefficient (oxidized and reduced) as compared to the oxygen and water vapor diffusion coefficients for SRL-131 melts (Schreiber et. al., 1988).

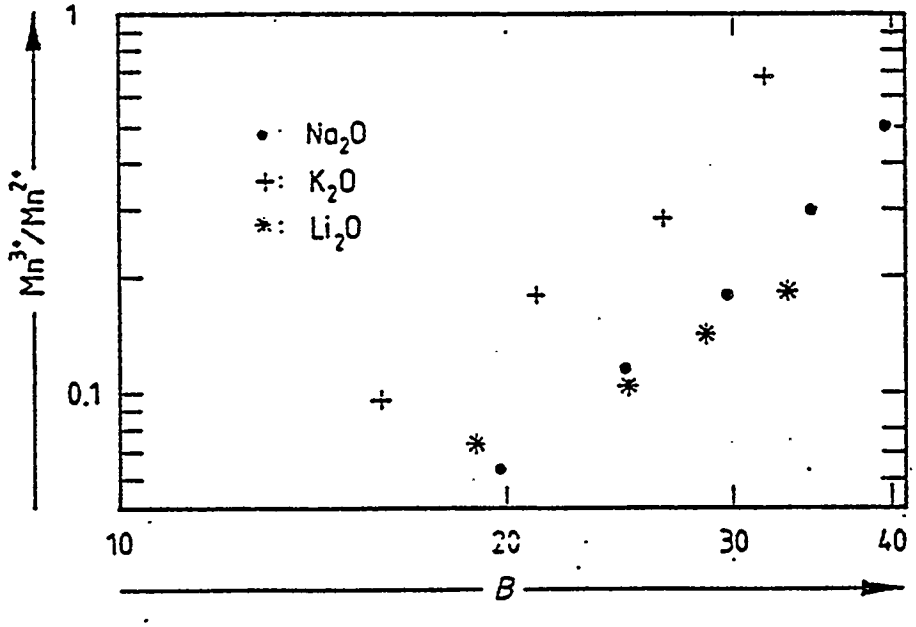

Figure 4.4.1. Manganese equilibrium as a function of the basicity number, B, at 900°C (Kramer)

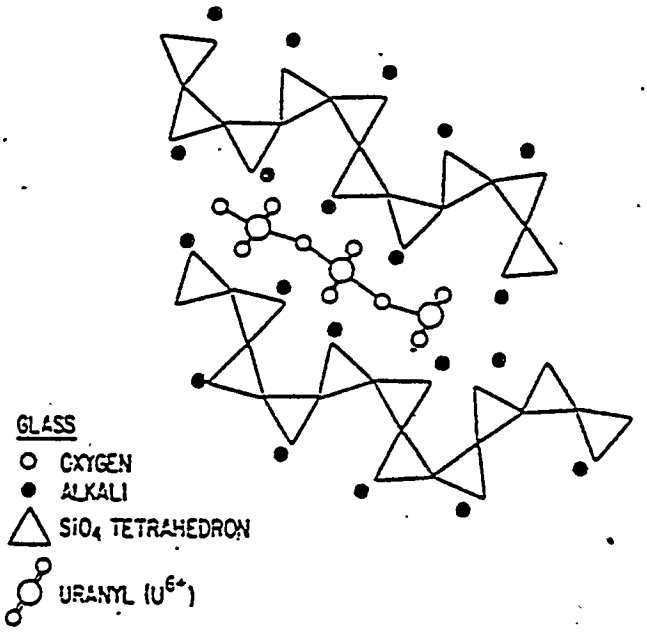

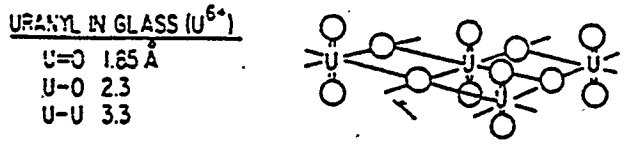

Figure 4.7.1. The Proposed Structure Model of U(VI) in an Alkali Silicate Glass. Layers of uranyl are dispersed between layers of silica. Bottom: Detailed view of the uranyl sheet. (Veal et al. /Knapp et al.)

APPENDIX

CALCULATIONS AND ASSUMPTIONS FOR THE PRELIMINARY WASTE LOADING ASSESSMENT (D. Kim)

Preliminary Feed Processability Assessment for Hanford High-Level Tank Wastes

Dong-Sang Kim
PNL

Glass Formulation Approach was used to estimate the possible maximum waste loading for each Tank Farm Waste, as summarized below:

(1) define the primary target property(s) for a given waste or a group of wastes,
(2) initially formulate glass to maximize or minimize the target property(s) within the revised single-component constraints (Table 1),
(3) determine specific component constraints for a given waste or a group of wastes, as required
(4) reformulate glass within the revised single-component constraints and the specific component constraints.

Glass formulation was based on various information available, such as CVS property models, component effects on the glass properties from the literature data, and past glass formulation experience with NCAW and Blend waste. CVS first-order models for viscosity, durability (7-day PCT B and Na), and liquidus temperature were used as the major tools for glass formulation. Electrical conductivity was predicted but not used as the requirements in glass formulation. When glass composition or temperature was outside of model validity range, certain adjustments were attempted to compensate the expected deviations from the model predictions if they are justified from any available information (qualitative in most cases).

The general strategy used in formulating glasses is described below

- Tried to keep the glass composition within CVS single-component limits (Table 1), if possible, especially for low-temperature glasses. However, CVS single component constraints were not used as limiting factors for waste loading. For the following components, revised single-component constraints were defined in Table 1 and explained below. These revised single-component constraints were used as waste loading limiting factors, unless otherwise superseded by the specific constraints for a given waste or a group of wastes.
  - SiO_2: Glass phase may become unstable at lower SiO2 concentration. The lower limit of SiO2 will depend on the compositions of other glass components. The 40 wt% was preliminarily set as the general limit because of lack of information on the component effects.
  - B_2O_3: $\geq$ 5 wt% B_2O_3 for low-T glasses for better property predictions. Allowed to be < 5 wt% B_2O_3, if necessary, for high-T glasses.

Li_2O: Lack of information at > 7 wt% Li_2O. (Never tested glasses with > 7 wt% Li_2O; compared to Na2O, the same increase in wt% corresponds to twice of increase in mole %) Na2O was primarily used for viscosity adjustment before Li2O was used.

CaO: Used within CVS limit (0-10 wt%) when it is necessary to reduce viscosity not significantly decreasing durability, especially when alkali components has reached their limits.

MgO: Not used as an additive component.

Above constraints are to be revised as new information becomes available. Component limits for Na2O, Fe2O3, Al2O3, and ZrO2 were dependent on the given waste. No component limit was used for "Others."

- Melting temperatures for low-temperature glasses were set at 1050°C and 1150°C. Melting temperature for high-temperature glass was primarily set at 1350°C, but was allowed to be within 1200-1450°C if necessary or significantly advantageous to achieve a higher waste loading.
- Viscosity at the melting temperature was set at 6 Pa·s for low-temperature glasses (1050 and 1150°C glasses) and 4 Pa·s for high-temperature glass. Viscosity of 4 Pa·s for high-T glass was to compensate the general underprediction of viscosity by CVS model at higher temperatures (>1250°C).
- Normalized PCT releases of B and Na were kept ≤ 2 g/m2/7-day. This is a conservative limit based on the possible uncertainties involved in model prediction, especially, for glass compositions outside of model validity range, waste composition, feed batch mixing , etc. In formulating example glass, minimizing the PCT B and Na releases were not attempted if they were lower than 2 g/m2/7-day.
- Example glass formulations are given for low-T (1050°C and 1150°C) and high-T (1250-1450°C) glasses with each waste.
- Assumed Joule-heated continuous melter types. May be applied to any melters with similar requirements for minor component phase separation and crystallinity requirements.

All tank farm wastes were divided into 7 different groups based on the primary limiting factors for waste loading. The different groups were initially based on the low-T glasses (1050°C and 1150°C) and, for some tank wastes, the primary limiting factors for high-T glass (1250-1450°C) were different from those for low-T glasses. In each group, the primary target property(s) and the specific constraints used for glass formulation were given separately for low-T and high-T glasses.

The limiting property values and the revised or specific component constraints used in this study are rather arbitrary because they are based on mostly qualitative information. They are intended to serve as alternatives until more complete

property models and better information on the component effects are available. They may also provide a list of areas that need investigation in the future.

TABLE 1. CVS Single-Component Constraints and Revised Single-Component Constraints Used in This Study

Component	CVS	Revised Constraints Used in This Study	
		Low-T glass	High-T glass
SiO_2	42 – 57	>40	
B_2O_3	5 – 20	5 – 20	0 – 20
Na_2O	5 – 20	waste dependent	
Li_2O	1 – 7	0 – 7	
CaO	0 – 10	0 – 10	
MgO	0 – 8	0 (from additive)	
Fe_2O_3	0.5 – 15	waste dependent	
Al_2O_3	0 – 17	waste dependent	
ZrO_2	0 – 13	waste dependent	
"Others"	1 – 10	None	

Detailed Glass Formulation Strategy

1. P_2O_5 limited (TF-B and TF-T)

3 wt% P_2O_5 limit for both Low-T and High-T glasses
(This limit is not based on the experimental data.)

a) Low-T glass

- Primary target:
  - PCT-B, PCT-Na ≤ 2 g/m^2/7-day
    Additions of both refractory (Al2O3 and ZrO2) and flux (B2O3, Na2O, and Li2O) components are needed to keep PCT releases low at a constant viscosity.
- Specific constraints:
  - No Li2O or CaO in the additive; possible formation of Li and Ca phosphate phases that may phase separate during melting of high-P2O5 glasses
  - Al2O3 ≤ 12 wt%; possible crystallization of Na-Al silicates after CCC, which can lead to a significant decrease of durability
  - ZrO2 ≤ 3 wt%; slow dissolution of ZrO2, which may lead to a slow melting rate

For 1050°C glasses, it was not possible to formulate glasses that satisfy the above constraints. The following adjustments were needed.

Case #1.

- η at T_M = 10 Pa·s
- Al_2O_3 = 13.5 - 14 wt%
- SiO_2 = 35 wt%

Possible outcome: slow melting due to high viscosity
crystallization of Na-Al silicates after CCC

Case #2.

- η at T_M = 10 Pa·s
- Li_2O = 2 wt%

Possible outcome: slow melting due to high viscosity
increased chance of Li_2PO_3 formation

For 1150°C glasses, no adjustments were needed.

b) High-T glass

- No primary target or specific constraint

2. Cr_2O_3 limited (TF-SX)

0.5 wt% Cr_2O_3 limit for Low-T and High-T glasses
(Original CVS limit.)

a) Low-T glass

- Primary target:
  - PCT-B, PCT-Na ≤ 2 g/m^2/7-day
- No specific constraint

b) High-T glass

- No primary target or specific constraint

3. Zr-containing crystal limited (TF-C and TF-DST)

Based on limited experience on glass formulations with NCAW and Blend Waste (Case C), the maximum predicted TL by the 1st-order T_L model that may satisfy the requirement, TM - TL (measured) > 100°C, was determined and used as the primary target.

a) Low-T glass

- Primary targets:
  - T_L (Zr-phase) ≤ 900 for 1050°C glass
    ≤ 1000 for 1150°C glass
  - PCT-B, PCT-Na ≤ 2 g/m^2/7-day (became a limiting factor for 1050°C glass with TF-DST only)
- No specific constraint

b) High-T glass

- Primary target:
  - T_L (Zr-phase) ≤ 1150
- No specific constraint

4. Spinel limited (TF-A, TF-AX, TF-TY, and TF-BY)

Based on limited experience on glass formulations for NCAW and Blend Waste (Case C), the maximum predicted TL by the 1st-order T_L model that may satisfy the requirement, TL (measured) < TM -100°C, was determined and used as the primary target for low-T glasses. Concentrations of MnO2, Cr2O3, NiO were taken into account when determining the TL limits (very crude estimates due to lack of

data; intended to be used as examples). Due to greater uncertainty of the model prediction at higher temperatures, the TL model was not used for high-T glasses. Instead, the high concentration limit was determined by comparing glass compositions with CVS glasses with satisfactory liquidus temperature data (TM - TL > 100°C).

a) Low-T glass

- Primary targets:
  - T_L (Spinel) ≤ 900 for 1050°C glass for TF-A
    ≤ 930 for 1150°C glass for TF-A
    ≤ 890 for 1050°C glass for TF-AX and TF-BY
    ≤ 920 for 1150°C glass for TF-AX and TF-BY
    ≤ 930 for 1050°C glass for TF-TY
    ≤ 980 for 1150°C glass for TF-TY
  - PCT-B, PCT-Na ≤ 2 g/m^2/7-day (became a limiting factor for TF-A and TF-AX)
- No specific constraint

b) High-T glass

- No primary target (Spinel TL model not used)
- Specific constraints
  For TF-A, 15 wt% Fe2O3 was used as the limit based on comparison with CVS data
  For TF-AX, Na2O and SiO2 concentrations became limiting factor before Fe2O3 = 15 wt%; 24 wt% Na2O was the maximum needed to keep SiO2 ≥ 40 wt% constraint at TM = 1250C
  For TF-TY and TF-BY, SiO2 ≥ 40 wt% became a limiting factor, SiO2 was used as an only additive component, TM was determined afterward

5. <u>Durability (Na2O) limited (TF-S, TF-DSSF, and TF-U)</u>

Based on the information on the durability of high-Na2O glasses from LLW glass formulation study, maximum Na2O concentration of Na2O was chosen: 25 wt% for low-T glasses and 27 wt% Na2O (even higher may be possible) for high-T glasses. Then, glass formulation was conducted to check if it is feasible to formulate glass within the revised single-component constraints.

a) Low-T glass

- Primary target:

- maximize Na2O concentration up to 25 wt% satisfying the revised single-component constraints and the specific constraints (SiO2 became a limiting factor for 1050°C glasses with TF-S and TF-U)

- Specific constraint:
  - Al2O3 ≤ 12 wt%; possible crystallization of Na·Al silicates after CCC
  - CaO ≤ 8 wt% (if Al2O3 ≥ 12 wt%) ; possible crystallization of (Ca,Na)·Al silicate after CCC

b) High-T glass

- Primary target:
  - maximize Na2O concentration up to 27 wt% satisfying the revised single-component constraints and the specific constraints (SiO2 became a limiting factor for TF-U)
- Specific constraint:
  - B2O3 ≥ 5 wt%; significantly low durability of high Na glass in the absence of B2O3 or CaO
  - Al2O3 ≤ 12 wt%; possible crystallization of Na·Al silicates after CCC

6. <u>SiO2 (minimum) limited (TF-TX)</u>

a) Low-T glass

- Primary target:
  - Maximize waste loading satisfying SiO2 ≥ 40 wt% and other revised single-component constraints
- No specific constraint

b) High-T glass

- Primary target:
  - Maximize waste loading satisfying SiO2 ≥ 40 wt% and other revised single-component constraints
- No specific constraint

7. <u>Al2O3 (maximum) limited (TF-BX)</u>

a) Low-T glass

- Primary target:
  - Maximize Al2O3 concentration satisfying the revised single-component constraints and the specific constraints
- Specific constraints:
  - Na2O ≤ 18 wt%; possible crystallization of Na·Al silicates after CCC

– $Li_2O \leq 5$ wt%; possible crystallization of Li·Al silicates after CCC

b) High-T glass

- Primary target:
  - Maximize Al_2O_3 concentration satisfying the revised single-component constraints and the specific constraints
- Specific constraints:
  - $Na_2O \leq 18$ wt%; possible crystallization of Na·Al silicates after CCC

P2O5 limited

TF-B		1050°C glass, #1		1050°C glass, #2		1150°C glass		High-T glass	
oxide	waste (wi)	add (di)	glass (gi)	add (di)	glass (gi)	add (di)	glass (gi)	add (di)	glass (gi)
SiO2	0.0076	0.4388	0.3477	0.5056	0.4003	0.5131	0.4063	0.6197	0.4904
B2O3		0.2040	0.1609	0.1395	0.1100	0.1902	0.1500	0.1268	0.1000
Na2O	0.5219	0.1518	0.2300	0.1433	0.2233	0.1356	0.2173	0.1046	0.1928
Li2O			0.0000	0.0253	0.0200		0.0000		0.0000
CaO	0.0003		0.0001		0.0001		0.0001		0.0001
MgO			0.0000		0.0000		0.0000		0.0000
Fe2O3	0.0793		0.0168		0.0168		0.0168		0.0168
Al2O3	0.0120	0.1680	0.1350	0.1489	0.1200	0.1489	0.1200	0.1489	0.1200
ZrO2	0.0022	0.0375	0.0300	0.0375	0.0300	0.0121	0.0100		0.0005
Others	0.3767		0.0796		0.0796		0.0796		0.0796
SUM	*1.0000*	*1.0000*	*1.0000*	*1.0000*	*1.0000*	*1.0000*	*1.0000*	*1.0000*	*1.0000*

waste loading (W)	0.2113	0.2113	0.2113	0.2113
Melting Temp. (°C)	1050	1050	1150	1350
Arrh.Vis at M.T. (Pa-s)	10.00	10.00	6.00	4.00
Ful.Vis at M.T. (Pa-s)	11.76	10.89	5.94	3.25
E.C. at M.T. (S/m)	28.21	39.89	36.22	52.87

Liq T/spinel (°C)	875	863	869	898	
LiqT/Zr-cont. phase (°C)	889	821	805	765	
					EA
7-d PCT B (g/m2)	1.99	1.76	1.96	0.54	8.35
7-d PCT Na (g/m2)	1.72	1.59	1.73	0.52	6.67
28-d MCC-1 B (g/m2)	25.45	20.18	22.44	10.92	
28-d MCC-1 Na (g/m2)	22.78	18.27	20.26	10.06	

Others components

oxide	wi	gi	gi	gi	gi	limit
Bi2O3	0.0643	0.0136	0.0136	0.0136	0.0136	
CeO2	0.0423	0.0089	0.0089	0.0089	0.0089	
Cr2O3	0.0002	0.0000	0.0000	0.0000	0.0000	0.005
F	0.0072	0.0015	0.0015	0.0015	0.0015	
La2O3	0.0004	0.0001	0.0001	0.0001	0.0001	
MnO2	0.0048	0.0010	0.0010	0.0010	0.0010	
NiO	0.0023	0.0005	0.0005	0.0005	0.0005	
P2O5	0.1420	0.0300	0.0300	0.0300	0.0300	0.03
SO3	0.0018	0.0004	0.0004	0.0004	0.0004	
SrO	0.0000	0.0000	0.0000	0.0000	0.0000	
U3O8	0.0995	0.0210	0.0210	0.0210	0.0210	
Subtotal	0.3647	0.0771	0.0771	0.0771	0.0771	
Balance	0.0120	0.0025	0.0025	0.0025	0.0025	

P2O5 limited (cont.)

TF-T		1050°C glass, #1		1050°C glass, #2		1150°C glass		High T glass	
oxide	waste (wi)	add (di)	glass (gi)	add (di)	glass (gi)	add (di)	glass (gi)	add (di)	glass (gi)
SiO2	0.0049	0.4306	0.3476	0.5054	0.4079	0.5015	0.4047	0.6162	0.4971
B2O3		0.2108	0.1697	0.1366	0.1100	0.1863	0.1500	0.1242	0.1000
Na2O	0.5603	0.1500	0.2300	0.1494	0.2295	0.1409	0.2227	0.1121	0.1995
Li2O			0.0000	0.0248	0.0200		0.0000		0.0000
CaO	0.0000		0.0000		0.0000		0.0000		0.0000
MgO			0.0000		0.0000		0.0000		0.0000
Fe2O3	0.0895		0.0175		0.0175		0.0175		0.0175
Al2O3	0.0066	0.1723	0.1400	0.1475	0.1200	0.1475	0.1200	0.1475	0.1200
ZrO2	0.0042	0.0362	0.0300	0.0362	0.0300	0.0238	0.0200		0.0008
Others	0.3345		0.0652		0.0652		0.0652		0.0652
SUM	*1.0000*	*1.0000*	*1.0000*	*1.0000*	*1.0000*	*1.0000*	*1.0000*	*1.0000*	*1.0000*

waste loading (W)	0.1949	0.1949	0.1949	0.1949
Melting Temp. (°C)	1050	1050	1150	1350
Arrh.Vis at M.T. (Pa·s)	10.00	10.00	6.00	4.00
Ful.Vis at M.T. (Pa·s)	12.00	11.00	6.02	3.22
E.C. at M.T. (S/m)	27.71	41.49	36.91	53.25

Liq T/spinel (°C)	880	861	872	897	
LiqT/Zr-cont. phase (°C)	895	817	840	762	
Target =	2.00	2.00	2.00		EA
7-d PCT B (g/m2)	1.94	1.89	1.94	0.58	8.35
7-d PCT Na (g/m2)	1.66	1.75	1.73	0.57	6.67
28-d MCC-1 B (g/m2)	25.58	20.39	22.36	11.08	
28-d MCC-1 Na (g/m2)	23.01	18.46	20.18	10.20	

Others components

oxide	wi	gi	gi	gi	gi	limit
Bi2O3	0.0883	0.0172	0.0172	0.0172	0.0172	
CeO2	0.0538	0.0105	0.0105	0.0105	0.0105	
Cr2O3	0.0002	0.0000	0.0000	0.0000	0.0000	0.005
F	0.0050	0.0010	0.0010	0.0010	0.0010	
La2O3	0.0012	0.0002	0.0002	0.0002	0.0002	
MnO2	0.0109	0.0021	0.0021	0.0021	0.0021	
NiO	0.0003	0.0001	0.0001	0.0001	0.0001	
P2O5	0.1539	0.0300	0.0300	0.0300	0.0300	0.03
SO3	0.0003	0.0000	0.0000	0.0000	0.0000	
SrO	0.0000	0.0000	0.0000	0.0000	0.0000	
U3O8	0.0188	0.0037	0.0037	0.0037	0.0037	
Subtotal	0.3327	0.0649	0.0649	0.0649	0.0649	
Balance	0.0018	0.0004	0.0004	0.0004	0.0004	

Cr2O3 limited

TF-SX		1050°C glass		1150°C glass		High T glass	
oxide	waste (wi)	add (di)	glass (gi)	add (di)	glass (gi)	add (di)	glass (gi)
SiO2	0.0937	0.5654	0.5226	0.6420	0.5721	0.7251	0.6445
B2O3		0.0802	0.0700	0.0573	0.0500		0.0000
Na2O	0.3393	0.1517	0.1756	0.1620	0.1846	0.1363	0.1622
Li2O		0.0802	0.0700	0.0688	0.0600	0.0688	0.0600
CaO	0.0124	0.0211	0.0200		0.0016		0.0016
MgO			0.0000		0.0000		0.0000
Fe2O3	0.1276		0.0163		0.0163		0.0163
Al2O3	0.2274	0.0814	0.1000	0.0699	0.0900	0.0699	0.0900
ZrO2	0.0001		0.0000		0.0000		0.0000
Others	0.1993		0.0254		0.0254		0.0254
SUM	*1.0000*	*1.0000*	*1.0000*	*1.0000*	*1.0000*	*1.0000*	*1.0000*

waste loading (W)	0.1276	0.1276	0.1276
Melting Temp. (°C)	1050	1150	1350
Arrh.Vis at M.T. (Pa·s)	6.00	6.00	4.00
Ful.Vis at M.T. (Pa·s)	6.12	5.92	3.95
E.C. at M.T. (S/m)	65.76	74.40	90.22

Liq T/spinel (°C)	849	843	875	
LiqT/Zr-cont. phase (°C)	597	597	593	
Target =	2.00	2.00		EA
7-d PCT B (g/m2)	1.64	1.47	0.40	8.35
7-d PCT Na (g/m2)	1.54	1.34	0.40	6.67
28-d MCC-1 B (g/m2)	15.81	12.47	6.16	
28-d MCC-1 Na (g/m2)	15.24	11.94	6.00	

Others components

oxide	wi	gi	gi	gi	limit
Bi2O3		0.0000	0.0000	0.0000	
CeO2	0.0207	0.0026	0.0026	0.0026	
Cr2O3	0.0392	0.0050	0.0050	0.0050	0.005
F	0.0004	0.0000	0.0000	0.0000	
La2O3		0.0000	0.0000	0.0000	
MnO2	0.0167	0.0021	0.0021	0.0021	
NiO	0.0030	0.0004	0.0004	0.0004	
P2O5	0.0042	0.0005	0.0005	0.0005	0.03
SO3	0.0022	0.0003	0.0003	0.0003	
SrO	0.0001	0.0000	0.0000	0.0000	
U3O8	0.0919	0.0117	0.0117	0.0117	
Subtotal	0.1784	0.0228	0.0228	0.0228	
Balance	0.0209	0.0027	0.0027	0.0027	

Zr-containing crystal limited

TF-C		1050°C glass		1150°C glass		High T glass	
oxide	waste (wi)	add (di)	glass (gi)	add (di)	glass (gi)	add (di)	glass (gi)
SiO2	0.0006	0.6888	0.4758	0.7733	0.5043	0.9227	0.5125
B2O3		0.0724	0.0500	0.0767	0.0500		0.0000
Na2O	0.1038	0.1374	0.1270	0.0426	0.0639		0.0462
Li2O		0.1014	0.0700	0.1074	0.0700	0.0773	0.0429
CaO	0.0939		0.0291		0.0327		0.0418
MgO			0.0000		0.0000		0.0000
Fe2O3	0.1100		0.0341		0.0383		0.0490
Al2O3	0.0755		0.0234		0.0263		0.0336
ZrO2	0.2585		0.0800		0.0900		0.1150
Others	0.3577		0.1107		0.1246		0.1591
SUM	*1.0000*	*1.0000*	*1.0000*	*1.0000*	*1.0000*	*1.0000*	*1.0000*

waste loading (W)	0.3095	0.3482	0.4449
Melting Temp. (°C)	1050	1150	1350
Arrh.Vis at M.T. (Pa·s)	6.00	6.00	4.00
Ful.Vis at M.T. (Pa·s)	4.98	5.72	5.96
E.C. at M.T. (S/m)	45.26	37.01	42.32

Liq T/spinel (°C)	871	928	1010	
LiqT/Zr-cont. phase (°C)	897	982	1147	
Target =	≤900	≤1000	<1150	EA
7-d PCT B (g/m2)	1.78	0.42	0.05	8.35
7-d PCT Na (g/m2)	1.48	0.31	0.04	6.67
28-d MCC-1 B (g/m2)	19.82	11.53	5.11	
28-d MCC-1 Na (g/m2)	18.66	11.23	4.92	

Others components

oxide	wi	gi	gi	gi	limit
Bi2O3	0.0005	0.0002	0.0002	0.0002	
CeO2	0.0003	0.0001	0.0001	0.0001	
Cr2O3	0.0001	0.0000	0.0000	0.0000	0.01
F	0.0156	0.0048	0.0054	0.0069	
La2O3		0.0000	0.0000	0.0000	
MnO2	0.0776	0.0240	0.0270	0.0345	
NiO	0.0569	0.0176	0.0198	0.0253	
P2O5	0.0028	0.0009	0.0010	0.0012	0.03
SO3	0.0016	0.0005	0.0005	0.0007	
SrO	0.0000	0.0000	0.0000	0.0000	
U3O8	0.1987	0.0615	0.0692	0.0884	
Subtotal	0.3540	0.1096	0.1233	0.1575	
Balance	0.0037	0.0012	0.0013	0.0017	

Zr-containing crystal limited (cont.)

TF-DST		1050°C glass		1150°C glass		High T glass	
oxide	waste (wi)	add (di)	glass (gi)	add (di)	glass (gi)	add (di)	glass (gi)
SiO2	0.0831	0.5688	0.4667	0.7614	0.5631	0.9210	0.5996
B2O3	0.0047	0.0644	0.0500	0.0706	0.0500		0.0018
Na2O	0.3198	0.1575	0.1967	0.0462	0.1318		0.1227
Li2O	0.0001	0.0923	0.0700	0.1018	0.0700	0.0790	0.0487
CaO	0.0079		0.0019		0.0025		0.0030
MgO	0.0027		0.0006		0.0008		0.0010
Fe2O3	0.0875		0.0211		0.0274		0.0336
Al2O3	0.0265	0.0970	0.0800		0.0083		0.0102
ZrO2	0.3520		0.0850		0.1100		0.1350
Others	0.1156		0.0279		0.0361		0.0443
SUM	*1.0000*	*1.0000*	*1.0000*	*1.0000*	*1.0000*	*1.0000*	*1.0000*

waste loading (W)	0.2415	0.3125	0.3836
Melting Temp. (°C)	1050	1150	1350
Arrh.Vis at M.T. (Pa·s)	6.00	6.00	4.00
Ful.Vis at M.T. (Pa·s)	5.35	5.94	5.52
E.C. at M.T. (S/m)	83.24	56.18	56.81

Liq T/spinel (°C)	855	863	924	
LiqT/Zr-cont. phase (°C)	895	968	1126	
Target =	≤900	≤1000	<1150	EA
7-d PCT B (g/m2)	1.87	1.82	0.33	8.35
7-d PCT Na (g/m2)	1.58	1.32	0.28	6.67
28-d MCC-1 B (g/m2)	16.75	14.77	6.86	
28-d MCC-1 Na (g/m2)	15.69	14.11	6.52	

Others components

oxide	wi	gi	gi	gi	limit
Bi2O3		0.0000	0.0000	0.0000	
CeO2	0.0008	0.0002	0.0003	0.0003	
Cr2O3	0.0040	0.0010	0.0012	0.0015	0.01
F	0.0143	0.0035	0.0045	0.0055	
La2O3	0.0065	0.0016	0.0021	0.0025	
MnO2	0.0087	0.0021	0.0027	0.0033	
NiO	0.0047	0.0011	0.0015	0.0018	
P2O5	0.0034	0.0008	0.0011	0.0013	0.03
SO3	0.0043	0.0010	0.0014	0.0017	
SrO	0.0002	0.0000	0.0001	0.0001	
U3O8	0.0267	0.0065	0.0084	0.0102	
Subtotal	0.0737	0.0178	0.0230	0.0283	
Balance	0.0419	0.0101	0.0131	0.0161	

Spinel limited

TF-A		1050°C glass		1150°C glass		High T glass	
oxide	waste (wi)	add (di)	glass (gi)	add (di)	glass (gi)	add (di)	glass (gi)
SiO2	0.0032	0.5927	0.5185	0.7269	0.6055	0.8714	0.6529
B2O3		0.0572	0.0500	0.0601	0.0500		0.0000
Na2O	0.1731	0.1769	0.1764	0.1018	0.1138	0.0484	0.0798
Li2O		0.0801	0.0700	0.0841	0.0700	0.0802	0.0600
CaO	0.0003		0.0000		0.0001		0.0001
MgO			0.0000		0.0000		0.0000
Fe2O3	0.5960		0.0750		0.1000		0.1500
Al2O3	0.0148	0.0932	0.0833	0.0271	0.0250		0.0037
ZrO2	0.0004		0.0000		0.0001		0.0001
Others	0.2123		0.0267		0.0356		0.0534
SUM	*1.0000*	*1.0000*	*1.0000*	*1.0000*	*1.0000*	*1.0000*	*1.0000*

waste loading (W)	0.1258	0.1678	0.2517
Melting Temp. (°C)	1050	1150	1350
Arrh.Vis at M.T. (Pa·s)	6.00	6.00	4.00
Ful.Vis at M.T. (Pa·s)	7.01	5.18	2.34
E.C. at M.T. (S/m)	71.00	51.68	59.28

Liq T/spinel (°C)	900	929	1018	
LiqT/Zr-cont. phase (°C)	629	651	707	
Target =	<900	<930		EA
7-d PCT B (g/m2)	2.00	1.66	0.53	8.35
7-d PCT Na (g/m2)	1.64	1.31	0.39	6.67
28-d MCC-1 B (g/m2)	18.99	17.81	11.39	
28-d MCC-1 Na (g/m2)	18.32	17.62	11.40	

Others components

oxide	wi	gi	gi	gi	limit
Bi2O3		0.0000	0.0000	0.0000	
CeO2	0.0048	0.0006	0.0008	0.0012	
Cr2O3	0.0000	0.0000	0.0000	0.0000	0.01
F	0.0000	0.0000	0.0000	0.0000	
La2O3		0.0000	0.0000	0.0000	
MnO2	0.0718	0.0090	0.0120	0.0181	
NiO	0.0022	0.0003	0.0004	0.0006	
P2O5	0.0002	0.0000	0.0000	0.0001	0.03
SO3	0.0041	0.0005	0.0007	0.0010	
SrO	0.0002	0.0000	0.0000	0.0000	
U3O8	0.1276	0.0160	0.0214	0.0321	
Subtotal	0.2109	0.0265	0.0354	0.0531	
Balance	0.0014	0.0002	0.0002	0.0003	

Spinel limited (continued)

TF-AX		1050°C glass		1150°C glass		High T glass	
oxide	waste (wi)	add (di)	glass (gi)	add (di)	glass (gi)	add (di)	glass (gi)
SiO2	0.0057	0.7151	0.5190	0.6036	0.5152	0.7582	0.4102
B2O3	0.0000	0.0691	0.0500	0.0783	0.0500	0.0311	0.0167
Na2O	0.5189	0.0251	0.1616		0.1875		0.2400
Li2O	0.0000	0.0987	0.0700	0.0453	0.0289		0.0000
CaO	0.0279		0.0077		0.0101		0.0129
MgO	0.0000		0.0000		0.0000		0.0000
Fe2O3	0.2352		0.0650		0.0850		0.1088
Al2O3	0.0146	0.0939	0.0720	0.0728	0.0518	0.2107	0.1200
ZrO2	0.0005		0.0001		0.0002		0.0002
Others	0.1971		0.0545		0.0712		0.0912
SUM	*1.0000*	*1.0000*	*1.0000*	*1.0000*	*1.0000*	*1.0000*	*1.0000*

waste loading (W)	0.2764	0.3614	0.4625
Melting Temp. (°C)	1050	1150	1250
Arrh.Vis at M.T. (Pa·s)	6.00	6.00	4.00
Ful.Vis at M.T. (Pa·s)	6.68	6.13	4.97
E.C. at M.T. (S/m)	62.48	47.59	63.61

Liq T/spinel (°C)	889	918	997	
LiqT/Zr-cont. phase (°C)	624	702	790	
Target =	<890	<920		EA
7-d PCT B (g/m2)	1.99	1.94	0.43	8.35
7-d PCT Na (g/m2)	1.65	1.92	0.56	6.67
28-d MCC-1 B (g/m2)	19.06	20.53	14.28	
28-d MCC-1 Na (g/m2)	18.34	18.98	12.77	

Others components

oxide	wi	gi	gi	gi	limit
Bi2O3		0.0000	0.0000	0.0000	
CeO2	0.0033	0.0009	0.0012	0.0015	
Cr2O3	0.0043	0.0012	0.0015	0.0020	0.01
F	0.0001	0.0000	0.0000	0.0001	
La2O3		0.0000	0.0000	0.0000	
MnO2	0.1148	0.0317	0.0415	0.0531	
NiO	0.0066	0.0018	0.0024	0.0030	
P2O5	0.0002	0.0001	0.0001	0.0001	0.03
SO3	0.0002	0.0001	0.0001	0.0001	
SrO	0.0000	0.0000	0.0000	0.0000	
U3O8	0.0651	0.0180	0.0235	0.0301	
Subtotal	0.1945	0.0538	0.0703	0.0900	
Balance	0.0026	0.0007	0.0009	0.0012	

Spinel limited (continued)

TF-BY		1050°C glass		1150°C glass		High T glass	
oxide	waste (wi)	add (di)	glass (gi)	add (di)	glass (gi)	add (di)	glass (gi)
SiO2	0.0584	0.7927	0.4564	0.8382	0.4438	1.0000	0.4000
B2O3		0.0918	0.0500	0.1012	0.0500		0.0000
Na2O	0.2375		0.1081		0.1201		0.1513
Li2O		0.1155	0.0629	0.0607	0.0300		0.0000
CaO	0.0566		0.0258		0.0286		0.0361
MgO			0.0000		0.0000		0.0000
Fe2O3	0.0989		0.0450		0.0500		0.0630
Al2O3	0.1233		0.0561		0.0624		0.0786
ZrO2	0.0022		0.0010		0.0011		0.0014
Others	0.4231		0.1926		0.2140		0.2696
SUM	*1.0000*	*1.0000*	*1.0000*	*1.0000*	*1.0000*	*1.0000*	*1.0000*

waste loading (W)	0.4552	0.5058	0.6372
Melting Temp. (°C)	1050	1150	1272
Arrh.Vis at M.T. (Pa·s)	6.00	6.00	4.00
Ful.Vis at M.T. (Pa·s)	5.71	6.03	5.41
E.C. at M.T. (S/m)	37.62	34.59	49.22

Liq T/spinel (°C)	883	917	960	
LiqT/Zr-cont. phase (°C)	657	731	786	
Target =	<890	<920		EA
7-d PCT B (g/m2)	1.19	0.61	0.21	8.35
7-d PCT Na (g/m2)	0.95	0.56	0.26	6.67
28-d MCC-1 B (g/m2)	18.49	15.21	10.90	
28-d MCC-1 Na (g/m2)	17.53	14.07	9.68	

Others components

oxide	wi	gi	gi	gi	limit
Bi2O3	0.0003	0.0001	0.0001	0.0002	
CeO2	0.0199	0.0091	0.0101	0.0127	
Cr2O3	0.0000	0.0000	0.0000	0.0000	0.01
F	0.0052	0.0023	0.0026	0.0033	
La2O3		0.0000	0.0000	0.0000	
MnO2	0.0041	0.0019	0.0021	0.0026	
NiO	0.1164	0.0530	0.0589	0.0742	
P2O5	0.0182	0.0083	0.0092	0.0116	0.03
SO3	0.0023	0.0010	0.0011	0.0014	
SrO	0.0345	0.0157	0.0174	0.0220	
U3O8	0.2199	0.1001	0.1112	0.1401	
Subtotal	0.4208	0.1915	0.2128	0.2681	
Balance	0.0023	0.0011	0.0012	0.0015	

Spinel limited (continued)

TF-TY		1050°C glass		1150°C glass		High T glass	
oxide	waste (wi)	add (di)	glass (gi)	add (di)	glass (gi)	add (di)	glass (gi)
SiO2	0.2920	0.7160	0.4694	0.7480	0.4375	1.0000	0.4032
B2O3		0.1201	0.0500	0.1566	0.0500		0.0000
Na2O	0.2229		0.1301		0.1517		0.1879
Li2O		0.1620	0.0675	0.0954	0.0305		0.0000
CaO	0.0000		0.0000		0.0000		0.0000
MgO			0.0000		0.0000		0.0000
Fe2O3	0.1542		0.0900		0.1050		0.1300
Al2O3	0.1006		0.0587		0.0685		0.0848
ZrO2	0.0252		0.0147		0.0172		0.0213
Others	0.2051		0.1197		0.1396		0.1729
SUM	*1.0000*	*1.0000*	*1.0000*	*1.0000*	*1.0000*	*1.0000*	*1.0000*

waste loading (W)	0.5835	0.6808	0.8428
Melting Temp. (°C)	1050	1150	1298
Arrh.Vis at M.T. (Pa·s)	6.00	6.00	4.00
Ful.Vis at M.T. (Pa·s)	6.70	6.38	5.15
E.C. at M.T. (S/m)	49.45	42.85	59.72

Liq T/spinel (°C)	924	969	1025	
LiqT/Zr-cont. phase (°C)	722	819	896	
Target =	<930	<980		EA
7-d PCT B (g/m2)	1.60	0.85	0.30	8.35
7-d PCT Na (g/m2)	1.10	0.67	0.31	6.67
28-d MCC-1 B (g/m2)	21.06	18.46	13.18	
28-d MCC-1 Na (g/m2)	20.21	17.17	11.82	

Others components

oxide	wi	gi	gi	gi	limit
Bi2O3	0.0033	0.0019	0.0022	0.0027	
CeO2	0.0105	0.0061	0.0072	0.0089	
Cr2O3	0.0003	0.0002	0.0002	0.0003	0.01
F	0.0004	0.0002	0.0003	0.0003	
La2O3		0.0000	0.0000	0.0000	
MnO2	0.0010	0.0006	0.0007	0.0008	
NiO	0.0000	0.0000	0.0000	0.0000	
P2O5	0.0347	0.0202	0.0236	0.0292	0.03
SO3	0.0059	0.0034	0.0040	0.0049	
SrO	0.0000	0.0000	0.0000	0.0000	
U3O8	0.1471	0.0859	0.1002	0.1240	
Subtotal	0.2032	0.1185	0.1383	0.1712	
Balance	0.0019	0.0011	0.0013	0.0016	

Durability (Na2O) limited

TF-S		1050°C glass		1150°C glass		High-T glass	
oxide	waste (wi)	add (di)	glass (gi)	add (di)	glass (gi)	add (di)	glass (gi)
SiO2	0.0213	0.6080	0.4049	0.6773	0.4407	0.8057	0.5002
B2O3		0.1377	0.0900	0.1564	0.1000	0.0819	0.0500
Na2O	0.6931		0.2400		0.2500		0.2700
Li2O		0.0183	0.0120		0.0000		0.0000
CaO	0.0000	0.1224	0.0800	0.0530	0.0339		0.0000
MgO			0.0000		0.0000		0.0000
Fe2O3	0.0270		0.0093		0.0097		0.0105
Al2O3	0.1320	0.1136	0.1200	0.1132	0.1200	0.1123	0.1200
ZrO2	0.0293		0.0101		0.0106		0.0114
Others	0.0974		0.0337		0.0351		0.0379
SUM	*1.0000*	*1.0000*	*1.0000*	*1.0000*	*1.0000*	*1.0000*	*1.0000*

waste loading (W)	0.3463	0.3607	0.3895
Melting Temp. (°C)	1050	1150	1306
Arrh.Vis at M.T. (Pa·s)	6.00	6.00	4.00
Ful.Vis at M.T. (Pa·s)	4.81	6.21	4.63
E.C. at M.T. (S/m)	34.19	41.96	72.84

Liq T/spinel (°C)	893	875	860	
LiqT/Zr-cont. phase (°C)	741	762	733	
Target =	2.00	2.00	2.00	EA
7-d PCT B (g/m2)	0.95	1.24	1.00	8.35
7-d PCT Na (g/m2)	1.75	1.72	1.29	6.67
28-d MCC-1 B (g/m2)	19.66	17.46	11.56	
28-d MCC-1 Na (g/m2)	17.61	15.59	10.28	

Others components

oxide	wi	gi	gi	gi	limit
Bi2O3		0.0000	0.0000	0.0000	
CeO2	0.0111	0.0039	0.0040	0.0043	
Cr2O3	0.0072	0.0025	0.0026	0.0028	0.01
F	0.0012	0.0004	0.0004	0.0005	
La2O3		0.0000	0.0000	0.0000	
MnO2	0.0046	0.0016	0.0017	0.0018	
NiO	0.0017	0.0006	0.0006	0.0007	
P2O5	0.0054	0.0019	0.0019	0.0021	0.03
SO3	0.0028	0.0010	0.0010	0.0011	
SrO	0.0000	0.0000	0.0000	0.0000	
U3O8	0.0589	0.0204	0.0212	0.0229	
Subtotal	0.0929	0.0322	0.0335	0.0362	
Balance	0.0044	0.0015	0.0016	0.0017	

Durability (Na2O) limited (continued)

TF-DSSF		1050°C glass		1150°C glass		High-T glass	
oxide	waste (wi)	add (di)	glass (gi)	add (di)	glass (gi)	add (di)	glass (gi)
SiO2	0.2944	0.5566	0.4573	0.5725	0.4672	0.7261	0.5495
B2O3	0.0000	0.0966	0.0600	0.1610	0.1000	0.0846	0.0500
Na2O	0.6600		0.2500		0.2500		0.2700
Li2O		0.0409	0.0254		0.0000		0.0000
CaO	0.0062	0.1250	0.0800	0.0855	0.0555		0.0025
MgO	0.0000		0.0000		0.0000		0.0000
Fe2O3	0.0000		0.0000		0.0000		0.0000
Al2O3	0.0200	0.1810	0.1200	0.1810	0.1200	0.1893	0.1200
ZrO2			0.0000		0.0000		0.0000
Others	0.0194		0.0073		0.0073		0.0079
SUM	*1.0000*	*1.0000*	*1.0000*	*1.0000*	*1.0000*	*1.0000*	*1.0000*

waste loading (W)	0.3788	0.3788	0.4091
Melting Temp. (°C)	1050	1150	1352
Arrh.Vis at M.T. (Pa·s)	6.00	6.00	4.00
Ful.Vis at M.T. (Pa·s)	4.57	6.00	4.22
E.C. at M.T. (S/m)	47.54	38.52	71.63

Liq T/spinel (°C)	870	874	850	
LiqT/Zr-cont. phase (°C)	646	713	678	
Target =	2.00	2.00	2.00	EA
7-d PCT B (g/m2)	0.98	1.05	0.91	8.35
7-d PCT Na (g/m2)	1.95	1.76	1.25	6.67
28-d MCC-1 B (g/m2)	16.35	16.25	9.88	
28-d MCC-1 Na (g/m2)	14.77	14.59	8.86	

Others components

oxide	wi	gi	gi	gi	limit
Bi2O3		0.0000	0.0000	0.0000	
CeO2		0.0000	0.0000	0.0000	
Cr2O3	0.0002	0.0001	0.0001	0.0001	0.01
F	0.0007	0.0002	0.0002	0.0003	
La2O3		0.0000	0.0000	0.0000	
MnO2	0.0000	0.0000	0.0000	0.0000	
NiO	0.0000	0.0000	0.0000	0.0000	
P2O5	0.0002	0.0001	0.0001	0.0001	0.03
SO3	0.0007	0.0003	0.0003	0.0003	
SrO	0.0000	0.0000	0.0000	0.0000	
U3O8	0.0001	0.0000	0.0000	0.0000	
Subtotal	0.0019	0.0007	0.0007	0.0008	
Balance	0.0175	0.0066	0.0066	0.0072	

Durability (Na2O) limited (continued)

TF-U		1050°C glass		1150°C glass		High-T glass	
oxide	waste (wi)	add (di)	glass (gi)	add (di)	glass (gi)	add (di)	glass (gi)
SiO2	0.1865	0.6666	0.4029	0.8149	0.4223	0.8249	0.4101
B2O3		0.1115	0.0500	0.1340	0.0500	0.1436	0.0500
Na2O	0.3989		0.2200		0.2500		0.2600
Li2O		0.0280	0.0126		0.0000		0.0000
CaO	0.0000	0.1939	0.0870	0.0512	0.0191		0.0000
MgO			0.0000		0.0000		0.0000
Fe2O3	0.0228		0.0126		0.0143		0.0149
Al2O3	0.1673		0.0922		0.1048	0.0315	0.1200
ZrO2	0.0030		0.0016		0.0019		0.0019
Others	0.2196		0.1211		0.1376		0.1431
SUM	*1.0000*	*1.0000*	*1.0000*	*1.0000*	*1.0000*	*1.0000*	*1.0000*

waste loading (W)	0.5515	0.6268	0.6518
Melting Temp. (°C)	1050	1150	1210
Arrh.Vis at M.T. (Pa-s)	6.00	6.00	4.00
Ful.Vis at M.T. (Pa-s)	4.09	6.55	4.83
E.C. at M.T. (S/m)	31.77	51.57	71.24

Liq T/spinel (°C)	884	853	849	
LiqT/Zr-cont. phase (°C)	694	709	713	
Target =	2.00	2.00	2.00	EA
7-d PCT B (g/m2)	0.88	1.36	1.37	8.35
7-d PCT Na (g/m2)	1.71	1.79	1.61	6.67
28-d MCC-1 B (g/m2)	19.14	16.84	16.06	
28-d MCC-1 Na (g/m2)	16.88	14.66	13.97	

Others components

oxide	wi	gi	gi	gi	limit
Bi2O3	0.0004	0.0002	0.0002	0.0002	
CeO2	0.0224	0.0123	0.0140	0.0146	
Cr2O3	0.0019	0.0010	0.0012	0.0012	0.01
F	0.0007	0.0004	0.0004	0.0005	
La2O3		0.0000	0.0000	0.0000	
MnO2	0.0021	0.0012	0.0013	0.0014	
NiO	0.0001	0.0000	0.0000	0.0000	
P2O5	0.0074	0.0041	0.0046	0.0048	0.03
SO3	0.0006	0.0004	0.0004	0.0004	
SrO	0.0000	0.0000	0.0000	0.0000	
U3O8	0.1835	0.1012	0.1150	0.1196	
Subtotal	0.2190	0.1208	0.1373	0.1428	
Balance	0.0006	0.0003	0.0004	0.0004	

SiO2 (minimum) limited

TF-TX		1050°C glass		1150°C glass		High-T glass	
oxide	waste (wi)	add (di)	glass (gi)	add (di)	glass (gi)	add (di)	glass (gi)
SiO2	0.1733	0.7613	0.4026	0.8153	0.4044	1.0000	0.4000
B2O3		0.1282	0.0500	0.1389	0.0500		0.0000
Na2O	0.3007		0.1834		0.1925		0.2182
Li2O		0.1105	0.0431	0.0458	0.0165		0.0000
CaO	0.0001		0.0001		0.0001		0.0001
MgO			0.0000		0.0000		0.0000
Fe2O3	0.0391		0.0238		0.0250		0.0284
Al2O3	0.1583		0.0965		0.1013		0.1149
ZrO2	0.0040		0.0024		0.0026		0.0029
Others	0.3245		0.1980		0.2077		0.2355
SUM	*1.0000*	*1.0000*	*1.0000*	*1.0000*	*1.0000*	*1.0000*	*1.0000*

waste loading (W)	0.6100	0.6400	0.7258
Melting Temp. (°C)	1050	1150	1278
Arrh.Vis at M.T. (Pa·s)	6.00	6.00	4.00
Ful.Vis at M.T. (Pa·s)	5.86	6.55	5.98
E.C. at M.T. (S/m)	53.89	50.75	77.14

Liq T/spinel (°C)	843	867	889	
LiqT/Zr-cont. phase (°C)	665	722	739	
Target =				EA
7-d PCT B (g/m2)	1.71	0.97	0.41	8.35
7-d PCT Na (g/m2)	1.44	0.89	0.47	6.67
28-d MCC-1 B (g/m2)	19.19	15.46	10.40	
28-d MCC-1 Na (g/m2)	17.42	13.80	9.06	

Others components

oxide	wi	gi	gi	gi	limit
Bi2O3	0.0005	0.0003	0.0003	0.0004	
CeO2	0.0276	0.0169	0.0177	0.0201	
Cr2O3	0.0001	0.0000	0.0000	0.0000	0.01
F	0.0012	0.0007	0.0008	0.0009	
La2O3		0.0000	0.0000	0.0000	
MnO2	0.0075	0.0046	0.0048	0.0054	
NiO	0.0025	0.0015	0.0016	0.0018	
P2O5	0.0410	0.0250	0.0263	0.0298	0.03
SO3	0.0051	0.0031	0.0033	0.0037	
SrO	0.0000	0.0000	0.0000	0.0000	
U3O8	0.2372	0.1447	0.1518	0.1722	
Subtotal	0.3227	0.1968	0.2065	0.2342	
Balance	0.0018	0.0011	0.0012	0.0013	

Al2O3 (maximum) limited

TF-BX		1050°C glass		1150°C glass		High-T glass	
oxide	waste (wi)	add (di)	glass (gi)	add (di)	glass (gi)	add (di)	glass (gi)
SiO2	0.2137	0.6387	0.4075	0.7302	0.4043	0.8444	0.4053
B2O3		0.1569	0.0715	0.1626	0.0600	0.1317	0.0400
Na2O	0.2514	0.0948	0.1800		0.1587		0.1751
Li2O		0.1096	0.0500	0.1072	0.0396	0.0239	0.0073
CaO	0.0012		0.0007		0.0008		0.0009
MgO			0.0000		0.0000		0.0000
Fe2O3	0.0591		0.0321		0.0373		0.0411
Al2O3	0.2298		0.1250		0.1450		0.1600
ZrO2	0.0033		0.0018		0.0021		0.0023
Others	0.2414		0.1313		0.1523		0.1681
SUM	*1.0000*	*1.0000*	*1.0000*	*1.0000*	*1.0000*	*1.0000*	*1.0000*

waste loading (W)	0.5440	0.6310	0.6963
Melting Temp. (°C)	1050	1150	1350
Arrh.Vis at M.T. (Pa-s)	6.00	6.00	4.00
Ful.Vis at M.T. (Pa-s)	6.29	6.41	4.92
E.C. at M.T. (S/m)	55.90	54.83	68.39

Liq T/spinel (°C)	876	924	965	
LiqT/Zr-cont. phase (°C)	681	734	801	
Target =				EA
7-d PCT B (g/m2)	1.12	0.32	0.11	8.35
7-d PCT Na (g/m2)	0.91	0.26	0.11	6.67
28-d MCC-1 B (g/m2)	17.09	10.61	7.01	
28-d MCC-1 Na (g/m2)	15.97	10.19	6.46	

Others components

oxide	wi	gi	gi	gi	limit
Bi2O3	0.0004	0.0002	0.0003	0.0003	
CeO2	0.0296	0.0161	0.0187	0.0206	
Cr2O3	0.0000	0.0000	0.0000	0.0000	0.01
F	0.0017	0.0009	0.0011	0.0012	
La2O3		0.0000	0.0000	0.0000	
MnO2	0.0084	0.0046	0.0053	0.0058	
NiO	0.0125	0.0068	0.0079	0.0087	
P2O5	0.0256	0.0139	0.0161	0.0178	0.03
SO3	0.0054	0.0029	0.0034	0.0038	
SrO	0.0005	0.0003	0.0003	0.0004	
U3O8	0.1412	0.0768	0.0891	0.0983	
Subtotal	0.2253	0.1225	0.1421	0.1568	
Balance	0.0162	0.0088	0.0102	0.0113	